

**UNIVERSITY OF MILANO-BICOCCA**  
**DOCTORAL DEGREE COURSE IN CHEMICAL SCIENCES**  
**XXVII CYCLE ENROLLMENT**



**RECYCLING OF TIRE RUBBER: INVESTIGATION AND OPTIMIZATION  
OF GREEN DEVULCANIZATION TECHNOLOGIES**

**Tutor:**  
**Prof. Marina LASAGNI**

**Ph.D. Dissertation by:**  
**Ivan MANGILI**  
**Student ID No. 703891**

**Academic Year 2013/2014**



“The only true voyage of discovery  
would be not to visit strange lands,  
but to possess other eyes.”

*Marcel Proust*



# CONTENTS

<b><u>LIST OF TABLES</u></b>	<b><u>V</u></b>
<b><u>LIST OF FIGURES</u></b>	<b><u>VII</u></b>
<b><u>LIST OF SYMBOLS AND ABBREVIATIONS</u></b>	<b><u>XI</u></b>
<b><u>1 INTRODUCTION AND AIM</u></b>	<b><u>1</u></b>
1.1 INTRODUCTION	1
1.2 SCOPE OF THE THESIS WORK	5
REFERENCES	7
<b><u>2 LITERATURE SURVEY AND BACKGROUND</u></b>	<b><u>9</u></b>
2.1 RECLAIMING AND RECYCLING	9
2.1.1 GENERAL CONSIDERATIONS	9
2.1.2 GRINDING	9
2.1.3 THERMO-MECHANICAL AND MECHANO-CHEMICAL METHODS	10
2.1.3.1 Mechano-chemical methods	11
2.1.3.2 Pan-mill method	12
2.1.3.3 Mixing mill with chemicals addition	12
2.1.3.4 Trelleborg process	12
2.1.3.5 De-Link process	12
2.1.3.6 Swelling in benzene with sulfoxide	13
2.1.4 CHEMICAL METHODS	13
2.1.4.1 Organic hydroperoxides	13
2.1.4.2 Thiols and disulfides	14
2.1.4.3 Triphenyl phosphine and phosphites	15
2.1.4.4 Lithium aluminum hydride	15
2.1.4.5 Methyl iodide	16
2.1.4.6 Phenyl hydrazine and peroxides (main chain degradation)	16
2.1.4.7 Other chemical methods	17
2.1.4.8 Ozonization	17
2.1.4.9 Supercritical CO <sub>2</sub>	18
2.1.5 PHYSICAL METHODS	20
2.1.5.1 Single- and twin- screw extruders	20

2.1.5.2	High speed mixing	22
2.1.5.3	Microwave	22
2.1.5.4	Ultrasound	22
2.1.6	BIOLOGICAL METHODS	26
	<b>REFERENCES</b>	<b>27</b>

### **3 CHARACTERIZATION OF CRYO-GTR AND PRELIMINARY SUPERCRITICAL CO<sub>2</sub>**

	<b><u>DEVULCANIZATION</u></b>	<b>35</b>
<b>3.1</b>	<b>EXPERIMENTAL</b>	<b>35</b>
3.1.1	MATERIALS AND REAGENTS	35
3.1.2	GTR COMPOSITION	35
3.1.3	DEVULCANIZATION PROCESS	36
3.1.4	CHARACTERIZATION OF THE MATERIALS	37
3.1.4.1	Comparison between E-GTR and TE-GTR	37
3.1.5	COMPOUNDS	41
<b>3.2</b>	<b>RESULTS AND DISCUSSION</b>	<b>43</b>
3.2.1	GTR COMPOSITION	43
3.2.1.1	Additives	45
3.2.2	COMPARISON OF E-GTR AND TE-GTR	48
3.2.3	MECHANICAL PROPERTIES OF VULCANIZED COMPOUNDS (VULCANIZATES)	52
3.2.4	CURING BEHAVIOR OF COMPOUNDS	54
<b>3.3</b>	<b>CONCLUSIONS</b>	<b>56</b>
	<b>REFERENCES</b>	<b>57</b>

### **4 MODELING AND INVESTIGATION OF SUPERCRITICAL CO<sub>2</sub>**

	<b><u>DEVULCANIZATION</u></b>	<b>61</b>
<b>4.1</b>	<b>INTRODUCTION</b>	<b>61</b>
<b>4.2</b>	<b>MATERIALS AND METHODS</b>	<b>62</b>
4.2.1	DESIGN OF EXPERIMENTS	62
4.2.2	EXPERIMENTAL AND ANALYTICAL PROCEDURES	64
<b>4.3</b>	<b>RESULTS AND DISCUSSION</b>	<b>67</b>
4.3.1	REGRESSION MODELS	67
4.3.2	VALIDATION	73
<b>4.4</b>	<b>CONCLUSIONS</b>	<b>74</b>
	<b>REFERENCES</b>	<b>75</b>

<b><u>5</u></b>	<b><u>MODELING AND INVESTIGATION OF ULTRASONIC DEVULCANIZATION</u></b>	<b><u>77</u></b>
5.1	INTRODUCTION	77
5.2	MATERIALS AND METHODS	79
5.2.1	MATERIALS AND EQUIPMENT	79
5.2.2	DESIGN OF EXPERIMENTS	79
5.2.3	RESPONSES FOR THE DEVULCANIZED GTR (D-GTR)	81
5.2.3.1	Horikx function	82
5.2.4	RESPONSES FOR THE REVULCANIZED GTR (R-GTR)	82
5.2.5	OPTIMIZATION	83
5.2.5.1	Derringer and Suich desirability functions	83
5.2.5.2	Kim and Lin desirability functions	84
5.3	RESULTS AND DISCUSSION	85
5.3.1	REGRESSION MODELS	85
5.3.2	D-GTR	89
5.3.2.1	Horikx function	91
5.3.3	R-GTR	92
5.3.4	VALIDATION	95
5.3.5	OPTIMIZATION	96
5.4	CONCLUSIONS	100
	REFERENCES	100
<b><u>6</u></b>	<b><u>MODELING AND INVESTIGATION OF BIOLOGICAL DEVULCANIZATION</u></b>	<b><u>105</u></b>
6.1	INTRODUCTION	105
6.2	MATERIALS AND METHODS	106
6.2.1	REAGENTS	106
6.2.1.1	Biological medium	107
6.2.2	DESIGN OF EXPERIMENTS	107
6.2.2.1	Experimental procedure	107
6.2.2.2	Full factorial design	107
6.2.2.3	Complex viscosity	110
6.2.3	HORIKX FUNCTIONS	110
6.2.4	AUTOMATED RIBOSOMAL INTERGENIC SPACER ANALYSIS (ARISA)	110
6.3	RESULTS AND DISCUSSION	111
6.3.1	REGRESSION MODEL	111
6.3.2	HORIKX FUNCTIONS	117
6.3.3	MICROBIAL CHARACTERIZATION	118

6.3.4	CONCLUSIONS	121
	REFERENCES	121
<b>7</b>	<b><u>INFLUENCE ON PROPERTIES OF NATURAL RUBBER COMPOUNDS</u></b>	
	<b><u>CONTAINING DEVULCANIZED GTRS</u></b>	<b><u>123</u></b>
<b>7.1</b>	<b>MATERIALS AND METHODS</b>	<b>123</b>
7.1.1	DEVULCANIZATION TECHNOLOGIES	123
7.1.1.1	scCO <sub>2</sub> devulcanization	123
7.1.1.2	Ultrasonic devulcanization	124
7.1.1.3	Biological devulcanization	125
7.1.2	COMPOUNDS	126
7.1.3	CHARACTERIZATION TECHNIQUES	128
7.1.3.1	GTR and X-GTRs sol and gel fractions	128
7.1.3.2	Compounds characterization	128
<b>7.2</b>	<b>RESULTS AND DISCUSSION</b>	<b>129</b>
7.2.1	GTR AND X-GTRS SOL AND GEL FRACTIONS	129
7.2.2	CHARACTERIZATION OF COMPOUNDS CONTAINING GTR AND X-GTRS SAMPLES	130
7.2.2.1	Curing behavior and crosslink density	130
7.2.2.2	Mechanical properties of vulcanized compounds	134
7.2.2.3	Dynamic viscoelastic properties of vulcanized compounds	137
<b>7.3</b>	<b>CONCLUSIONS</b>	<b>139</b>
	REFERENCES	<b>140</b>
	<b><u>SCIENTIFIC CONTRIBUTIONS</u></b>	<b><u>143</u></b>
	RESEARCH PAPERS	<b>143</b>
	CONFERENCE CONTRIBUTIONS	<b>143</b>
	<b><u>ACKNOWLEDGMENTS</u></b>	<b><u>145</u></b>



## LIST OF TABLES

TABLE 2.1: DISSOCIATION ENERGY OF BONDS IN VULCANIZED RUBBER [3].	11
TABLE 3.1: TEMPERATURE, PRESSURE, TIME AND DEVULCANIZING AGENT USED IN THE DEVULCANIZATION PROCESS.	37
TABLE 3.2: COMPOUNDS FORMULATION.	42
TABLE 3.3: GTR COMPOSITION.	45
TABLE 3.4: ADDITIVES FOUND BY GC-MSD ANALYSIS IN THE ACETONE EXTRACT.	46
TABLE 3.5: ADDITIVES FOUND BY GC-MSD ANALYSIS IN THE CHLOROFORM EXTRACT.	47
TABLE 3.6: CHARACTERIZATION OF THE E-GTR AND TE-GTR.	48
TABLE 4.1: FACTORS AND LEVELS OF THE EXPERIMENTAL DESIGN.	62
TABLE 4.2: FULL FACTORIAL DESIGN AND EXPERIMENTAL RESPONSES.	65
TABLE 4.3: ANALYSIS OF VARIANCE FOR THE INTERACTION MODEL.	68
TABLE 4.4: ESTIMATED EFFECTS AND STANDARD ERROR (SE) CALCULATED THROUGH THE THREE CENTRAL EXPERIMENTS (EQUATION 4.2).	69
TABLE 4.5: ESTIMATED EFFECTS AND STANDARD ERROR (SE) CALCULATED THROUGH HIGHER ORDER INTERACTIONS (EQUATION 4.3).	69
TABLE 4.6: REGRESSION COEFFICIENTS WITH STANDARD ERROR (SE) AND COEFFICIENTS OF DETERMINATION FOR EACH EXPERIMENTAL RESPONSE REFERRED TO THE SCALED AND CENTERED VARIABLES.	71
TABLE 4.7: VALIDATION EXPERIMENT CONDITIONS WITHIN THE STUDIED DOMAIN.	73
TABLE 5.1: FACTORS AND LEVELS OF THE EXPERIMENTAL DESIGN.	80
TABLE 5.2: CENTRAL COMPOSITE DESIGN AND EXPERIMENTAL RESPONSES.	86
TABLE 5.3: REGRESSION COEFFICIENTS AND STANDARD ERROR (SE) FOR EACH EXPERIMENTAL RESPONSE RELATED TO THE SCALED AND CENTERED VARIABLES.	87
TABLE 5.4: COEFFICIENTS OF DETERMINATIONS OF REDUCED MODELS.	89
TABLE 5.5: VALIDATION EXPERIMENT CONDITIONS.	95
TABLE 5.6: PARAMETERS FOR DESIRABILITY FUNCTIONS.	98
TABLE 5.7: DESIRABILITY FUNCTIONS OPTIMIZATION RESULTS.	99
TABLE 6.1: FACTORS AND LEVELS OF THE EXPERIMENTAL DESIGN.	108
TABLE 6.2: FULL FACTORIAL DESIGN AND EXPERIMENTAL RESPONSE.	108
TABLE 6.3: CONTROL SAMPLES WITHOUT BACTERIAL INOCULUM.	109
TABLE 6.4: ANALYSIS OF VARIANCE FOR THE INTERACTION MODEL.	112

TABLE 6.5: ESTIMATED EFFECTS AND STANDARD ERROR (SE) CALCULATED THROUGH THE THREE CENTRAL EXPERIMENTS AND THREE CONTROL SAMPLES (EQUATION 6.2).	112
TABLE 6.6: REGRESSION COEFFICIENTS WITH THE STANDARD ERROR (SE) AND COEFFICIENTS OF DETERMINATION REFERRED TO THE SCALED AND CENTERED VARIABLES.	113
TABLE 7.1: EXPERIMENTAL CONDITIONS FOR THE SCCO <sub>2</sub> DEVULCANIZATION.	124
TABLE 7.2: EXPERIMENTAL CONDITIONS FOR THE ULTRASONIC DEVULCANIZATION.	125
TABLE 7.3: EXPERIMENTAL CONDITIONS FOR THE BIOLOGICAL DEVULCANIZATION.	126
TABLE 7.4: COMPOUNDS FORMULATION.	127
TABLE 7.5: INGREDIENTS ADDED TO THE MASTER-BATCH IN TWO-ROLL MILL.	128
TABLE 7.6: SOL AND GEL FRACTION OF GTR/X-GTRS SAMPLES.	130

## LIST OF FIGURES

FIGURE 1.1: THREE-DIMENSIONAL CROSSLINK NETWORK FORMATION (ADAPTED FROM REF. [4]).	2
FIGURE 1.2: EFFECT OF CROSSLINK DENSITY ON PROPERTIES OF VULCANIZATES (ADAPTED FROM REF [4]).	3
FIGURE 2.1: RECLAIMING AGENTS USED IN MECHANO-CHEMICAL METHODS (ADAPTED FROM REF.[3]).	11
FIGURE 2.2: ORGANIC HYDROPEROXIDES REACTION MECHANISM WITH THE SULFUR CROSSLINKS (ADAPTED FROM REF.[3]).	13
FIGURE 2.3: OPENING OF SULFUR CROSSLINKS BY REARRANGEMENT.	14
FIGURE 2.4: OPENING OF SULFUR CROSSLINKS BY SUBSTITUTION.	14
FIGURE 2.5: REACTION MECHANISM BETWEEN 2-PROPANE THIOL/PIPERIDINE SYSTEM AND POLYSULFIDIC CROSSLINKS (ADAPTED FROM REF.[3]).	14
FIGURE 2.6: TRIPHENYL PHOSPHINE CLEAVAGE REACTION MECHANISMS OF DI- AND POLYSULFIDIC CROSSLINKS (ADAPTED FROM REF.[3]).	15
FIGURE 2.7: CLEAVEGE OF DI- AND POLYSULFIDIC CROSSLINKS BY TRIALKYL PHOSPHITES (ADAPTED FROM REF.[2]).	15
FIGURE 2.8: CLEAVEGE OF DI- AND POLYSULFIDIC CROSSLINKS BY SODIUM DIBUTYL PHOSPHITE, (ADAPTED FROM REF.[3]).	15
FIGURE 2.9: REACTION OF LITHIUM ALUMINUM HYDRIDE WITH DI- AND POLYSULFIDIC CROSSLINKS (ADAPTED FROM REF.[2]).	15
FIGURE 2.10: REACTION MECHANISM OF METHYL IODIDE (ADAPTED FROM REF.[2]).	16
FIGURE 2.11: OXIDATION MECHANISM FOR PHENYL HYDRAZINE-IRON (II) CHLORIDE SYSTEM (ADAPTED FROM REF.[3]).	16
FIGURE 2.12: RUBBER CHAIN OXIDATION MECHANISM BY RADICALS (ADAPTED FROM REF.[3]).	17
FIGURE 2.13: DECOMPOSITION OF PEROXIDES BY IONS OF METALS (ADAPTED FROM REF.[3]).	17
FIGURE 2.14: CO <sub>2</sub> PRESSURE-TEMPERATURE PHASE DIAGRAM.	18
FIGURE 2.15: CO <sub>2</sub> DENSITY-PRESSURE PHASE DIAGRAM (ADAPTED FROM REF. [21]).	19
FIGURE 2.16: BREAKAGES OF CROSSLINKING POINTS IN HIGH SHEAR (ADAPTED FROM REF. [46]).	21
FIGURE 2.17: ULTRASOUND CAVITATION BUBBLE GROWTH AND COLLAPSE (ADAPTED FROM REF. [51]).	24

FIGURE 3.1: SCHEMATIC OF SFE $\mu$ -PLANT.	37
FIGURE 3.2: GTR PARTICLES SIZE DISTRIBUTION.	43
FIGURE 3.3: SEM PICTURE OF GTR PARTICLES.	44
FIGURE 3.4: TGA/dTGA OF THE GTR IN N <sub>2</sub> ATMOSPHERE AND HEATING RATE OF 20 °C/min.	44
FIGURE 3.5: NORMALIZED GEL FRACTION AS A FUNCTION OF NORMALIZED CROSSLINK DENSITY COMPARED TO THE HORIKX FUNCTION.	49
FIGURE 3.6: ATR SPECTRA OF E-GTR AND TE-GTR.	50
FIGURE 3.7: REACTION SCHEME FOR THE DD AND NR.	51
FIGURE 3.8: STRESS–STRAIN CURVES FOR NR VULCANIZATE COMPOUND AND VULCANIZED COMPOUNDS CONTAINING VARIOUS AMOUNTS OF (a) GTR / T-GTR AND (b) E-GTR / TE-GTR.	53
FIGURE 3.9: MODULI AT (a) 100% AND AT (b) 300% ELONGATION, (c) TENSILE STRENGTH AND (d) ELONGATION AT BREAK AS A FUNCTION OF THE DEVULCANIZED RUBBER CONTENT (PHR).	54
FIGURE 3.10: CURING CURVES FOR NR COMPOUND AND COMPOUNDS CONTAINING VARIOUS AMOUNTS OF (a) GTR / T-GTR AND (b) E-GTR / TE-GTR.	55
FIGURE 3.11: (a) MAXIMUM TORQUE (M <sub>H</sub> ) AND (b) $\Delta M$ AS A FUNCTION OF THE DEVULCANIZED RUBBER CONTENT (PHR).	56
FIGURE 4.1: PROCEDURE USED FOR THE TREATMENT AND CHARACTERIZATION.	66
FIGURE 4.2: NORMAL PROBABILITY PLOT OF RESIDUALS FOR (a) CROSSLINK DENSITY, (b) SOL FRACTION, (c) GEL FRACTION AND (d) SULFUR CONTENT.	71
FIGURE 4.3: 3-D PLOT FOR THE FOUR EXPERIMENTAL RESPONSES AS A FUNCTION OF DD AND T. (a) CROSSLINK DENSITY, (b) SOL FRACTION, (c) GEL FRACTION AND (d) SULFUR CONTENT.	72
FIGURE 4.4: VALIDATION EXPERIMENT RESULTS WITHIN THE MODELS ERROR BARS AT 99 % OF CONFIDENCE LEVEL.	74
FIGURE 5.1: SCHEMATIC OF THE SCREW CONFIGURATION.	79
FIGURE 5.2: NORMAL PROBABILITY PLOT OF RESIDUALS FOR (a) $\eta^*$ , (b) CD, (c) GF, (d) TS, (e) M100 AND (f) Eb.	88
FIGURE 5.3: POWER LAW FITTING EXAMPLES ON SAMPLES (a) E1, (b) E12 AND (c) C4 CORRESPONDING TO TABLE 5.2.	90
FIGURE 5.4: NORMALIZED GEL FRACTION AS A FUNCTION OF NORMALIZED CROSSLINK DENSITY COMPARED TO THE HORIKX FUNCTION.	91

FIGURE 5.5: RESPONSES SURFACES OF (a) $\eta^*$ , (b) CD, (c) GF, (d) M100, (e) TS AND (f) Eb AS A FUNCTION OF T AND US AT HIGHEST VALUE OF SS (250 RPM) AND MIDDLE VALUE OF FR (6 g/min).	94
FIGURE 5.6: RESULTS OF VALIDATION EXPERIMENTS WITH THE MODELS ERROR BARS AT 95 % CONFIDENCE LEVEL.	96
FIGURE 5.7: CONTOUR PLOTS OF (a) $\eta^*$ , (b) CD, (c) GF, (d) M100, (e) TS AND (f) Eb AS A FUNCTION OF T AND US FIXING SS=250 RPM AND FR = 6 g/min.	97
FIGURE 6.1: NORMAL PROBABILITY PLOT OF RESIDUALS.	113
FIGURE 6.2: 3-D PLOT FOR $\eta^*$ AS A FUNCTION OF DBT AND Gc, FIXING OD AT (a) 0.1, (b) 0.55 AND (c) 1 AU.	115
FIGURE 6.3: 3-D PLOT FOR $\eta^*$ AS A FUNCTION OF OD AND DBT, FIXING Gc AT (a) 10 (b) 15 AND (c) 20 g/l.	116
FIGURE 6.4: NORMALIZED GEL FRACTION AS A FUNCTION OF NORMALIZED CROSSLINK DENSITY COMPARED TO THE HORIKX FUNCTIONS.	117
FIGURE 6.5: CONTROL1 AND VGNR ARISA PROFILES.	119
FIGURE 6.6: <i>G. DESULFURICANS</i> 213E ARISA PROFILE.	120
FIGURE 6.7: ARISA PROFILES OF THE EXPERIMENTS E3, E4, E5 AND E6 IN TABLE 6.2.	120
FIGURE 7.1: SCHEMATIC OF THE BIOREACTOR.	125
FIGURE 7.2: (a) MAXIMUM TORQUE ( $M_H$ ) AND MINIMUM TORQUE ( $M_L$ ), (b) SCORCH TIME ( $T_{s2}$ ) AND OPTIMAL CUTTING TIME ( $T_{95}$ ) FOR THE COMPOUNDS.	131
FIGURE 7.3: CROSSLINK DENSITY OF VULCANIZATES.	133
FIGURE 7.4: (a) MODULI AT 100% (M100) AND AT 300% (M300) OF ELONGATION, (b) TENSILE STRENGTH (TS) AND ELONGATION AT BREAK (Eb) FOR THE VULCANIZED COMPOUNDS.	136
FIGURE 7.5: (a) STORAGE MODULUS ( $G'$ ) AND (b) LOSS TANGENT ( $\tan \delta$ ) OF VULCANIZED COMPOUNDS AS A FUNCTION OF FREQUENCY.	137
FIGURE 7.6: COLE-COLE PLOT FOR VULCANIZED COMPOUNDS.	139



## LIST OF SYMBOLS AND ABBREVIATIONS

6PPD	N-(1,3-Dimethylbutyl)-N'-phenyl-p-phenylenediamine
ANOVA	Analysis of Variance
APA	Advanced Polymer Analyzer
ARISA	Automated Ribosomal Intergenic Spacer Analyses
ASTM	American Society for Testing and Materials
BR	Butadiene Rubber
C	Filler Constant
CBS	N-Cyclohexyl-2-benzothiazole sulfonamide
CCDF	Central Composite Design Faced-Centered
CD	Crosslink Density
<i>D</i>	Overall Desirability Function
DBT	Dibenzothiophene
DD	Diphenyl Disulfide
DD-GTRs	Ground Tire Rubber Treated At Optimal Conditions for Supercritical CO <sub>2</sub> Treatment (DD0-GTR, DD1.5-GTR, DD5-GTR)
D-GTR	Ground Tire Rubber Devulcanized by Ultrasonic Treatment
DOE	Design of Experiments
DVGNR	Vulcanized/Ground Natural Rubber Devulcanized by Biological Treatment
Eb	Elongation at Break
E-GTR	Ground Tire Rubber Extracted by Acetone in Soxhlet Apparatus
EPDM	Ethylene-Propylene Diene Monomer Rubber
FR	Flow Rate
<i>G'</i>	Elastic or Storage Modulus
<i>G''</i>	Viscous or Loss Modulus
Gc	Glucose Concentration
GC-MSD	Gas Chromatography-Mass Spectrometer Detector
GF	Gel Fraction
G-GTR	Ground Tire Rubber Treated at Optimal Conditions of the Biological Treatment
GPC	Gel Permeation Chromatography
GTR	Ground Tire Rubber
IIR	Isobutylene-Isoprene Rubber

IR	Isoprene Rubber, Synthetic
ISO	International Organization for Standardization
K	Number of Factors of the Experimental Design
$K, n$	Empirical Constants for the Power Law Equation
L	Number of Levels of the Experimental Design
LTB	Large the Best
M100	Elastic Modulus at 100 % of Elongation
M300	Elastic Modulus at 300 % of Elongation
MDR	Moving Die Rheometer
$M_H$	Maximum Torque
$M_L$	Minimum Torque
MLR	Multiple Linear Regression
$M_n$	Number Average Molecular Weight
MSM	Minimum Salt Medium
$M_w$	Weight Average Molecular Weight
n	Number of Experiments
$N_A$	Number of Control Samples in the Experimental Design
$N_C$	Number of Central Points in the Experimental Design
NR	Natural Rubber
NTB	Nominal the Best
OD	Optical Density
OTU	Operative Taxonomic Unit
OVAT	One Variable at a Time
P	Pressure
PDI	Polydispersity Index
PRESS	Predicted Sum of Squares
$Q^2$	Coefficient of Determination in Prediction
$R^2$	Coefficient of Determination in Regression
$R^2$ adj	$R^2$ Adjusted for Degrees of Freedom
R-GTR	Revulcanized GTR after Ultrasonic Devulcanization and Compounding
RPA	Rubber Process Analyzer
RSM	Response Surface Methodology
rt	Reaction Time
S.S.	Sum of Squares
SBR	Styrene-Butadiene Rubber



SC	Sulfur Content
scCO <sub>2</sub>	Supercritical CO <sub>2</sub>
SE	Standard Error
SEM	Scanning Electron Microscope
SF	Sol Fraction
SS	Screw Speed
STB	Small the Best
t	Student's t
T	Temperature
t <sub>95</sub>	Optimal Curing Time
tan δ	Loss Angle
TE-GTR	Ground Tire Rubber Devulcanized in Supercritical CO <sub>2</sub> and Extracted by Acetone in Soxhlet apparatus
TGA	Thermogravimetric Analysis
T-GTR	Ground Tire Rubber Devulcanized in Supercritical CO <sub>2</sub> Treatment
TMQ	2,2,4-trimethyl-1,2-dihydroquinoline
TS	Tensile Strength
T <sub>s2</sub>	Scorch Time
US	Ultrasonic Amplitude
US-GTRs	Ground Tire Rubber Treated at Optimal Conditions of Ultrasonic Treatment (US5-GTR, US7.2-GTR, US12-GTR)
$v_f$	Crosslink Density of the Vulcanizate after Devulcanization
VNGR	Vulcanized/Ground Natural Rubber
$W_{GF}$	Weight of Dried Sample after Toluene Evaporation
$W_i$	Initial Sample Weight for Crosslink and Sol/Gel Fraction Measurements
$w_i$	Weights in the Overall Desirability Function in Derringer and Suich's approach
$W_{SF}$	Weight of Toluene Extract after Toluene Evaporation
wt%	Weight percent
X-GTRs	Ground Tire Rubber Treated at the Optimal Conditions for Each Technology (DD0-GTR; DD1.5-GTR; DD5-GTR; US5-GTR; US7.2-GTR; US12-GTR; G-GTR)
$x_i - x_j$	Variables
z	Standardized Parameter Representing Distance of Estimated Response from its Target

$\beta$	Coefficients
$\nu_f$	Crosslinking Index (Average number of crosslinks per chain in the remaining network after devulcanization treatment)
$\nu_i$	Crosslinking Index (Average number of crosslinks per chain in the network of the untreated vulcanizate)
$\Delta M$	Difference between Maximum and Minimum Torque
$\varepsilon$	Residuals
$\eta^*$	Complex Viscosity
$\nu_e$	Crosslink Density
$\nu_i$	Crosslink Density of the Untreated Vulcanizates
$\nu_r$	Polymer Volume Fraction in Vulcanizates
$\nu_{ro}$	Volume Fraction in Analogous Filled Vulcanizates (with respect to $\nu_r$ )
$\tau$	Constant in Kim and Lin's Desirability Function Approach
$\tau'$	Function of $\tau$
$\tau^{max}$	Maximum Value for $\tau$
$\chi$	Flory-Huggins Interaction Parameter
$\omega$	Angular Frequency
$\phi$	Volume Fraction of Filler in Vulcanizates

# 1 INTRODUCTION AND AIM

---

This chapter introduces the topic of the present thesis work: the problem of waste rubber, in particular End-of-Life Tires and possible solutions.

---

## 1.1 INTRODUCTION

Polymers (from the Greek words “poly” = many and “meroi” = units) are high molecular weight macromolecules consisting of up to millions of repeated linked units. Generally, polymers can be either natural, synthetic or artificial and can be divided into two different categories: thermoplastic and thermosetting. The former, such as poly(methyl methacrylate) (PMMA), polyethylene (PE) or polystyrene (PS) represent polymers which are soft and easily formable above their melting temperature and turn to a solid state decreasing the temperature. The latter, such epoxy resins (EP), polyurethane (PUR) or vulcanized rubber are generally liquid and soft materials at their initial stage and cure with the temperature, through a chemical process that generates a cross-link network among the polymer chains. Since this three-dimensional network generally involves covalent bonds, or ionic bonds the thermosetting materials cannot be softened by increasing the temperature. For this reason, while the thermoplastic materials are easily recyclable, just by a thermal treatment that allows remolding, for the thermosetting ones it is necessary to break the infusible three-dimensional network [1].

Rubber materials are viscoelastic polymers able to withstand multiple high elastic deformations and recover their initial state. They can be divided in two different categories: natural rubber (NR) and synthetic rubber.

NR is the only natural elastomer available which is a coagulated or precipitated product extracted as latex (milky exudations) from barks of trees (i.e. *Hevea brasiliensis*) belonging to several botanical families which grow mostly in the tropical zone. All other elastomers are synthetic and must be prepared by polymerization or modification [2,3].

In order to improve the mechanical properties, especially increasing elasticity and resistance to the deformation required for tires and industrial applications, rubber is generally vulcanized (or cured) by heating between 120 °C and 200 °C in presence of a vulcanizing (or curing) agent (usually sulfur or peroxides). The most common and used vulcanization (or curing) system for the

industry has been attributed to Charles Goodyear and it was first used in Springfield, Massachusetts, in 1841. This chemical process acts generating three-dimensional sulfur crosslinks between polymer chains (Figure 1.1), modifying the mechanical properties of the rubber with elongation decreasing and resistance to deformation increasing [4,5].

The long rubber molecules (molecular weight usually between 100000 and 500000 Da) become linked together with junctures (crosslinks) spaced along the polymeric chains, with the average distance between junctures corresponding to a molecular weight between crosslinks of about 4000 to 10000 Da. As a result of this network formation, the rubber becomes essentially insoluble in any solvent and it cannot be processed by any means which requires it to flow, e.g., in a mixer, in an extruder, on a mill, on a calender, or during shaping, forming, or molding [4].

Initially, vulcanization was accomplished by using elemental sulfur at a concentration of 8 parts per 100 parts of rubber (phr). It required 5 hours at 140 °C. The addition of zinc oxide and curing agents has reduced the time to few minutes. As a result, vulcanization by sulfur without accelerators is no longer employed [4].

Depending on the formulation of the rubber recipe and on the vulcanization parameters applied, both polysulfidic, disulfidic and monosulfidic cross-links are formed [6].

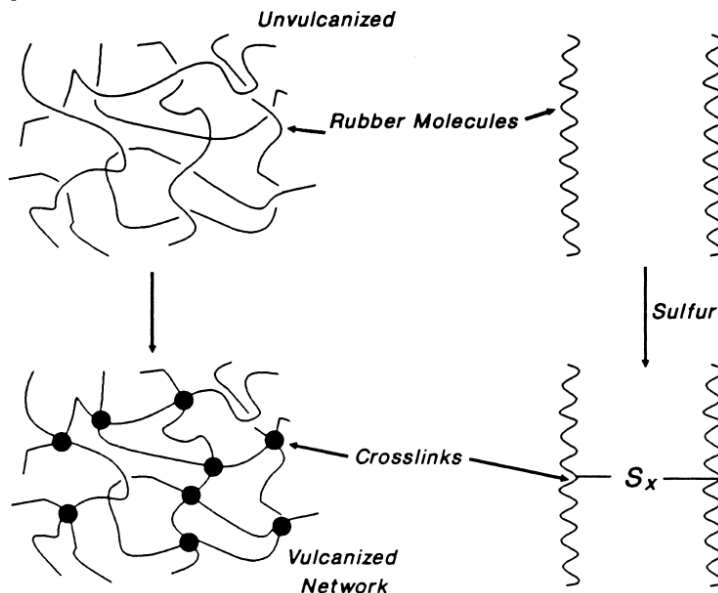


FIGURE 1.1: THREE-DIMENSIONAL CROSSLINK NETWORK FORMATION (ADAPTED FROM REF. [4]).

In general the crosslink density, which is a measure of the extent of vulcanization, increases with curing time. The properties of the resulting materials are a function of the crosslink density, as shown in Figure 1.2.

Static modulus (equilibrium modulus or slow-strain-rate modulus) increases with vulcanization to a greater extent than does the dynamic modulus. Dynamic modulus (measured under sinusoidal, small strain at a frequency of 1–100 Hz) is a composite of viscous and elastic behavior, whereas static modulus is largely a measure of only the elastic component of rheological behavior. Hysteresis is reduced with increasing crosslink formation. Hysteresis is the ratio of the rate-dependent or viscous component to the elastic component of deformation resistance. It is also a measure of deformation energy that is not stored, but that is converted to heat. Tear strength fatigue life and toughness are related to the breaking energy. Values of these properties increase with small amounts of crosslinking, but they are reduced by further crosslink formation. Properties related to the energy-to-break increase with increases in both the number of network chains and hysteresis. Since hysteresis decreases as more network chains are developed, the energy-to-break related properties are maximized at some intermediate crosslink density [4,5].

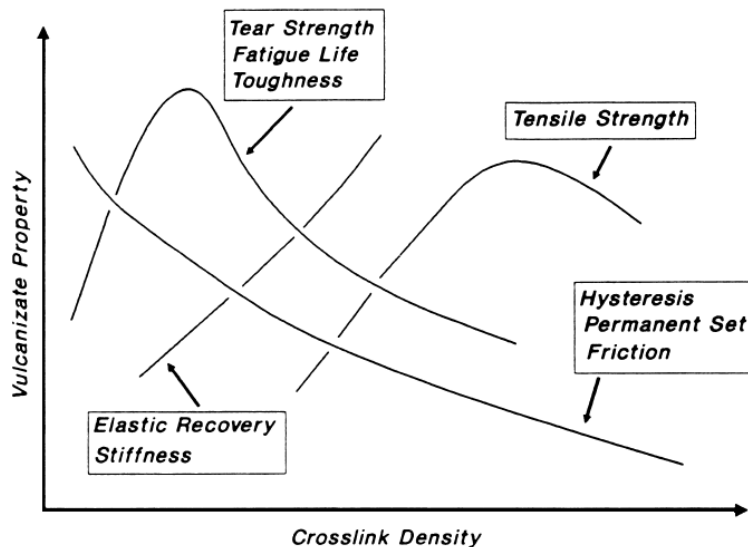


FIGURE 1.2: EFFECT OF CROSSLINK DENSITY ON PROPERTIES OF VULCANIZATES  
(ADAPTED FROM REF [4]).

The three-dimensional network, required to adjust the mechanical properties, represents a stable, solid, insoluble and infusible network resulting difficult to recycle and reprocess. Therefore, when vulcanized elastomeric products are no longer sufficiently safe or efficient to be used, they become a waste, hard to reuse and recycle. These materials cannot be easily and naturally decomposed and therefore represent a challenging issue. Moreover, these waste materials may cause severe environmental problems if not correctly disposed [1,7].

Several are the sources of waste rubber, however End-of-Life Tires (ELTs) are the most representative ones. In the last decades, the generation of ELTs is increasing and represents a main issue. According to a 2008 survey [8], approximately 900 million ELTs are generated each year around the world. When ELTs are disposed in landfill, they consume soil and natural resources, spoiling the ground and surface waters. They also represent threats for public health and safety because of the risk for diseases and fires that may release toxic chemicals into the air. Several are the reasons for the application of tire and rubber recycling on a small scale, such as the increasing quality requirements of rubber products and the high costs for the reclaiming processes. However, over the last 15 years recovery rates for ELTs have increased in Europe, Japan and the United States. Japan started recycling programs even earlier. In Europe, the directive 2006/53/CE concerning the End of Life Vehicles obliges to recover 85 % of scrap cars since 2006. At the same time, the cost of recycling for the consumer of ELTs has decreased in some areas due to both increased efficiency in management structures and new recovery routes.

ELTs and in general tires, are complex systems with multiple constituents and a large amount of raw materials. Indeed, they contain different kind of rubber compounds, reinforcing fillers such as several types of carbon black, clay and silica and a variety of chemicals and minerals. Several chemicals are also added as antidegradants (i.e. antioxidants, antiozonants) to protect tires against deterioration by ozone, oxygen and heat or as accelerators during vulcanization process. Tire also contain several types of textile (i.e. polyester and nylon) and steel cables, added as a reinforcement [9-11].

ELTs can be mainly recovered through two ways: the recovery of material and the recovery of energy [1,7,12,13]. Their derived products can be legitimately recognized as a valuable secondary raw material or as an alternative fuel. Indeed, the high calorific value of ELTs, close to the one of coal [12], allows their use as a

source of energy in paper mills, cement works or in thermoelectric power plants. The recovery of material is more difficult. It requires specific treatments with the resulting material having worse features than the starting one. Retreading of the whole tire is the easiest method for the recovery of tires as material. Other methods that allow reusing rubber from ELTs in several civil engineering applications and for composite materials require a strong size-reduction and the separation of metallic and textile materials. Therefore, most of the recovery techniques involve a grinding process leading to a significant reduction of tire dimensions. During the grinding process, temperature can be lower than the glass transition temperature (i.e. cryogenic grinding) of the polymers in the tires or next to the room temperature (dry ambient grinding or wet ambient grinding). The ground tire rubber (GTR) having dimension less than 2 mm can be widely reused as a filler in some applications (civil buildings, mulching materials, etc.), but its introduction is more difficult in systems that have to withstand high dynamic stresses. Furthermore, the GTR is not suitable to be processed in new compounds due to the presence of the sulfur crosslink network that prevents the full compatibility with raw rubber leading to weak adhesion and deterioration of the final properties of the revulcanizates. As a result, it can be used as a filler and added just in small amount only after a strong reduction in size [14,15].

In order to increase the compatibility with raw rubber, ELTs must be devulcanized by selectively breaking the three-dimensional crosslink network or should undergo some surface modification. In order to break the sulfur crosslink network, several chemical, thermo-mechanical, physical and biological methods have been studied [1,7,12,13]. Most of the chemical techniques are dangerous for health and environment since they require reactions that involve organic compounds, oils and solvents. On the other hand, thermal and mechanical techniques require large amount of energy and are generally expensive. A microbial desulfurization was suggested over the last years as an alternative with respect to the methods requiring hazardous chemicals or energy consuming operating conditions.

## 1.2 SCOPE OF THE THESIS WORK

Supercritical fluid, ultrasonic and biological devulcanization technologies were chosen as focus of the present thesis work. These three devulcanization technologies were primarily chosen considering their impact on the environment and in particular their tendency to minimize the use of solvents, chemicals or energy.

The supercritical carbon dioxide devulcanization was first proposed by Kojima et al. [16]. In this technique the supercritical CO<sub>2</sub> (scCO<sub>2</sub>) has been used as a reaction medium for some devulcanizing agents, in particular diphenyl disulfide (DD). Supercritical fluids, in particular scCO<sub>2</sub>, show the ability to permeate into polymers and represent excellent *green* solvents for these materials [17]. This technique minimizes the use of swelling agents, generally required for chemical techniques and leads to a bulk treatment. Nevertheless, it requires both energy to reach supercritical fluids conditions and chemicals as devulcanizing agents. As just mentioned, this technology is based on a well-studied process in scientific and patent literature [16,18], however it has never been modeled and optimized so far.

The ultrasonic devulcanization, which has been widely investigated and patented by Isayev et al. [7], is carried out without involving any chemical, since ultrasounds can generate cavitation leading to the rupture of three-dimensional network in the rubber matrix within a time of several seconds. The incorporation of an ultrasonic device in extruders makes this process continuous. This technology avoids the usage of any devulcanizing or swelling agents, generally required for chemical techniques. It is a continuous process that allows to treat large amount of material and it is a bulk treatment. However, this technique requires energy to reach the treatment temperatures and to generate the ultrasonic waves. The ultrasonic technology has been extensively studied, however a coupled system ultrasonic/twin-screw extrusion has never been optimized for the devulcanization of tire rubber.

The third considered devulcanization technology is the biological one, involving microorganism strains able to metabolize the sulfur present in the rubber matrix. Just few microorganisms were found with the ability to devulcanize waste rubber and GTR, due to their complex structure.

This process was reported in 1997 by Romine and Romine [19]. They used *Sulfolobus acidocaldarius* on GTR and proposed a “4s”-like mechanism for the desulfurization. Other studies were successively carried out on other microorganisms. One of the most efficient chemoorganotroph bacterium described in literature is *Gordonia desulfuricans* 213E. It was patented by Christofi et al. in 2006 [20]. This bacterium is reported to be able to reduce the content of sulfur between 23 % and 35 %.

Out of the known technologies, the biological one represents the *greenest* devulcanization technique since no swelling or chemical devulcanizing agents are



required and it is a low energy consumption technique. It has been proven that this process is highly selective towards sulfur, however the treatment is limited to the surface and has low reaction yields. Therefore long treatment time is generally required. The bio-devulcanization has already been patented and studied, however this technology has never been optimized considering the influence of bacterial growth parameters on the devulcanization.

The aim of the present thesis work is to extensively investigate these three devulcanization technologies, to gain important information regarding the devulcanization mechanism and the influencing conditions and to provide a comparison among the optimal conditions on a commercial GTR.

## REFERENCES

1. B. Adhikari, D. De, S. Maiti; Reclamation and recycling of waste rubber. *Progress in Polymer Science* 2000;25:909–948.
2. S. Kohjiya, Y. Ikeda; *Chemistry, manufacture and applications of natural rubber*, Elsevier, 2014.
3. K. Rose, A. Steinbuchel; Biodegradation of natural rubber and related compounds: Recent insights into a hardly understood catabolic capability of microorganisms. *Applied and Environmental Microbiology* 2005;71:2803-2812.
4. A.Y. Coran; In J.E. Mark, B. Erman, M. Roland, editors. *The science and technology of rubber*, 4th ed., Boston: Elsevier Academic Press, 2014, p. 337-381.
5. C.P. Rader; In K.C. Baranwal, H.L. Stephens, editors. *Basic elastomer technology*, Akron: The rubber Division American Chemical Society, 2001, p.165-190.
6. O. Holst, B. Stenberg, M. Christiansson; Biotechnological possibilities for waste tyre-rubber treatment. *Biodegradation* 1998,9:301-310.
7. A.I. Isayev. In J.E. Mark, B. Erman, M. Roland, editors. *The science and technology of rubber*, 4th ed., Boston: Elsevier Academic Press, 2014, p. 697-764.
8. *Managing End-of-Life Tires*, The World Business Council for Sustainable Development (WBCSD), 2008.
9. A. Evans, R. Evans; *The composition of a tyre: Typical components* EER Limited, The Waste & Resources Action Programme, 2006.
10. B.E. Lindenmuth; *The pneumatic tire*. Akron: US Department of Transportation, 2005.

11. W.H. Waddell, R.S. Bhakuni, W.W. Barbin, P.H. Sandstrom; Pneumatic tire compounding, The Goodyear Tire & Rubber Company, 1990.
12. T. Amari, N.J. Themelis, I.K. Wernick; Resource recovery from used rubber tires. *Resource Policy* 1999;25:179-188.
13. V.V. Rajan, W.K. Dierkes, R. Joseph, J.W.M. Noordermeer; Science and technology of rubber reclamation with special attention to NR-based waste latex products. *Progress in Polymer Science* 2006;31:811-834.
14. S. Li, J. Lamminmäki, K. Hanhi; Effect of ground rubber powder on properties of natural rubber. *Macromolecular Symposia* 2004;216:209-216.
15. A.K. Naskar, S.K. De, A.K. Bhowmick, P.K. Pramanik, R. Mukhopadhyay; Characterization of ground rubber tire and its effect on natural rubber compound. *Rubber Chemistry and Technology* 2000;73:902-911.
16. M. Kojima, K. Ogawa, H. Mizushima, M. Tosaka, S. Kohjiya, Y. Ikeda; Devulcanization of sulfur-cured isoprene rubber in supercritical carbon dioxide. *Rubber Chemistry and Technology* 2003;76:957-968.
17. M. Kojima, S. Kohjiya, Y. Ikeda; Role of supercritical carbon dioxide for selective impregnation of decrosslinking reagent into isoprene rubber vulcanizate. *Polymer* 2005;46:2016-2019.
18. M.J. Forrest, L. W. Lloyd; WO 2011158024 A1, 2011.
19. R.A. Romine, M.F. Romine; Rubbercycle: A bioprocess for surface modification of waste tyre rubber. *Polymer Degradation and Stability* 1998;59:353-358
20. N. Christofi, J. Geoffrey, D. Edward; US 7737191 B2, 2010.

## 2 LITERATURE SURVEY AND BACKGROUND

---

This chapter gives a comprehensive overview of the available methods for the reclaiming and recycling of waste rubber: Particular attention is given to the devulcanization methods experimentally investigated in the present thesis work.

---

### 2.1 RECLAIMING AND RECYCLING

#### 2.1.1 GENERAL CONSIDERATIONS

Waste rubber represents a potential *green* source of material, replacing the raw natural and synthetic rubber. Recycling of vulcanized rubber and tires represents a main concern to the industrial world. The more stringent environmental regulations and the fluctuating price of raw material have become driving forces for the development of several innovative technologies for rubber reclaiming.

Reclaiming is a procedure in which scrap tires or rubber are converted, using mechanical or thermal energy, chemicals or microorganisms, into a state in which they can be mixed, reprocessed and vulcanized. However, the rubber recovery from such materials is not an easy matter due to their complex structure and to the presence of three-dimensional chemical crosslinks.

Since the formation of this network is a non-reversible chemical process, many studies have focused their attention on this issue over the last decades. Generally, the reclaiming approaches can be divided into two categories. The first approach involves a grinding process leading to a reduction of rubber particle size without a significant rupture of the chemical bonds. The second approach that attempts to devulcanize the waste rubber by breaking the three-dimensional network involves mechanical, chemical, biological, microwaves and ultrasonic technologies [1-3].

#### 2.1.2 GRINDING

Reuse of waste vulcanized rubber and ELTs generally requires reduction of particles and therefore a grinding process. This method was invented by Goodyear more than 150 years ago [4]. Three different grinding techniques can be identified according to their processing conditions: ambient grinding,

cryogenic grinding and wet-ambient grinding. However, the first two methods are the most employed.

A primary reduction of whole tires down to 5x5 cm<sup>2</sup> or 2.5x2.5 cm<sup>2</sup> chips is done by using the guillotine, the cracker mill, the high impact hammer mill and the rotary shear shredder. Then, a magnetic separator and a fiber separator (cyclone) remove all the steel and polyester fragments. After that, the material can be further reduced by using ambient ground mill or can be ground into fine particles while is being frozen by a cryogenic grinding.

The cryo-grinding process can produce much finer particles between 30 and 100 mesh. However, this process requires a large amount of liquid nitrogen to cool the sample during the size reduction.

The ambient grinding is often used as a conventional inexpensive method to produce 10 to 30-mesh material and relatively large crumbs. However, ambient grinding produces an irregular shaped particle and results in higher oxidation [2]. The lowest particle limit for the process is the production of 40-mesh material. The process, however, generates a significant amount of heat. Excessive heat can induce degradation and if not properly cooled combustion can occur upon storage [1].

It has been reported that the addition at 5-10 phr in new compounds of fine GTR obtained from the cryogenic grinding leads to better properties than the one obtained from ambient grinding. Although the nature of surface in cryogenically ground material facilitates the ventilation of trapped air, reducing the tendency for cure blistering in rubber products, providing better flow characteristics than ambient ground material, the mechanical properties of rubber compounds, even if containing this cryogenically GTR, worsen with the increase of content and of particle dimensions [2].

### 2.1.3 THERMO-MECHANICAL AND MECHANO-CHEMICAL METHODS

Mechanical and thermo-mechanical techniques consist of non-selective processes based on thermal and mechanical degradation due to high temperature and mechanical shearing. The differences in bond energies (Table 2.1) between C-C, C-S and S-S bonds are very small and hence unselective cleavage may occur under stress and heat.

These methods can be implemented by adding and mixing several reclaiming agents, solvents, plasticizers, oils, or rubber previously devulcanized in order to improve the treatment [2].

TABLE 2.1: DISSOCIATION ENERGY OF BONDS IN VULCANIZED RUBBER [5].

Bond Type	Dissociation energy, kcal/mole
alkyl-C-alkyl	80
alkyl-C-S-C-alkyl	74
alkyl-C-S-S-C-alkyl	54
alkyl-C-S <sub>n</sub> -S <sub>m</sub> -C-alkyl	34

## 2.1.3.1 MECHANO-CHEMICAL METHODS

Usually chemical reclaiming agents are used in combination with a mechanical force applied to the rubber powder in air atmosphere and at room temperature. The most common reclaiming agents used in combination with the mechanical processes were described by Rajan et al. [3] and are listed in Figure 2.1. These reclaiming agents show ability to act as radical acceptors and hinder radical formation on the rubber chain. An often proposed reaction mechanism is the opening of crosslinks or the scission of the main chain by heat or shearing force and its reaction with disulfides or thiols, which prevent the recombination.

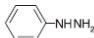

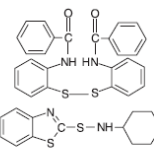
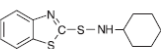
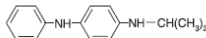
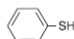
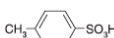
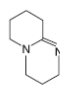
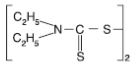
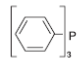
No.	Chemical name/abbreviation	Reclaiming accelerator	Reclaiming catalyst
1	Peroxide-methyl halides	ROOR	Me <sub>n</sub> X <sub>m</sub>
2	Phenyl hydrazine-ferrous chloride (PH-FeCl <sub>2</sub> )		FeCl <sub>2</sub> ·4H <sub>2</sub> O
3	Tributylamine-cuprous chloride (TBA-CuCl)	( <i>n</i> -C <sub>4</sub> H <sub>9</sub> ) <sub>3</sub> N	Cu <sub>2</sub> Cl <sub>2</sub>
4	Dixylyldisulfide		
5	2,2'-Dibenzamidodiphenyl disulfide		
6	<i>N</i> -cyclohexylbenzothiazole-2-sulfenamide (CBS)		
7	<i>N</i> -isopropyl- <i>N'</i> -phenyl- <i>p</i> -phenylenediamine (IPPD)		
8	Thiophenol- <i>n</i> -butylamine (TP-BA)		<i>n</i> -BuNH <sub>2</sub>
9	Toluene sulfonic acid-1,8-diazabicyclo 5.4.0]undec-7-ene (TS-DBU)		
10	Tetraethylthiuramdisulfide-triphenyl phosphine (TETD-TTP)		

FIGURE 2.1: RECLAIMING AGENTS USED IN MECHANO-CHEMICAL METHODS (ADAPTED FROM REF.[3]).

#### 2.1.3.2 PAN-MILL METHOD

In this procedure, the devulcanization is carried out in a pan-mill mechano-chemical reactor. The pan-mill equipment was designed for solid state mechano-chemical reactions of polymers. Theoretical analysis demonstrated that this equipment can exert a strong squeezing force in the normal direction and a shearing force in both radial and tangential directions on milled materials, functioning like pairs of three-dimensional scissors [6].

#### 2.1.3.3 MIXING MILL WITH CHEMICALS ADDITION

Grigoryeva et al. [7] used a mechanical procedure followed by a thermal treatment. GTR and ingredients of devulcanizing mixture (industrial processing oil, rosin, mineral rubber and phthalic anhydride) were mixed by rolls at 50 °C for 20 min, without pre-swelling GTR with processing oil. Then, the obtained mixture was subjected to thermal heating at 130 °C for 0-6 hours in an oven. In another test series, the GTR was first swollen in industrial processing oil (mixture of naphthenic hydrocarbons) and then treated.

Adhikari and coworkers [2] have developed a simple process, involving a vegetable product, which is ecofriendly and renewable resource material (RRM). The major constituent of RRM is diallyl disulfide. Other constituents of RRM are different disulfides, monosulfides, polysulfides and thiol compounds. Vulcanized and aged ground rubber of known composition was milled in a two roll mixing mill with simultaneous addition of the RRM and spindle oil or diallyl disulfide and spindle oil separately [2]. Other authors employed benzoic acid [8] or thiuram disulfides, such as tetrabenzyl thiuram disulfide [9]. For instance, Mandal et al. devulcanized GTR mixing 2 wt% of tetrabenzyl thiuram disulfide and spindle oil with powder rubber. The mixture was then mechanically milled in an open two-roll mill for 40 min close to room temperature [9].

#### 2.1.3.4 TRELLEBRORG PROCESS

This process is realized in a powder mixer at room (or slightly higher) temperature, where the cryogenically ground rubber is mixed with phenyl hydrazine-methyl halide or diphenyl guanidine [2].

#### 2.1.3.5 DE-LINK PROCESS

Ground rubber is mixed in a two-roll mill at a temperature below 50 °C with a chemical mixture prepared from zinc salt of dimethyldithiocarbamate and mercaptobenzothiazole with stearic acid, sulfur and zinc oxide dispersed in diols.

Tetramethyl thiuram disulfide can be also used. The number of crosslinks can decrease by a factor of two. The application of this technology for devulcanization of synthetic rubber is more difficult than NR [2,3].

#### 2.1.3.6 SWELLING IN BENZENE WITH SULFOXIDE

Vulcanized NR is swollen in benzene at room temperature in presence of a sulfoxide compound like dimethyl sulfoxide, di-*n*-propyl sulfoxide or a mixture of these with thiophenol, methyl iodide or *n*-butyl amine during a mechano-chemical process in a mill. The process generates low sol fraction and selective crosslink scission, but is extremely toxic. NR is more attacked by this treatment than synthetic rubber [2,3].

#### 2.1.4 CHEMICAL METHODS

The majority of the devulcanization techniques focused on the use of chemical reagents. Several organic and inorganic chemicals have been employed for this purpose. The devulcanization reactions are complex and have been investigated by several studies. However, depending on the reagent type, these reactions can occur by main chain degradation or selectively, by breaking the crosslink network. The most employed reagents belong to disulfides, mercaptans and thiols acting at high temperatures. These chemicals can initiate the breakdown of sulfur crosslinks and interact with radicals formed during the degradation of rubber [2,3]. The most important techniques will now be described in more detail.

##### 2.1.4.1 ORGANIC HYDROPEROXIDES

Organic hydroperoxides act by opening the sulfur crosslinks through an oxidation reaction [3] (Figure 2.2).

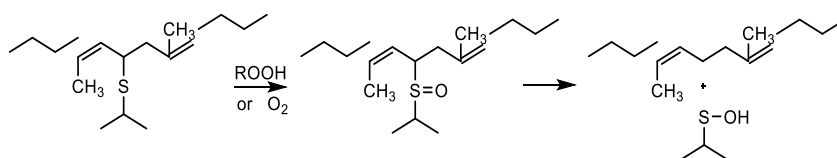


FIGURE 2.2: ORGANIC HYDROPEROXIDES REACTION MECHANISM WITH THE SULFUR CROSSLINKS (ADAPTED FROM REF.[3]).

#### 2.1.4.2 THIOLS AND DISULFIDES

Thiols and disulfides can initiate the breakdown of sulfur crosslinks and the degradation of the rubber chain (Figure 2.3 and Figure 2.4) and they can interact with radicals formed during the degradation of rubber.

Thiols in combination with organic bases are able to selectively break the sulfur crosslinks, e.g., hexanethiol can break the di- and polysulfidic crosslinks [10]; 2-propane thiol in combination with piperidine as organic base can selectively break the polysulfidic crosslinks in a nucleophilic reaction [2]. In this case, the reagents give a complex combination as a piperidinium propane-2-thiolate ion pair, in which the sulfur atom has enhanced nucleophilic properties, able to cleave polysulfidic crosslinks at 20 °C. Polysulfidic crosslinks cleavage is faster than disulfidic ones due to the  $p\pi-d\pi$  delocalization of the  $\sigma$ -electron pair [11] (Figure 2.5).

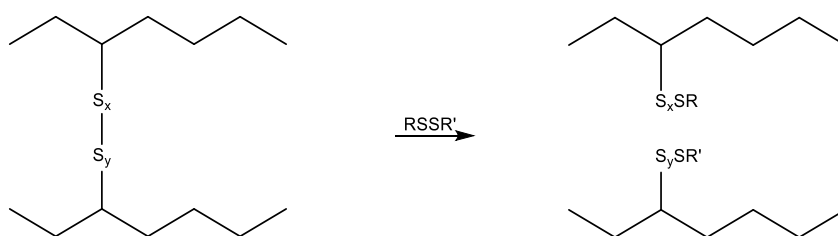


FIGURE 2.3: OPENING OF SULFUR CROSSLINKS BY REARRANGEMENT.

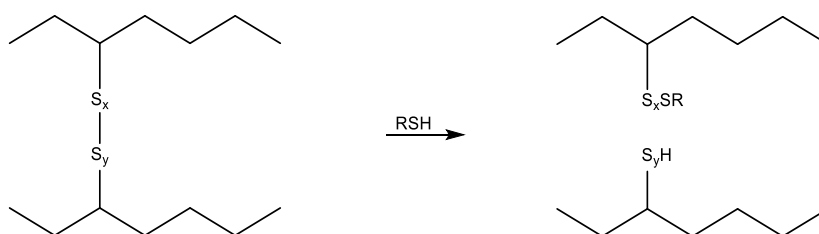


FIGURE 2.4: OPENING OF SULFUR CROSSLINKS BY SUBSTITUTION.

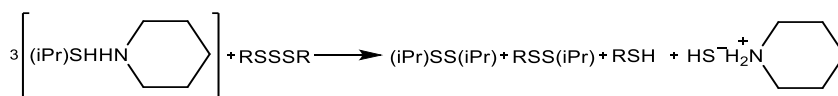


FIGURE 2.5: REACTION MECHANISM BETWEEN 2-PROPANE THIOL/PIPERIDINE SYSTEM AND POLYSULFIDIC CROSSLINKS (ADAPTED FROM REF.[3]).



## 2.1.4.3 TRIPHENYL PHOSPHINE AND PHOSPHITES

The triphenyl phosphine selectively reacts with the sulfur crosslinks as reported in Figure 2.6 [2,3,12].

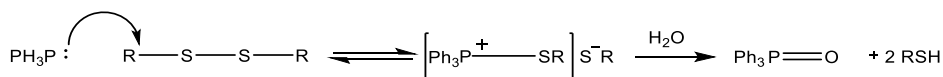


FIGURE 2.6: TRIPHENYL PHOSPHINE CLEAVAGE REACTION MECHANISMS OF DI- AND POLYSULFIDIC CROSSLINKS (ADAPTED FROM REF.[3]).

Trialkyl phosphites and sodium dibutyl phosphite and have been studied for the di- and polysulfidic crosslinks rupture and they act as reported in Figure 2.7 and Figure 2.8 [12,13].

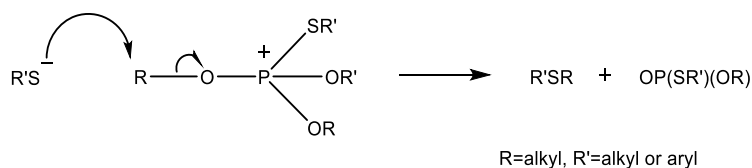
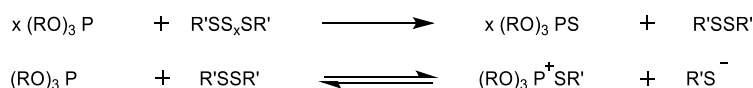


FIGURE 2.7: CLEAVAGE OF DI- AND POLYSULFIDIC CROSSLINKS BY TRIALKYL PHOSPHITES (ADAPTED FROM REF.[2]).



FIGURE 2.8: CLEAVAGE OF DI- AND POLYSULFIDIC CROSSLINKS BY SODIUM DIBUTYL PHOSPHITE, (ADAPTED FROM REF.[3]).

## 2.1.4.4 LITHIUM ALUMINUM HYDRIDE

Lithium aluminum hydride (LAH) reacts with di- and polysulfidic crosslinks with a weak acid. Terminal sulfidic groups are converted into thiols, while the interior groups are converted to hydrogen sulfide (Figure 2.9) [2,3].



FIGURE 2.9: REACTION OF LITHIUM ALUMINUM HYDRIDE WITH DI- AND POLYSULFIDIC CROSSLINKS (ADAPTED FROM REF.[2]).

#### 2.1.4.5 METHYL IODIDE

Methyl iodide reacts very slowly with disulfidic crosslinks. The allylic sulfides easily break down to trimethyl sulfonium salts (Figure 2.10).

The reaction can be catalyzed by mercury iodide, even with monosulfidic crosslinks [2,3].

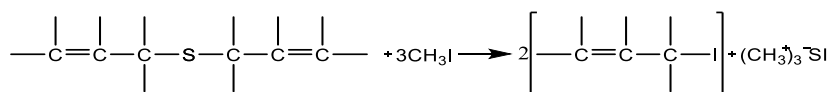


FIGURE 2.10: REACTION MECHANISM OF METHYL IODIDE (ADAPTED FROM REF.[2]).

#### 2.1.4.6 PHENYL HYDRAZINE AND PEROXIDES (MAIN CHAIN DEGRADATION)

In this process, phenyl hydrazine-iron (II) chloride system is employed for the oxidative degradation of the rubber chain. In this process, the selectivity is low and it leads to the main-chain scission. The phenyl hydrazine is the main reagent, while FeCl<sub>2</sub> acts as a catalyst. The reactions that take place during this process are shown in Figure 2.11 and Figure 2.12 [3,14].

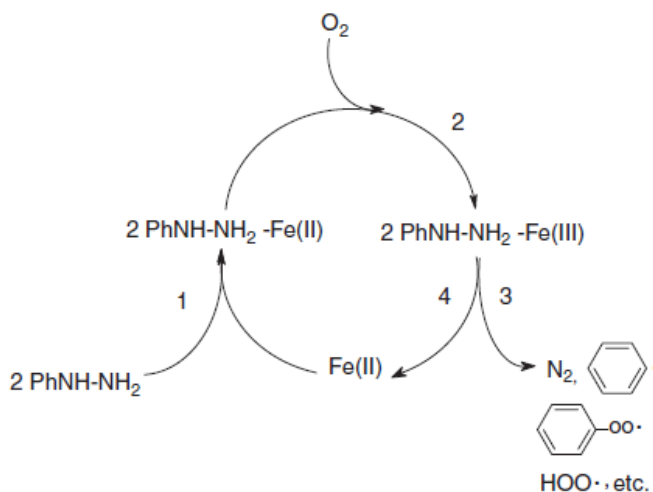


FIGURE 2.11: OXIDATION MECHANISM FOR PHENYL HYDRAZINE-IRON (II) CHLORIDE SYSTEM (ADAPTED FROM REF.[3]).

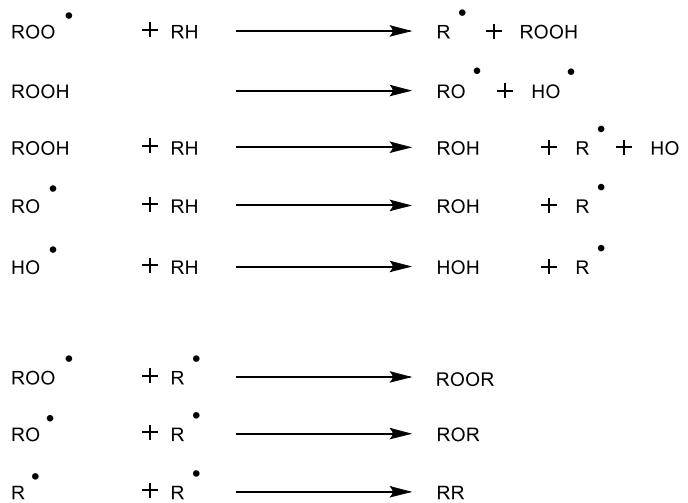


FIGURE 2.12: RUBBER CHAIN OXIDATION MECHANISM BY RADICALS (ADAPTED FROM REF.[3]).

Peroxides decompose in presence of transition metals, generating free RO-radicals, which can give degradation reactions (Figure 2.13) [3,15].

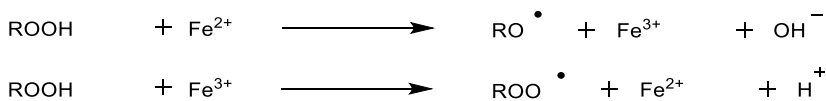


FIGURE 2.13: DECOMPOSITION OF PEROXIDES BY IONS OF METALS (ADAPTED FROM REF.[3]).

#### 2.1.4.7 OTHER CHEMICAL METHODS

Tributyl amine used in a mixture with copper (I) chloride can degrade rubber, especially the isoprene rubber [3]. Many other chemicals such as thiocarboxylic acid, alkyl phenol sulfides, 2-Mercaptobenzothiazole [2,3], benzoyl peroxide [16] and thiosalicylic acid [17] have been studied for devulcanization purposes.

#### 2.1.4.8 OZONIZATION

Cataldo et al. [18] used ozone as active agent to cause surface oxidation and functionalization of rubber crumbs. Most researchers agreed that ozone attack is notably a surface reaction, in contrast to thermo-oxidative degradation, which takes place in the entire volume of the polymer specimen. However, for natural rubber, in contrast to synthetic rubber, published data suggest that the ozonization does continue into the bulk of the specimen. The GTR can be deeply oxidized to break up some crosslinks in bulk with enough time ozone exposure [19].

#### 2.1.4.9 SUPERCRITICAL CO<sub>2</sub>

Supercritical fluids are substances at a temperature and pressure above their critical point. At this point, liquid and gas phases do not exist separately but coexist. For this reason, these fluids show properties that are proper of the supercritical phase, different from the ones of either liquids or gases [20].

Density can be easily varied, since small changes in pressure or temperature result in large changes in density. Their viscosities are nearer to the ones of normal gaseous states, but densities and diffusivities are similar to liquids and solubility can be orders of magnitude higher. Due to these properties, they are able to penetrate porous materials as gas and to dissolve materials as a liquid. Since the solvent strength is correlated to the density, it can be manipulated by changing the supercritical conditions [20].

Carbon dioxide and water are the most commonly used supercritical fluids. Figure 2.14 shows a pressure-temperature phase diagram of the CO<sub>2</sub>. The boiling line separates the gas and liquid region and terminates in the critical point, where the liquid and gas coexist in the supercritical phase.

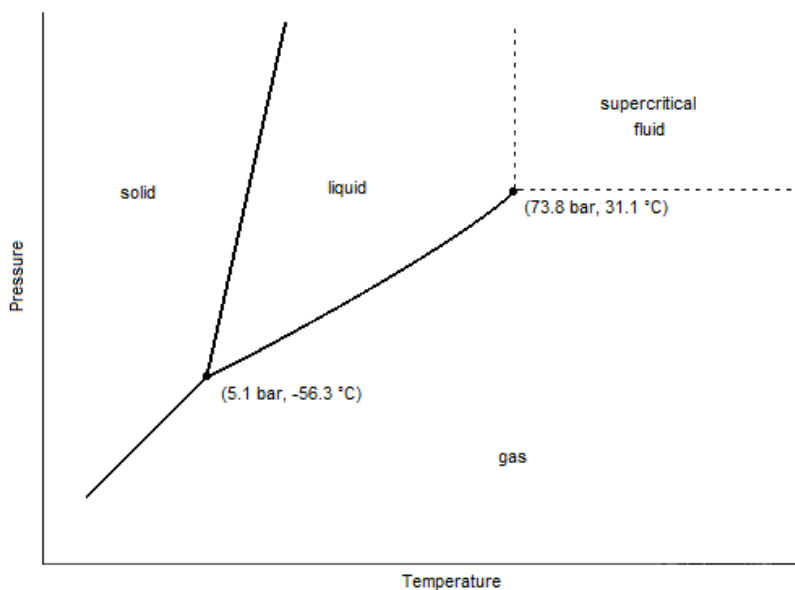


FIGURE 2.14: CO<sub>2</sub> PRESSURE-TEMPERATURE PHASE DIAGRAM.

Below the critical temperature, in the discontinuity two-phase region, as the pressure increases, the gas compresses and eventually condenses into a denser liquid, resulting in a discontinuity (vertical dotted lines in Figure 2.15). This region

is characterized by two phases in equilibrium, consisting of dense liquid and a low-density gas. As the critical temperature is approached (31.1 °C), the densities of the gas and liquid at equilibrium become closer. At the critical point, 31.1 °C (304.25 K) and 7.38 MPa (73.8 bar and 1070 psi), there is no difference in density and the two phases become one supercritical fluid phase. In the region above the critical temperature, a small increase in pressure causes a large increase in density [21].

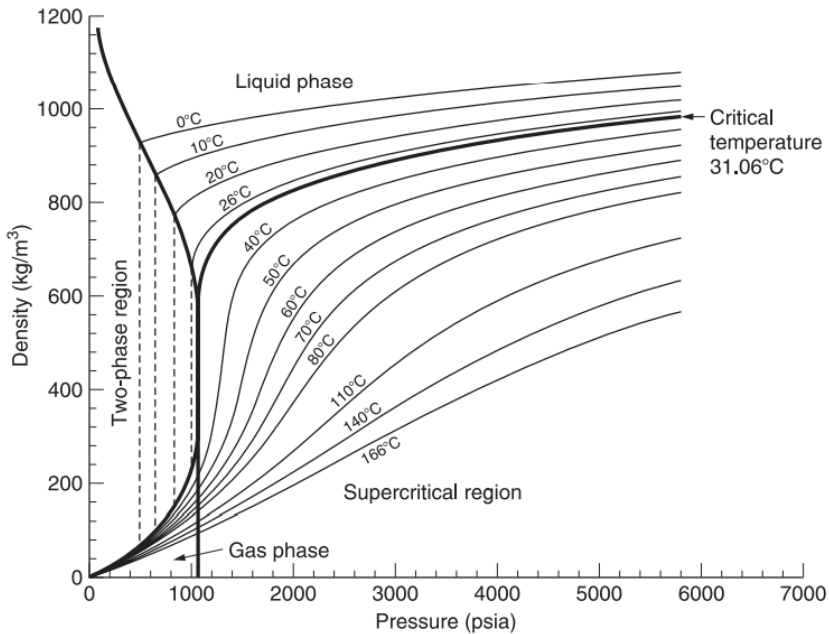


FIGURE 2.15: CO<sub>2</sub> DENSITY-PRESSURE PHASE DIAGRAM (ADAPTED FROM REF. [21]).

Supercritical fluids, in particular scCO<sub>2</sub>, show ability to permeate into polymers and represent excellent solvents for these materials. Therefore, in the last years several researches focused on their possible applications, including polymer blending and composites, polymer modification and polymer foaming [20,22-24]. Other studies investigated the application of supercritical fluids to environmental friendly processes such as treatment of hazardous wastes [25], decomposition and reclaiming of pneumatic tires [26]. In particular, an environmental friendly process was developed for the recycling of waste rubber materials such as waste tires to generate valuable fuels or chemicals in a closed oxidation process, which is free of hazardous emissions [26]. This process involves the breakdown of rubber polymer materials by selective oxidation

decoupling of C-C, C-S and S-S bonds by water as a solvent at or near its supercritical condition. Moreover, some authors developed a *green* devulcanization process for cured rubber employing scCO<sub>2</sub> as a reaction medium for devulcanizing agents [27], in particular diphenyl disulfide (DD) [28-32].

ScCO<sub>2</sub> has high diffusivity, low viscosity and high thermal conductivity depending on temperature and pressure. This fluid is non-toxic, inexpensive, non-flammable and easily removable from rubber and has an accessible critical point. ScCO<sub>2</sub> is a good swelling agent and the distribution coefficient of DD in scCO<sub>2</sub> is about four orders of magnitude higher than in toluene [29]. Several agents, such as thiophenol, n-butylamine, triphenyl phosphine and diphenyl disulfide (DD) have been used for the devulcanization of rubber in scCO<sub>2</sub> [27], however the thiol-amine system and DD were found to be the most effective agents for devulcanization of rubber in scCO<sub>2</sub> and DD has been the most studied. The studies, employing DD as a devulcanizing agent, investigated this process on several types of rubber, in particular, Natural Rubber (NR) and synthetic rubber [28,30,32]. Some studies were also conducted on ground rubber [31,33]. Most commercial tires contain a great amount of carbon black (CB) and other fillers. It was demonstrated that the CB content does not interfere with the devulcanization reaction through scCO<sub>2</sub> [32]. The reaction mechanism was studied on natural rubber [3,28] and butyl rubber [30].

Although most of these researches were carried out in order to find the best devulcanizing conditions, these studies have analyzed the process variables just considering one variable at a time (OVAT) [28,30,32]. The studies showed that temperature, pressure, amount of devulcanizing agent and treatment time were the variables that mainly affect the devulcanization process, especially decreasing the crosslink density and increasing the sol fraction of the devulcanized rubber.

Some studies analyzed the effect of the presence of unreacted DD on the devulcanization process of natural and butyl rubber [30,31] and just few researches evaluated the effect of a large amount of residual DD on the devulcanization process of the devulcanized rubber [33].

## 2.1.5 PHYSICAL METHODS

### 2.1.5.1 SINGLE- AND TWIN- SCREW EXTRUDERS

Several researches have investigated a devulcanization process based only on shear stress and high temperature produced in single and twin-screw extruders

at several conditions and varying several screw configurations [34-44]. Most of these studies were carried out in order to find the best devulcanization conditions by analyzing the process parameters. These studies mainly pointed out that temperature, screw shape, screw speed and flow rate have significant effect on the devulcanization process. This process could be also enhanced by adding swelling or chemical devulcanizing agents [2]. In [45], waste tires were pretreated and swollen at a temperature around 180-200 °C for 24-36 h in a mixture of aromatic, naphthenic and paraffinic hydrocarbons and then extruded. In [42,45], some devulcanizing and promoting agents such as alkylphenol polysulfides and dixylen disulfide were added during the extrusion.

Devulcanization using twin-screw extruders is one of the relatively new methods of devulcanization. During this process, shear and elongational stresses along with high temperature are used to break the three-dimensional crosslink network. However, the high stress and heat generated during the extrusion of rubber can also cause a breakage of the main chain. A basic understanding for the cleavage of crosslinking bonds under high shear stress has been suggested in [46]. As shown in Figure 2.16 there appears to be a small difference in the bonding energy between C-C and C-S or S-S bonds. Hence, by simple heating, the cleavages of both the C-C and C-S or S-S bonds may occur unselectively. On the other hand, with regard to the elastic constant for these bonds, the constant value of S-S bonds can be estimated to be about 1/30th of the C-C one. Therefore, under high shear stress, the bonds having lower value of elastic constant (S-S) may become more extended compared to the ones having higher value (C-C), thus favoring a selective cleavage of S-S bonds [46].

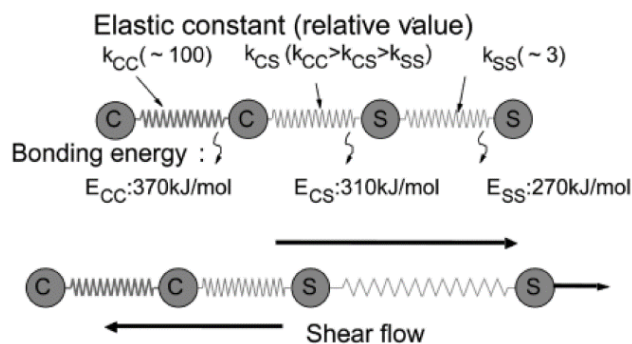


FIGURE 2.16: BREAKAGES OF CROSSLINKING POINTS IN HIGH SHEAR (ADAPTED FROM REF. [46]).

Another method for devulcanization involving a twin-screw extruder was developed and patented by Tzoganakis [47].

This process of devulcanization in twin-screw extruder makes use of mechanical elongation and shear forces in presence of supercritical carbon dioxide (scCO<sub>2</sub>). The purpose of injecting scCO<sub>2</sub> in the extruder is to facilitate the extrusion process and this is achieved by penetration of scCO<sub>2</sub> in the rubber crumb particles, which causes them to swell. Swelling results in exerting more stress on less elastic crosslinks (C-S and S-S bonds), thus making them more susceptible for cleavage. Studies were carried out to investigate the effect of processing parameters and properties of devulcanized rubber obtained using this method [48].

#### 2.1.5.2 HIGH SPEED MIXING

In this technique, the rubber is stirred at high speed (500 rpm) for 15-20 min and the temperature increases till 200 °C [3].

#### 2.1.5.3 MICROWAVE

In this procedure, the microwave energy is used at specific frequencies, able to generate heat quickly and uniformly on the waste rubber. Because of the relative bond energies of C-C, C-S and S-S, it has been reported that the process can selectively break the C-S and crosslink bonds in the vulcanizates. In particular, waves at 950 or 2450 MHz should be sufficient to break the crosslink bonds, but insufficient to break the polymer chain. In this way, the rubber waste can be reclaimed without depolymerization and can be revulcanized. This process showed good applicability to EPDM and IIR, reaching better properties than the ones obtained by other methods. However, the main problem pointed out with this technique is that during the treatment the microwave energy generates heat causing a temperature increase of the material above 260 °C [1-3].

#### 2.1.5.4 ULTRASOUND

The range of human hearing is from about 16 Hz to 16 kHz. Ultrasound is generally defined as any sound with a frequency beyond the limit which the human ear can respond to. The upper limit for the ultrasonic frequency is usually taken to be 5 MHz for gases and 500 MHz for liquids and solids.

The uses of ultrasound can be divided into two different categories. The first one, involving low amplitude (high frequency) waves, is referred to as



“low power” or “high frequency” ultrasound. This kind of ultrasound deals with the physical effect of the medium on the wave and generally, these low amplitude waves are used for analytical purposes such as the measurement of the velocity and absorption coefficient of the wave in a medium, for medical imaging, chemical analysis and the study of relaxation phenomena. The latter, involving high amplitude (low frequency) waves, is referred to as “high power” ultrasound (between 20 and 100 kHz). This ultrasound range is usually applied for the chemical reactivity and is used for cleaning, plastic welding and, more recently, for sonochemistry, with the employment of high power equipment capable of generating cavitation within liquid systems at these high frequencies [1].

It is believed that high power ultrasound influences chemical reactivity through an effect known as cavitation. Cavitation is the production of bubbles in a medium when a region is subjected to a rapidly alternating of pressures of high amplitude generated by high power ultrasound. The released energy depends on the value of acoustic pressure amplitude. When a sufficiently intense sound wave is applied to a medium, bubbles are formed during the expansion portion of the wave. These bubbles then undergo repeated expansion and compression. During the negative half of cycle, the liquid is subjected to a stress and during the positive one undergoes a compression. These bubbles can collapse rapidly and release a large amount of energy (Figure 2.17). Moreover, the intensity experienced by individual bubbles is not constant due to surrounding bubbles forming and resonating around them. This causes some bubbles to suddenly reach an unstable size and to collapse.

In case of polymer solutions, it is known that the irradiation by ultrasound waves produces cavitation of bubbles. The collapse of these bubbles is responsible for the degradation of polymers in solution, which arises as a result of the ultrasound effect on the solvent medium. When applied to solid polymers, the term *cavitation* usually corresponds to the effect of formation and unrestricted growth of voids, induced by existing cavities, voids and density fluctuations.

The viscoelasticity of rubber tremendously affects the dynamics of cavitation, acting to reduce the amplitude of oscillations and to decelerate the violent collapse contractions. As described by Yashin and Isayev [49,50] the collapse is not the primary mechanism of the ultrasonic devulcanization. When acoustic pressure is high enough to cause high levels of strain during cavitation, network

degradation around pulsating cavities should be considered. Therefore, ultrasonic cavitation without collapse is a possible mechanism of devulcanization. Very high acoustic pressure can be generated in a cured rubber compressed in a narrow gap. It has been demonstrated that high amplitude cavitation with no-collapse like effects is capable of a significant reduction of the crosslink density [49,50].

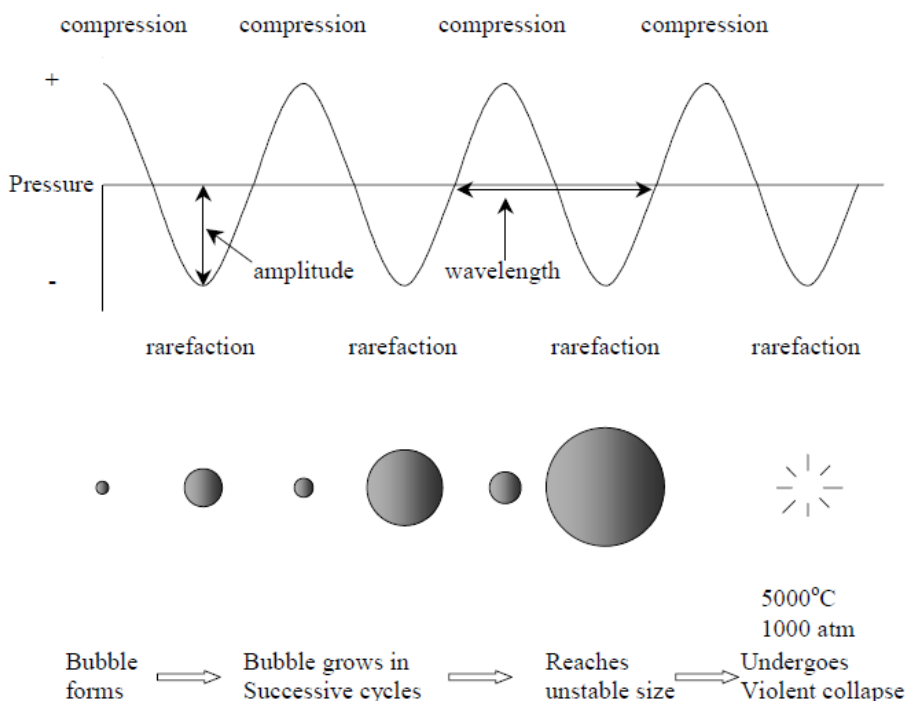


FIGURE 2.17: ULTRASOUND CAVITATION BUBBLE GROWTH AND COLLAPSE  
(ADAPTED FROM REF. [51]).

Rubber devulcanization, using the ultrasonic energy, was first reported by Pelofsky in 1973 [52]. In this patented process, solid rubber has to be immersed into a liquid solution and then subjected to a source of ultrasonic waves at a frequency of 20 kHz. The rubber underwent a degradation process and dissolved in the liquid solution. In 1987, Okuda and Hatano patented a new ultrasonic devulcanization process based on a 20 min treatment with 50 kHz ultrasonic waves under static conditions (no flow). In this study, the treated rubber was revulcanized.

After these researches, a completely new continuous devulcanization process has been developed by Isayev at the University of Akron. In this case, the ultrasonic treatment was coupled to the extrusion of waste rubber resulting in a fast, continuous and chemical free process. The ultrasonic waves, in presence of heat and pressure, during the extrusion, can quickly lead to the three-dimensional rubber network breakage. Isayev and co-authors claimed a preferentially cleavage of sulfidic crosslinks in vulcanized rubber [1].

At first, the system they used consisted of a single-screw extruder with an ultrasonic cone-shaped die attachment. In this case, an ultrasonic power supply, an acoustic converter, a booster and a cone-tipped horn were used. The rubber coming from the extruder flowed through the uniform clearance between the horn and the die, undergoing an ultrasonic wave treatment; the wave propagation was perpendicular to the flow direction and with a frequency of 20 kHz.

Later, the ultrasonic source was moved from the die to the barrel and two different systems were developed: the first one consisted of a barrel ultrasonic reactor with the rectangular cross section ultrasonic water-cooled horn installed on the barrel. Two bronze restrictors, placed on the barrel, blocked the flow of rubber and forced the rubber to flow through the cavity between the screw and the tip of the horn. The second one, similar to the previous one, consisted of a grooved barrel. In this case, two helical channels were installed on the barrel surface. Rubber was forced to flow into these channels.

Extensive studies were conducted using these different systems for the devulcanization of several types of vulcanized rubbers; these technologies were successfully investigated on GTR, synthetic rubber, unfilled and filled NR. After the devulcanization, the mechanical and rheological properties of revulcanizates were investigated and showed good results, comparable to the one of virgin materials.

Recently, a new devulcanization system was introduced by Isayev in his laboratories. In this new system, the ultrasonic device has been installed on a barrel of a co-rotating twin-screw extruder. The ultrasonic waves have frequency of 40 kHz. The rubber passing through the gap in the ultrasonic zone is subjected to a longitudinal waves, being perpendicular to the flow direction. The devulcanization reaction has already been tested on GTR of several dimensions by Isayev et al. [53], but this research just considered several conditions and analyzed the results, without giving a global view of the problem.

#### 2.1.6 BIOLOGICAL METHODS

The possibility to apply microorganisms to catalyze desulfurization reactions for industrial applications has been extensively investigated. In particular, some chemolithotrophes microorganisms, able to derive energy from the oxidation of inorganic sulfur compounds, have been isolated for desulfurization of inorganic compounds (i.e. pyrite, copper sulfide) from coal and mineral oil [54-56]. Among them, the most studied were *Thiobacillus* strains and some Archaea bacteria, such as Sulfolobales [57].

Nevertheless, the majority of existing biodesulfurization researches and applications have focused on the microbial desulfurization of organic molecules, such as dibenzothiophene (DBT), often present as chemicals in fuels and as a consequence in the contaminated soils. Most of these studies pointed out that several microorganisms are able to remove the sulfur content from the DBT and use it as a micronutrient without introducing any change in the carbon structure [58-60]. The DBT desulfurization pathway was described and characterized by Oldfield et al. and it is known as “4s” pathway [61]. Several chemoorganotrophic bacteria, which require organic compounds for growth, were studied and some strains of the genera *Pseudomonas*, *Rhodococcus*, *Paenibacillus* and *Bacillus* are reported for their ability to oxidize DBT [62].

Since the biodesulfurization process on these compounds is similar to the biodesulfurization process of vulcanized rubber, several researches tried to extend and apply this technique to the rubber devulcanization, using the known ability of the chemoorganotrophs and chemolithotrophes microorganisms to selectively break the C-S bond. However, just few microorganisms were found with the ability to devulcanize waste rubber, due to its complex structure.

A “4s”-like mechanism was suggested by Romine and Romine [63] for the desulfurization of GTR by *Sulfolobus acidocaldarius*. The sulfur crosslinks were metabolized into sulfoxide / sulfone / sulfonate / sulfate. Jiang et al. [64] reported the activity of *Thiobacillus ferrooxidans* on GTR. *Thiobacillus*, grown in 30 days in presence of GTR, maintained a high biomass and was able to desulfurize rubber [65].

Li et al. [66] used *Sphingomonas* sp. isolated from coalmine soil for GTR desulfurization. The strain showed sulfur oxidizing capacity after a 20-day treatment. *Acidianus brierleyi* and *TH2 Lund*, isolated Archaea, broke sulfur bonds in cryo-GTR in 20 days, leaving oxidized sulfur species on the surface [67].

In addition, Eukarya were studied for rubber devulcanization. Some species of white-rot and brown-rot fungi, such as *Ceriporiopsis subvermispora*, were able to break sulfur crosslinks [68,69].

Since the biological devulcanization represents a promising technique, due to its low energy consumption and high selective nature, several microorganisms with a biodesulfurization ability were isolated and patented for this purpose. *Thiobacillus ferroxidans*, *Rhodococcus rhodochrous* and *Solfobus acidocaldarius* were patented for a selective devulcanization [70]. Others strains such as *Bacillus sphaericus* or *Rhodococcus rhodochrous* were claimed for their selectivity towards C-S bonds. Christofi et al. [71] described different strains of mycolata bacteria such as *Corynebaclerium*, *Rhodococcus*, *Nocardia*, *Gordonia*, *Tsukamurella*, *Dietzia*, *Mycobacterium* and in particular *Gordonia desulfuricans* strain 213E. In this patent, the bacterium *G. desulfuricans* 213E was employed for the desulfurization of vulcanized rubber. The sulfur content in the rubber decreased between 23 % and 35 %. Before the treatment, benzothiophene was added to the culture medium as a desulfurization pathway inducer.

Nevertheless, several might be the problems with the microbial devulcanization. Vulcanized rubber and culture medium have no affinity, resulting in a two-phase system. Moreover, some microorganisms might break the polymer chain in addition to the crosslink network and some rubber additives and soluble compounds released by the rubber might inhibit their growth. Nevertheless, the main limiting factor to the bacterial devulcanization process is the low yield of the process that by its nature is limited to the rubber surface, requiring a long treatment time [65,72].

## REFERENCES

1. A.I Isayev; In J.E. Mark, B. Erman, M. Roland, editors. The science and technology of rubber, 4th ed., Boston: Elsevier Academic Press, 2014, p. 697-764.
2. B. Adhikari, D. De, S. Maiti; Reclamation and recycling of waste rubber. Progress in Polymer Science 2000;25:909–948.
3. V.V. Rajan, W.K. Dierkes, R. Joseph, J.W.M. Noordermeer; Science and technology of rubber reclamation with special attention to NR-based waste latex products. Progress in Polymer Science 2006;31:811-834.
4. C. Goodyear; British Patent 2933, 1853.

5. C.P. Rader; In K.C. Baranwal, H.L. Stephens, editors. Basic elastomer technology, Akron: The rubber Division American Chemical Society, 2001, p.165-190.
6. X. Zhang, L. Canhui, M. Liang; Properties of natural rubber vulcanizates containing mechanochemically devulcanized ground tire rubber. *Journal of Polymer Research* 2009;16:411–419.
7. O. Grigoryeva, A. Fainleib, O. Starostenko, I. Danilenko, N. Kozak, G. Dudarenko; Ground tire rubber (GTR) reclamation: Virgin rubber / reclaimed GTR (RE)vulcanizates. *Rubber Chemistry and Technology* 2004;77:131-146.
8. M.M. Hassan, R.O. Aly, S.EA. Aal, A.M. El-Masry, E.S. Fathy; Mechanochemical devulcanization and gamma irradiation of devulcanized waste rubber/high density polyethylene thermoplastic elastomer. *Journal of Industrial and Engineering Chemistry* 2013;19:1722-1729.
9. S.K. Mandal, M.N. Alam, K. Roy, S.C. Debnath; Reclaiming of ground rubber tire by safe multifunctional rubber additives: II Virgin natural rubber/reclaimed ground rubber tire vulcanizates. *Rubber Chemistry and Technology* 2014;87:152-167.
10. D. Kiroski, J. Sims, D.E. Packham, A.L. Gregory; The use of thiol–amine chemical probes in network characterization of NBR vulcanizates. *Kautschuk Gummi Kunststoffe* 1997;50:716–20.
11. B. Saville, A.A. Watson; Structural characterization of sulfur-vulcanized rubber networks. *Rubber Chemistry and Technology* 1967;40:100-148.
12. R.E. Humphey, J.L. Potter; Reduction of disulfide with tributylphosphine. *Analytical Chemistry* 1965;37:164–165.
13. C.G. Moore, B.R. Trego; Structural characterization of vulcanizates Part IV: Use of triphenylphosphine and sodium-di-n-butyl phosphite to determine the structure of sulfur linkages in natural rubber, cis-1,4-polyisoprene and ethylene–propylene rubber vulcanizate networks. *Journal of Applied Polymer Science* 1964;8:1957–1983.
14. F.R. Mayo, J. Heller, R.L. Walrath, K.C. Irwin; Accelerated oxidation of polyisoprene II: Effects of hydrazines, sulfur compounds and phenyl-b-naphthylamine in solution. *Rubber Chemistry and Technology* 1968;41:289–295.
15. J.L. Bolland; Kinetic studies in the chemistry of rubber and related material I: The thermal oxidation of ethyl linoleate. *Proceedings Royal Society* 1943;186:218–236.

16. S. Rooj, G.C. Basak, P.K. Maji, A.K. Bhowmick; New route for devulcanization of natural rubber and the properties of devulcanized rubber. *Journal of Polymer and Environment* 2011;19:382–390.
17. P. Thaicharoen, P. Thamyongkit, S. Poompradub; Thiosalicylic acid as a devulcanizing agent for mechano-chemical devulcanization. *Korean Journal of Chemical Engineering* 2010;27:1177-1183.
18. F. Cataldo, O. Ursini, G. Angelini; Surface oxidation of rubber crumb with ozone. *Polymer Degradation and Stability* 2010;95:803-810.
19. X. Cao, J. Luo, Y. Cao, X. Yin, G. He, X. Peng, B. Xu; Structure and properties of deeply oxidized waste rubber crumb through long time ozonization. *Polymer Degradation and Stability* 2014;109:1-6.
20. V. Goodship, E.O. Ogar; *Polymer processing with supercritical fluids*. Shawbury: Rapra Technology Ltd., 2004.
21. W. Tumas, J.M. DeSimone; *Green chemistry using liquid and supercritical carbon dioxide*, Oxford University Press, 2003.
22. M. Kojima, M. Tosaka, E. Funami, K. Nitta, M. Ohshima, S. Kohjiya; Phase behavior of crosslinked polyisoprene rubber and supercritical carbon dioxide. *The Journal of Supercritical Fluids* 2005;35:175–181.
23. M.A. Jacobs, M.F. Kemmere, J.T.F. Keurentjes; Foam processing of poly(ethylene-co-vinyl acetate) rubber using supercritical carbon dioxide. *Polymer* 2004;45:7539–7547.
24. I. Hong, S. Lee; Microcellular foaming of silicone rubber with supercritical carbon dioxide. *Korean Journal of Chemical Engineering* 2014;31:166-171.
25. V. Jain; Supercritical fluids tackle hazardous wastes. *Environmental Science & Technology* 1993;5:806-808.
26. P. Sangdo, E.F. Gloyna; Statistical study of the liquefaction of used rubber tyre in supercritical water. *Fuel* 1997;76:999-1003.
27. M. Kojima, K. Ogawa, H. Mizushima, M. Tosaka, S. Kohjiya, Y. Ikeda; Devulcanization of sulfur-cured isoprene rubber in supercritical carbon dioxide. *Rubber Chemistry and Technology* 2003;76:957-968.
28. M. Kojima, M. Tosaka, Y. Ikeda; Chemical recycling of sulfur-cured natural rubber using supercritical carbon dioxide. *Green Chemistry* 2004;6:84-89.
29. M. Kojima, S. Kohjiya, Y. Ikeda; Role of supercritical carbon dioxide for selective impregnation of decrosslinking reagent into isoprene rubber vulcanizate. *Polymer* 2005;46:2016-2019.

30. K. Jiang, J. Shi, Y. Ge, R. Zou, P. Yao, X. Li, L. Zhang; Complete devulcanization of sulfur-cured butyl rubber by using supercritical carbon dioxide. *Journal of Applied Polymer Science* 2012;127:2397-2406.
31. J. Shi, K. Jiang, D. Ren, H. Zou, Y. Wang, X. Lv, L. Zhang; Structure and performance of reclaimed rubber obtained by different methods. *Journal of Applied Polymer Science* 2013;129:999–1007.
32. M. Kojima, M. Tosaka, Y. Ikeda, S. Kohjiya; Devulcanization of carbon black filled natural rubber using supercritical carbon dioxide. *Journal of Applied Polymer Science* 2005;95:137-143.
33. V.V. Rajan, W.K. Dierkes, R. Joseph, J.W.M. Noordermeer; Recycling of NR based cured latex material reclaimed with 2,2'-dibenzamidodiphenyldisulphide in a truck tire tread compound. *Journal of Applied Polymer Science* 2006;102:419-426.
34. K. Formela, M. Cysewska, J. Haponiuk, A. Stasiak; The influence of feed rate and shear forces on the devulcanization process of ground tire rubber (GTR). *Polimery* 2013;58:906-912.
35. K. Formela, M. Cysewska, J. Haponiuk; The influence of screw configuration and screw speed of co-rotating twin screw extruder on the properties of products obtained by thermomechanical reclaiming of ground tire rubber. *Polimery* 2014;59:170-177.
36. J. Shi, K. Jiang, D. Ren, H. Zou, Y. Wang, X. Lv, L. Zhang; Structure and performance of reclaimed rubber obtained by different methods. *Journal of Applied Polymer Science* 2013;129: 999-1007.
37. G. Tao, Q. He, Y. Xia, G. Jia, H. Yang, W. Ma; The effect of devulcanization level on mechanical properties of reclaimed rubber by thermal-mechanical shearing devulcanization. *Journal of Applied Polymer Science* 2013;129:2598-2605.
38. B. Maridass; Cure modeling and mechanical properties of counter rotating twin screw extruder devulcanized ground rubber tire-natural rubber blends. *Journal of Polymer Research* 2009;16:133-141.
39. H. Si, T. Chen, Y. Zhang; Effects of high shear stress on the devulcanization of ground tire rubber in a twin-screw extruder. *Journal of Applied Polymer Science* 2013;128:2307-2318.
40. B. Maridass, B.R. Gupta; Effect of extruder parameters on mechanical properties of revulcanized ground rubber tire powder. *Polimery* 2007;52:456-460.



41. B. Maridass, B.R. Gupta; Process optimization of devulcanization of waste rubber powder from syringe stoppers by twin screw extruder using response surface methodology. *Polymer Composite* 2008;29:1350-1357.
42. H. Yazdani, I. Ghasemi, M. Karrabi, H. Azizi, G.R. Bakhshandeh; Continuous devulcanization of waste tires by using a co-rotating twin screw extruder: Effects of screw configuration, temperature profile, and devulcanization agent concentration. *Journal of Vinyl Additives Technology* 2013;19:65-72.
43. B. Maridass, R.B. Gupta; Performance optimization of a counter rotating twin screw extruder for recycling natural rubber vulcanizates using response surface methodology. *Polymer Testing* 2004;23:377-385.
44. E. Bilgili, H. Arastoopour, B. Bernstein; Analysis of rubber particles produced by the solid state shear extrusion pulverization process. *Rubber Chemistry and Technology* 2000;73:340-355.
45. H. Si, T. Chen, Y. Zhang; Effects of high shear stress on the devulcanization of ground tire rubber in a twin-screw extruder. *Journal of Applied Polymer Science* 2013;128:2307–2318.
46. K. Fukumori, M. Matsushita, M. Mouri, H. Okamoto, N. Sato, K. Takeuchi, Y. Suzuki; Dynamic devulcanization and dynamic vulcanization for recycling of crosslinked rubber. *Kautschuk Gummi Kunststoffe* 2006;59:405-41.
47. C. Tzoganakis, US 7189762, 2007.
48. C. Tzoganakis, Q. Zhang; Devulcanization of recycled tire rubber using supercritical carbon dioxide. *Antec-Conference Proceedings* 2004;3:3509-3513.
49. V.V. Yashin, A.I. Isayev; A model for rubber degradation under ultrasonic treatment: Part I. Acoustic cavitation in viscoelastic solid. *Rubber Chemistry and Technology* 1999;72:741-757.
50. V.V. Yashin, A.I. Isayev; A model for rubber degradation under ultrasonic treatment: Part II. Rupture of rubber network and comparison with experiments. *Rubber Chemistry and Technology* 2000;73:325-339.
51. X. Sun; The devulcanization of unfilled and carbon black filled isoprene rubber vulcanizates by high power ultrasound. Ph.D. Dissertation, The University of Akron, 2007.
52. A.H. Pelofsky; US:3725314, 1971.
53. A.I. Isayev, T. Liang, T.M. Lewis; Effect of particle size on ultrasonic devulcanization in twin-screw extruder. *Rubber Chemistry and Technology* 2014;87:86-102.

54. H.L. Ehrlich, C. L. Brierley; Microbial mineral recovery, McGraw-Hill, 1990.
55. G. Olsson, B. M. Pott, L. Larsson, O. Holst, H.T. Karlsson; Microbial desulfurization of coal by *Thiobacillus-ferrooxidans* and thermophilic archaea. Fuel Processing Technology 1994;40:277-282.
56. G. Olsson, B. M. Pott, L. Larsson, O. Holst, H.T. Karlsson; Microbial desulfurization of coal and oxidation of pure pyrite by *Thiobacillus-ferrooxidans* and *Acidianus-brierleyi*. Journal of Industrial Microbiology 1995;14:420-423.
57. O. Holst, B. Stenberg, M. Christiansson; Biotechnological possibilities for waste tyre-rubber treatment. Biodegradation 1998;9:301-310.
58. A. Aminsefat, B. Rasekh, M.R. Ardakani; Biodesulfurization of dibenzothiophene by *Gordonia* sp. AHV-01 and optimization by using of response surface design procedure. Microbiology 2012;81:154-159.
59. M. Papizadeh, M.R. Ardakani, H. Motamedi, I. Rasouli, M. Zarei; C-S targeted biodegradation of dibenzothiophene by *Stenotrophomonas* sp. NISOC-04. Applied Biochemistry and Biotechnology 2011;165:938-948.
60. F. Davoodi-Dehaghani, M. Vosoughi, A.A. Ziaee; Biodesulfurization of dibenzothiophene by a newly isolated *Rhodococcus erythropolis* strain. Bioresource Technology 2010;101:1102–1105.
61. C. Oldfield, O. Pogrebinsky, J. Simmonds, E.S. Edwin, C.F. Kulpa; Elucidation of the metabolic pathway for dibenzothiophene desulphurization by *Rhodococcus* sp. strain IGTS8 (ATCC 53968). Microbiology 1997;143:2961-2973.
62. J. Konishi, Y. Ishii, T. Onaka, K. Okumura, M. Suzuki; Thermophilic carbon-sulfur-bond-targeted biodesulfurization. Applied and Environmental Microbiology 1997;63:3164-3169.
63. R.A. Romine, M.F. Romine; Rubbercycle: A bioprocess for surface modification of waste tyre rubber. Polymer Degradation and Stability 1998;59:353-358.
64. G. Jiang, S. Zhao, J. Luo, Y. Wang, W. Yu, C. Zhang; Microbial Desulfurization for NR Ground Rubber by *Thiobacillus ferrooxidans*. Journal of Applied Polymer Science 2010;116:2768–2774.
65. Y. Li, S. Zhao, Y. Wang; Microbial desulfurization of ground tire rubber by *Thiobacillus ferrooxidans*. Polymer Degradation and Stability 2011,96;1662-1668.

66. Y. Li, S. Zhao, Y. Wang; Microbial desulfurization of ground tire rubber by *Sphingomonas* sp.: A novel technology for crumb rubber composites. *Journal of Polymers and the Environment* 2012;20:372-380.
67. M. Christiansson; B. Stenberg, L. R. Wallenberg, O. Holst; Reduction of surface sulphur upon microbial devulcanization of rubber materials. *Biotechnology Letters* 1998;20:637-642.
68. K. Bredberg, B. E. Andersson, E. Landfors, O. Holst; Microbial detoxification of waste rubber material by wood-rotting fungi. *Bioresource Technology* 2002;83:221-224.
69. S. Sato, Y. Honda, M. Kuwahara, T. Watanabe; Degradation of vulcanized and nonvulcanized polyisoprene rubbers by lipid peroxidation catalyzed by oxidative enzymes and transition metals. *Biomacromolecules* 2003;4:321-329.
70. A.R. Romine, J.L. Snowden-Swan; US 5597851 A, 1997.
71. N. Christofi, J. Geoffrey, D. Edward; US 7737191 B2, 2010.
72. C. Yao, S. Zhao, Y. Wang, B. Wang, M. Wei, M. Hu; Microbial desulfurization of waste latex rubber with *Alicyclobacillus* sp.. *Polymer Degradation and Stability* 2013;98:1724-1730.



## 3 CHARACTERIZATION OF CRYO-GTR AND PRELIMINARY SUPERCRITICAL CO<sub>2</sub> DEVULCANIZATION

---

The present chapter focuses on the characterization of the ground tire rubber (GTR) used in the entire thesis work. After an extensive characterization, the GTR is subsequently devulcanized in supercritical CO<sub>2</sub> in presence of diphenyl disulfide (DD) as devulcanizing agent, keeping the treatment conditions as suggested in literature. The effect of the devulcanization process on mechanical properties and on curing behavior of compounds containing devulcanized GTR is investigated. The obtained results shown in this chapter has been published in *Polymer Degradation and Stability* (2014) [1].

---

### 3.1 EXPERIMENTAL

#### 3.1.1 MATERIALS AND REAGENTS

The ground truck-tire rubber (GTR) characterized and devulcanized in the present chapter was the same studied in the entire thesis work. It had dimensions smaller than 0.4 mm and it was a cryo-ground rubber from whole truck tires. The rubber fraction was mainly composed by natural rubber (NR).

The other reagents used in this chapter were diphenyl disulfide, DD (99% assay) from Sigma Aldrich (Germany); liquid carbon dioxide (99.995% assay) from Sapio (Italy); sulfur certified standard (NCS FC28107) from LabService Analytica (Italy); acetone, toluene and dichloromethane (>99% assay) from Panreac (Spain); polystyrene standards from Pressure Chemical Company (USA). N-Cyclohexyl-2-benzothiazole sulfenamide was Vulkacit CZ/EG-C from Lanxess (Germany); stearic acid was Stearina TP8 from Undesa (Italy); sulfur was from Zolfoindustria (Italy), zinc oxide was from Zincol (Italy), NR was STR20-1,4-cis polyisoprene from Von Buntit (Thailand) and carbon black (CB) was N330 from Cabot Corporation (USA).

#### 3.1.2 GTR COMPOSITION

The dimensions of the GTR particles were determined by sieving through ASTM E-11 standard sieves and weighing the respective fractions. Scanning electron microscope was used to investigate the particle surface morphology.

The moisture content was determined by drying the sample in a vacuum oven at 70 °C for 24 h and by thermogravimetric analysis (Perkin Elmer TGA 7) at

isothermal conditions (70 °C for 7 h). The ashes content was determined by muffle calcination at 550 °C for 5 h and by TGA at 900 °C in air atmosphere.

Further details on the rubber composition were obtained by TGA. Approximately 10 mg of sample had previously been extracted to remove the extractable and dried in vacuum oven. Thus, the sample was introduced in the TGA and heated from room temperature up to 600 °C at a heating rate of 20 °C/min in N<sub>2</sub> atmosphere. The sample weight and its rate of weight loss were continuously measured as a function of temperature.

The characterization also focused on the extractable fraction through two consecutive Soxhlet extractions. Approximately 3 g of GTR were dried and extracted with acetone and subsequently with chloroform. The extraction was performed using an automatic Soxhlet (Büchi Extraction System B-811) in standard Soxhlet mode, according to the ISO 1407 and ASTM D 297 standards. The Soxhlet cycles were optimized in order to obtain the largest amount of extractable. This corresponded to 384 and 90 cycles for acetone and chloroform, respectively. These two solvents are suggested by the ASTM D 297 standard in order to reach a total extraction. They were chosen due to their higher Hildebrand solubility parameter in comparison with NR and BR, since this parameter provides a numerical estimation of the degree of interaction between solvent and polymer.

The extracts were dried (Büchi Rotavapor R-200) and the remaining solid fraction was weighed. In order to identify the extractable chemicals, the extracts were re-suspended in 25 ml of hexane and analyzed using a gas chromatograph (GC 6890N, Agilent) equipped with a 7683 Series injector (Agilent), combined with a mass selective detector (AG5973N MSD, Agilent). The separation column (Phenomenex ZB-5ms, Torrance, CA, USA) had a length of a 60 m and internal diameter of 0.25 mm with 0.25 µm film thickness. The GC conditions were as follows: column carrier gas, helium, injection volume, 2 µL in splitless mode with an injection temperature of 260 °C. The oven temperature program was from 60 °C (holding time 5 min) to 320 °C (holding time 10 min) at 5 °C/min. The mass spectra detector (MSD) conditions were as follows: full scan mode, m/z 40–550 amu, positive EI mode, ion-source temperature 230 °C.

### 3.1.3 DEVULCANIZATION PROCESS

GTR was dried under vacuum to remove moisture and subsequently underwent the devulcanization process. The reaction was carried out in an

industrial prototype plant (SFE  $\mu$ -Plant) realized by Q-Ation Ltd (Italy), designed for supercritical extractions. The instrument, shown in Figure 3.1, has maximum operating temperature of 500 °C and pressure of 70 MPa. It was equipped with a reactor cell of a capacity up to 100 ml.

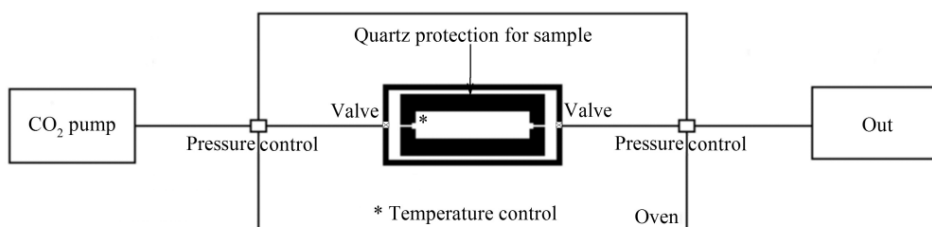


FIGURE 3.1: SCHEMATIC OF SFE  $\mu$ -PLANT.

Temperature (T), pressure (P), time (rt) and the amount of devulcanizing agent (DD), shown in Table 3.1, were chosen considering the operating level and the rubber type [2-7]. These experimental conditions provided a large excess of devulcanizing agent.

TABLE 3.1: TEMPERATURE, PRESSURE, TIME AND DEVULCANIZING AGENT USED IN THE DEVULCANIZATION PROCESS.

Parameter	Value
Temperature (°C)	180
Pressure (MPa)	15
Time (min)	180
Ratio DD/rubber (wt%)	10

#### 3.1.4 CHARACTERIZATION OF THE MATERIALS

The GTR and devulcanized GTR (T-GTR) were passed in a two-roll mill at 40 °C keeping conditions constant in order to obtain 1-mm-thick sheets. These sheets were suitable to avoid loss of material, especially during the swelling measurements. Additives were removed from GTR and T-GTR (E-GTR, TE-GTR) sheets by extraction using hot acetone. Each sample was then dried.

##### 3.1.4.1 COMPARISON OF E-GTR AND TE-GTR

The content of sulfur, the molecular weight of the sol fraction, the crosslink density, the sol and gel fractions parameters were determined on E-GTR and on TE-GTR sheets and each measurement was repeated at least three times in order

to estimate the standard error and to test statistical differences between the two samples.

Sulfur was determined by elemental analysis (Perkin Elmer 2400 Series II CHNS/O System) and the NCS Coal Certified Reference Material, containing 2.10 wt% of sulfur for K factor calculation, was used as a standard.

About 1 g of E-GTR or TE-GTR was used for the determination of the crosslink density, of the sol and gel fraction and for the gel permeation chromatography (GPC) analysis ( $W_i$ ).

The crosslink density and the estimation of the devulcanization percentage were carried out according to ASTM D 6814-02 standard through swelling measurements. Toluene was chosen as a solvent considering the Hildebrand solubility parameter. The Flory-Rehner equation was used in order to calculate the crosslink density [8]:

$$v_e = - \frac{\ln(1-v_r)+v_r+\chi v_r^2}{v_s(v_r^{1/3}-0.5v_r)} \quad (\text{EQUATION 3.1})$$

where  $v_e$  is the crosslink density of the rubber,  $v_r$  is the volume fraction of the rubber at swelling equilibrium calculated considering the rubber and solvent densities,  $v_s$  is the molar volume of the solvent and  $\chi$  is the interaction parameter between the rubber and the solvent.

The density of rubber was approximated to the density of the NR, considering the content of sulfur and it was 0.92 g/cm<sup>3</sup> [9]. The  $\chi$  interaction parameter between the rubber and the swelling solvent (toluene) was set equal to 0.39. The interaction parameter was chosen considering NR as the main polymer.

In reinforced filler-rubber systems, the Flory-Rehner equation cannot be directly used. It is assumed that the filler does not swell in solvents, therefore Equation 3.1 has to be modified using the Kraus correction [10,11] as follows:

$$\frac{v_{ro}}{v_r} = 1 - \frac{m\phi}{(1-\phi)} \quad (\text{EQUATION 3.2})$$

$$m = 3C \left(1 - v_{ro}^{1/3}\right) + v_{ro} - 1 \quad (\text{EQUATION 3.3})$$



where  $v_{ro}$  and  $v_r$  are the volume fraction of rubber in the swollen gels of unfilled and analogous filled vulcanizates,  $C$  is a universal constant for a given filler and  $\phi$  is the volume fraction of the filler in the dried gel. The CB density was taken to be  $1.85 \text{ g/cm}^3$  and the constant  $C$  in the correction was chosen equal to 1.17.

The sol fraction represents the soluble polymeric fraction extracted by a suitable solvent. To achieve the dissolution of the unbound rubber chains, the sample was swollen in cold toluene for 72 h and the solvent replaced with fresh solvent every 24 h [12-14]. The following equation was used for the sol fraction calculation:

$$\text{Sol fraction (\%)} = \left( \frac{W_{SF}}{W_i} \right) * 100 \quad (\text{EQUATION 3.4})$$

where  $W_{SF}$  is the weight of the toluene extract after solvent evaporation.

The gel fraction, which represents the insoluble fraction after removing the sol fraction, was calculated using the equation:

$$\text{Gel fraction (\%)} = \left( \frac{W_{GF}}{W_i} \right) * 100 \quad (\text{EQUATION 3.5})$$

where  $W_{GF}$  is the dried sample weight after toluene evaporation.

Furthermore, since it is difficult to determine the type of bond rupture during devulcanization processes, the dependence of experimental normalized sol fraction (or gel fraction) versus normalized crosslink density was analyzed and compared to the Horikx function, which is based on the statistical theory dealing with the sol fraction (or gel fraction) – crosslink density relationship. The analysis of the soluble polymeric material (or gel fraction) generated during the devulcanization process can be used to investigate the ratio between the main chain and crosslink scission [15,16]. Horikx functions can be calculated as:

$$1 - \frac{v_f}{v_i} = 1 - \frac{(1-SF_f^{1/2})^2}{(1-SF_i^{1/2})^2} \quad (\text{EQUATION 3.6})$$

$$1 - \frac{v_f}{v_i} = 1 - \frac{\gamma_f(1-SF_f^{1/2})^2}{\gamma_i(1-SF_i^{1/2})^2} \quad (\text{EQUATION 3.7})$$

where  $v_i$  and  $v_f$  are the crosslink density of initial and devulcanized material, respectively;  $SF_i$  and  $SF_f$  are the sol fraction of initial and devulcanized material, respectively.  $\gamma_i$  and  $\gamma_f$  are the crosslinking indices before and after the devulcanization process. If gel fraction is the only available measurement, the sol fraction can be calculated from the content of gel fraction.

Equation 3.6 is used to plot the relationship between the normalized sol fraction (or gel fraction) and the normalized crosslink density in case of the only main chain breakage. Equation 3.7 is used just in case of crosslink cleavage. By these equations, it is possible to describe the type bond breakage occurred during the devulcanization process.

$\gamma_i$  and  $\gamma_f$  numbers are calculated from  $M_n$ , the density of rubber and the crosslink density. If the value of  $M_n$  is known, it is possible to easily calculate the Horikx function for the crosslink scission. In case of GTR devulcanization, it is possible to calculate only the function for the main chain breakage, but not the function for the selective crosslink breakage, since the value of  $M_n$  is not available for GTR that represents a waste and vulcanized material.

GPC was used to investigate the sol fraction molecular weight and its distribution. The dried toluene extract was re-suspended in 1 ml of chloroform and the sample was filtered with a 0.45  $\mu\text{m}$  filter. 30 mg of the solution were dried again and suspended again in 1 ml of dichloromethane. A volume of 40  $\mu\text{L}$  was injected in a GPC equipped with Isocratic Pump (Waters 1515), 4 columns (Shodex, KF-802.5, KF-803, KF-804, KF-805) and a DAD detector (Waters 2487). The dichloromethane flow rate was 1 ml/min at room temperature and at the wavelength of 244 nm. Monodisperse polystyrene standards (the weight average Molecular weight,  $M_w$  between  $1.6 \times 10^6$  and 478 Da) were used for the quantification.

In order to obtain information on structural changes in the functional groups after the devulcanization treatment, Fourier transform infrared spectra (Nicolet iS10 FT-IR Spectrometer) with the attenuated total reflectance mode were collected at room temperature with a 4  $\text{cm}^{-1}$  resolution and 32 scans signal average. Spectra were registered from 4500 to 650  $\text{cm}^{-1}$ .

The acetone and cold toluene extracts were analyzed in GC-MSD in order to gain information on devulcanization reaction mechanism. The GC and MSD conditions were already reported in section 3.1.2.

### 3.1.5 COMPOUNDS

GTR or T-GTR were mixed with raw NR in order to obtain several compounds and then cured. Formulations are shown in Table 3.2. As reference, a compound with NR as the only polymeric material was prepared (Ref in Table 3.2). The compounds were formulated considering the composition of the starting material in order to reach the same amount of rubber and CB in each compound.

In order to evaluate the influence of the DD on the revulcanization process, not only GTR and T-GTR, but also E-GTR and TE-GTR samples were compounded. Each compound was mixed for 30 min using a two-roll mill and the curing behavior was studied according to the ISO 6502 standard using a Moving Die Rheometer (MDR 200, Alpha Technologies) at an oscillation angle of  $0.5^\circ$ , a temperature equal to  $150^\circ\text{C}$ , a pressure equal to 4.3 bar and a frequency of 1.7 Hz. All the specimens for MDR analyses were cut by a Constant Volume Rubber Sample Cutter (CUTTER 2000, Alpha Technologies) from the uncured compounds sheets (diameter = 3.5 cm, thickness = 0.2 cm and weight =  $4.5 \pm 0.3$  g). The resulting curves allowed evaluating the maximum and minimum torque ( $M_H$ ,  $M_L$ ), the scorch time ( $T_{S2}$ ) and was especially used to evaluate the optimal curing time for the tensile test.

Tensile test properties were measured according to the ISO 37 standard, using ring as specimens shape. At least three samples were prepared by compression molding at the optimum cure temperature and time for each sample. Mechanical properties were measured at room temperature using a Zwick dynamometer.

TABLE 3.2: COMPOUNDS FORMULATION.

Formulation (phr) <sup>a</sup>	Ref	5		10		10T		20		20T		5E		10E		10TE		20E		20TE	
		GTR	GTR	GTR	GTR	GTR	GTR	GTR	GTR	GTR	GTR	GTR	GTR	GTR	GTR	GTR	GTR	GTR	GTR	GTR	GTR
NR	100.0	97.5	97.5	95.0	95.0	95.0	90.0	90.0	90.0	90.0	90.0	97.5	97.5	95.0	95.0	95.0	95.0	90.0	90.0	90.0	90.0
GTR	0.0	5.0	0.0	10.0	0.0	0.0	20.0	0.0	0.0	0.0	0.0	0.0	0.0	0.0	0.0	0.0	0.0	0.0	0.0	0.0	0.0
T-GTR	0.0	0.0	5.0	0.0	10.0	10.0	0.0	0.0	0.0	20.0	0.0	0.0	0.0	0.0	0.0	0.0	0.0	0.0	0.0	0.0	0.0
E-GTR	0.0	0.0	0.0	0.0	0.0	0.0	0.0	0.0	0.0	0.0	0.0	5.0	0.0	10.0	0.0	0.0	0.0	20.0	0.0	0.0	0.0
TE-GTR	0.0	0.0	0.0	0.0	0.0	0.0	0.0	0.0	0.0	0.0	0.0	0.0	5.0	0.0	0.0	10.0	0.0	0.0	0.0	20.0	0.0
Carbon Black	37.0	35.5	35.5	34.0	34.0	34.0	31.0	31.0	31.0	31.0	35.5	35.5	35.5	34.0	34.0	34.0	34.0	31.0	31.0	31.0	31.0
Silicon Dioxide	15.0	15.0	15.0	15.0	15.0	15.0	15.0	15.0	15.0	15.0	15.0	15.0	15.0	15.0	15.0	15.0	15.0	15.0	15.0	15.0	15.0
Zinc Oxide	3.5	3.5	3.5	3.5	3.5	3.5	3.5	3.5	3.5	3.5	3.5	3.5	3.5	3.5	3.5	3.5	3.5	3.5	3.5	3.5	3.5
Zinc Salts of Fatty Acids	2.0	2.0	2.0	2.0	2.0	2.0	2.0	2.0	2.0	2.0	2.0	2.0	2.0	2.0	2.0	2.0	2.0	2.0	2.0	2.0	2.0
Stearic Acid	2.0	2.0	2.0	2.0	2.0	2.0	2.0	2.0	2.0	2.0	2.0	2.0	2.0	2.0	2.0	2.0	2.0	2.0	2.0	2.0	2.0
Waxes	1.0	1.0	1.0	1.0	1.0	1.0	1.0	1.0	1.0	1.0	1.0	1.0	1.0	1.0	1.0	1.0	1.0	1.0	1.0	1.0	1.0
TMQ-6PPD (25%-75%) <sup>b</sup>	4.0	4.0	4.0	4.0	4.0	4.0	4.0	4.0	4.0	4.0	4.0	4.0	4.0	4.0	4.0	4.0	4.0	4.0	4.0	4.0	4.0
Sulfur	1.3	1.3	1.3	1.3	1.3	1.3	1.3	1.3	1.3	1.3	1.3	1.3	1.3	1.3	1.3	1.3	1.3	1.3	1.3	1.3	1.3
CBS <sup>c</sup>	1.2	1.2	1.2	1.2	1.2	1.2	1.2	1.2	1.2	1.2	1.2	1.2	1.2	1.2	1.2	1.2	1.2	1.2	1.2	1.2	1.2
Resin	0.3	0.3	0.3	0.3	0.3	0.3	0.3	0.3	0.3	0.3	0.3	0.3	0.3	0.3	0.3	0.3	0.3	0.3	0.3	0.3	0.3
Silane Coupling Agent	3.0	3.0	3.0	3.0	3.0	3.0	3.0	3.0	3.0	3.0	3.0	3.0	3.0	3.0	3.0	3.0	3.0	3.0	3.0	3.0	3.0

<sup>a</sup> The values are expressed parts per hundred of rubber (phr).

<sup>b</sup> 2,2,4-trimethyl-1,2-dihydroquinoline and N-(1,3-Dimethylbutyl)-N'-phenyl-p-phenylenediamine.

<sup>c</sup> N-Cyclohexylbenzothiazole-2-sulfenamide.

## 3.2 RESULTS AND DISCUSSION

### 3.2.1 GTR COMPOSITION

The relative and cumulative distributions of particles size (Figure 3.2) show that the 95 % of the particles were smaller than 0.4 mm with the majority (about 80 %) between 0.4 and 0.15 mm (40-100 mesh).

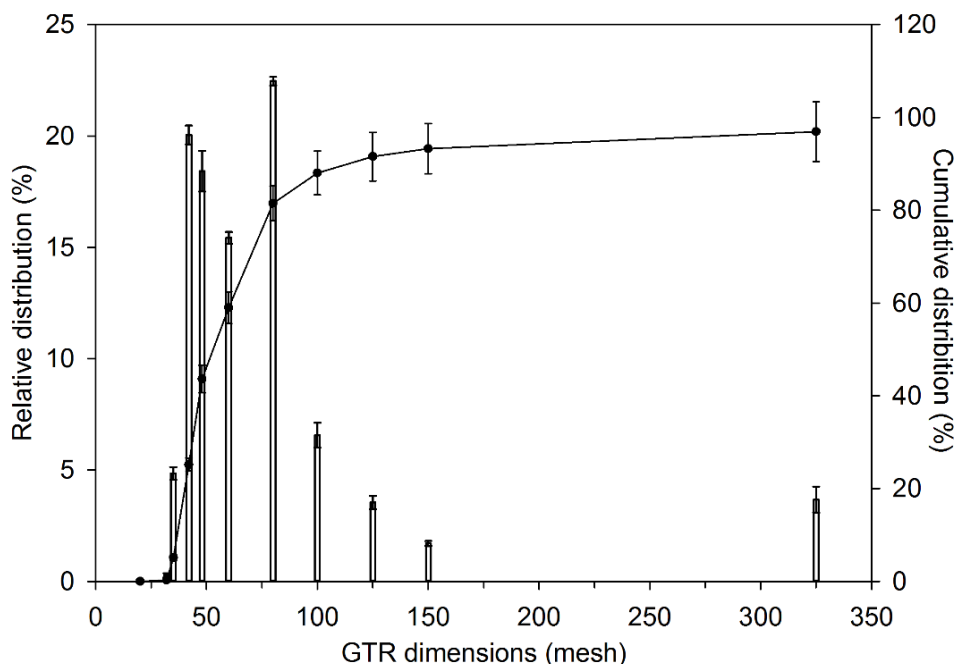


FIGURE 3.2: GTR PARTICLES SIZE DISTRIBUTION.

The particles surface morphology is shown in Figure 3.3. During the milling process, the nitrogen steam hindered a temperature increase and prevented the degradation and oxidation of the sample. As a result, the surface of the cryo-GTR appears quite smooth. The dimensions of several GTR particles can be also observed in Figure 3.3.

The moisture content determined by drying the sample through vacuum oven and through TGA were respectively  $1.2 \pm 0.2$  wt% and  $0.9 \pm 0.1$  wt%. The amount of ashes determined by calcination and by TGA were respectively  $7.2 \pm 0.8$  wt% and  $7 \pm 1$  wt%.

The thermogravimetric (TGA/dTGA) curves of the GTR sample are shown in Figure 3.4. This analysis allowed the quantification of the polymeric fraction. The weight losses with a maximum rate at 385 °C and 430 °C correspond to the

decomposition of NR and synthetic rubber, respectively [17]. From the TGA analysis and the amount of the extractable, the rubber fraction was proved to be the 53 wt% and it was made up of 70 % NR and less than 30 % of synthetic rubber (BR and SBR).

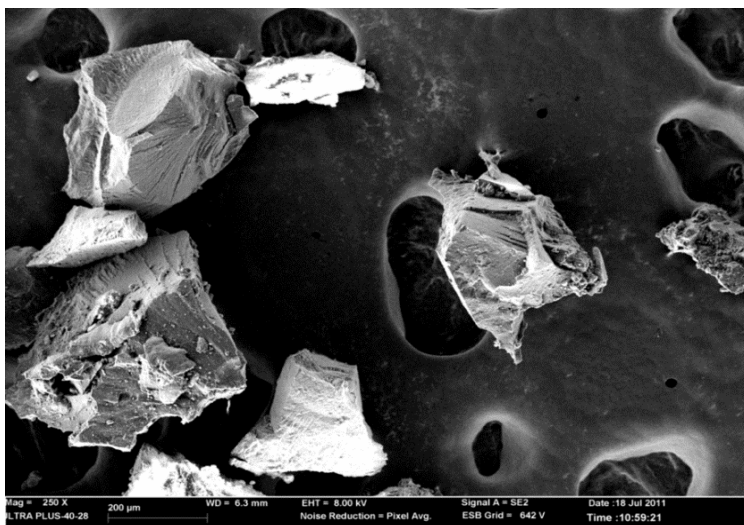


FIGURE 3.3: SEM PICTURE OF GTR PARTICLES.

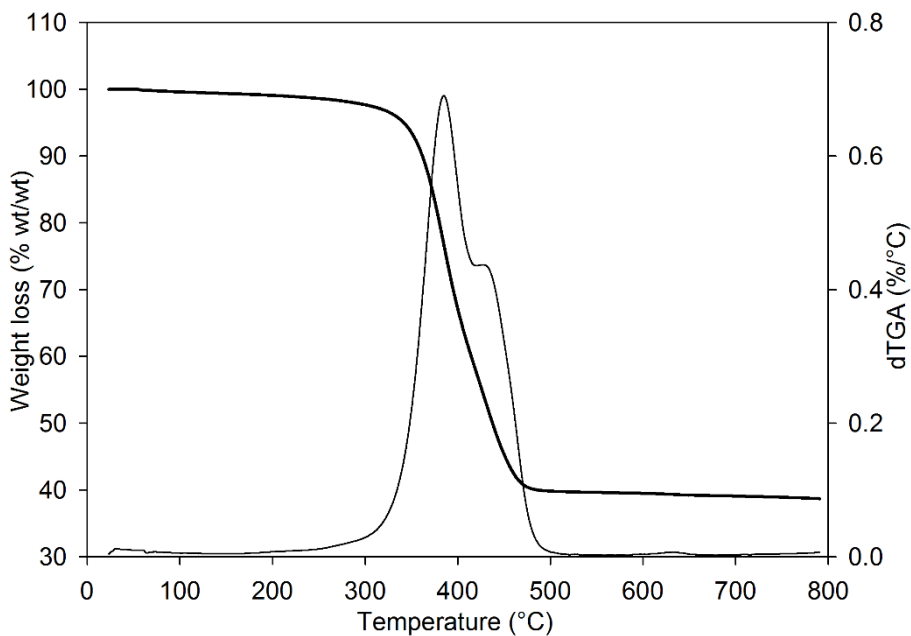


FIGURE 3.4: TGA/dTGA OF THE GTR IN N<sub>2</sub> ATMOSPHERE AND HEATING RATE OF 20 °C/min.

The polymeric fraction, moisture and ashes were determined through TGA measurements, the extractable fraction was determined through the extraction procedure and the CB was determined as the difference between the starting weight and the weight of the other fractions (Table 3.3).

TABLE 3.3: GTR COMPOSITION.

Parameter <sup>a</sup>	Value (wt%) <sup>a</sup>	Standard deviation
Polymer	53	1
Carbon black	30	3
Extractable	9.4	0.2
Moisture	0.9	0.1
Ashes	7.2	0.8

<sup>a</sup>wt% on the initial weight.

#### 3.2.1.1 ADDITIVES

The GC-MSD analysis of the extracts led to the identification of several compounds that are shown in Table 3.4 and Table 3.5. The mass spectra of the National Institute of Standards and Technology library was used for the identification of the compounds. The MSD peaks were identified and assigned to a specific compound only when the match probability was higher than 80 %.

Most of these compounds belong to three main categories of additives: plasticizers, accelerators and antioxidants. The accelerators had previously reacted during the vulcanization reaction. It was possible to identify some products of the reaction, in particular N,N-dicyclohexyl and benzothiazolone.

Some peaks exhibited peculiar mass spectra. Many of these peaks resulted from degradation fragments of the basic structure of natural and synthetic rubber rather than from additives [18].

TABLE 3.4: ADDITIVES FOUND BY GC-MSD ANALYSIS IN THE ACETONE EXTRACT.

Time (min)	Chemical	Time (min)	Chemical	Time (min)	Chemical
8.96	Toluene	26.40	Neodecanoic acid	45.89	Benzothiazole, 2-phenyl-
9.76	3-Penten-2-one, 4-methyl-	28.72	Oxalic acid, cyclohexyl isohexyl ester	47.38	Polymer
10.20	Acetic acid, butyl ester	30.55	3-Tetradecene	48.17	Oleic acid
11.19	2-Pentanone, 4-hydroxy-4-methyl-	31.13	Cyclohexanamine, N-cyclohexyl-	48.67	Octadecanoic acid
13.23	Styrene	32.33	Quinoline, 1,2-dihydro-2,2,4-trimethyl-	49.30	Polymer
13.38	Cyclohexanone	32.94	o-Cyanobenzoic acid	49.42	Polymer
13.61	2-Butoxyethanol	34.98	Dodecanoic acid	50.86	2-Naphthalenamine, N-phenyl-
14.17	Hexylene Glycol	35.97	Hexadecene	51.15	Polymer
16.94	o-Cyanobenzoic acid	36.53	p-Anisic acid, 4-nitrophenyl ester	52.59	1,4-Benzenediamine, N-(1,3-dimethylbutyl)-N'-phenyl-
17.51	Cyclohexane, isocyanato-	38.45	2(3H)-Benzothiazolone	52.91	Polymer
18.35	Butanedioic acid, dimethylester	39.98	Tetradecanoic acid	53.05	Polymer
22.14	Pentanedioic acid, dimethyl ester	40.85	Quinoline, 6-methyl-2-phenyl-	54.61	Polymer
22.61	Oxalic acid, cyclohexyl pentyl ester	40.98	2-Naphthalenamine, N-phenyl-	56.26	Polymer
24.23	2-Dodecene	43.23	Nonadecane	58.40	N,N-Diphenyl-p-phenylenediamine
25.74	Hexanedioic acid, dimethyl ester	44.54	n-Hexadecanoic acid	58.97	N-(2,4-Dinitrophenyl)-1,4-phenylenediamine
25.87	Benzothiazole	45.27	2-Mercaptobenzothiazole		



TABLE 3.5: ADDITIVES FOUND BY GC-MSD ANALYSIS IN THE CHLOROFORM EXTRACT.

Time (min)	Chemical	Time (min)	Chemical
30.13	2,2,4-Pentanone, 4-hydroxy-4-methyl	39.95	Tetradecanoic acid
32.35	Cyclohexanamine, N-cyclohexyl-	40.43	Benzene, (1-ethyldecyl)-
32.95	Benzoic acid, 4-cyano-	40.98	Nonadecane
34.59	Benzene, (1-butylhexyl)-	41.37	Benzene, (1-methylundecyl)-
34.85	Benzene, (1-propylheptyl)-	41.60	Benzene, (1-pentylloctyl)-
35.39	Benzene, (1-ethylloctyl)-	41.87	Benzene, (1-butylonyl)-
36.40	Benzene, (1-methylnonyl)-	42.18	Benzene, (1-propyldecyl)-
37.02	Benzene, (1-pentylhexyl)-	42.53	1,2-Benzenedicarboxylic acid, bis(2-methylpropyl) ester
37.13	Benzene, (1-butylheptyl)-	42.78	Benzene, (1-ethylundecyl)-
37.42	Benzene, (1-propylloctyl)-	43.68	Benzene, (1-methylododecyl)-
38.00	Benzene, (1-ethylloctyl)-	44.54	Hexanedioic acid
38.42	2(3H)-Benzothiazolone	45.25	2-Mercaptobenzothiazole
39.42	Benzene, (1-pentylheptyl)-	50.86	2-Naphthalenamine, N-phenyl-
39.53	Benzene, (1-butylloctyl)-	50.94	Octadecanoic acid
39.87	Benzene, (1-prpoynyl)-		

### 3.2.2 COMPARISON BETWEEN E-GTR AND TE-GTR

The content of sulfur, crosslink density, sol and gel fractions and estimated molecular weight are shown in Table 3.6 for E-GTR and TE-GTR.

TABLE 3.6: CHARACTERIZATION OF THE E-GTR AND TE-GTR.

Parameter <sup>a</sup>	E-GTR	SE <sup>d</sup> (Number of observations)	TE-GTR	SE (Number of observations)
Sol-fraction (s) % (wt%)	1.08	0.05 (16)	8.3	0.2 (3)
Gel-fraction (g) % (wt%)	98.78	0.06 (16)	91.12	0.03 (3)
Crosslink density, ( $\nu_e$ ) (mmol/cm <sup>3</sup> )	0.082	0.005 (11)	0.037	0.001 (3)
Sulfur % (wt%)	2.29	0.04 (5)	2.69	0.03 (4)
$M_n$ (Da) <sup>b</sup>	7000	300 (3)	5200	300 (3)
PDI <sup>c</sup>	2.01	0.1 (3)	2.68	0.03 (3)

<sup>a</sup>All parameters were determined on sample extracted with hot acetone and then dried.

<sup>b</sup>The number average molecular weight,  $M_n$

<sup>c</sup>Poly dispersity index.

<sup>d</sup>Standard error.

All these parameters were useful to evaluate the yield of devulcanization reaction. Each parameter of TE-GTR significantly differed from the ones determined for E-GTR (t-test, confidence level at 95 %).

The degree of devulcanization was calculated as:

$$\% \text{ Devulcanization} = \left(1 - \frac{\nu_f}{\nu_i}\right) * 100 \quad (\text{EQUATION 3.8})$$

where  $\nu_f$  and  $\nu_i$  are the crosslink density of the material after devulcanization and of the initial material. This percentage was  $55 \pm 6$  %.

The reduction of the crosslink density showed that the devulcanization reaction had occurred. The increase of the sol fraction, the decrease of the  $M_n$  and the increase of PDI confirm that during the treatment a partial main chain scission occurred. During this process, it was possible to reach a substantial degree of devulcanization and low sol fraction indicating an efficient crosslink scission.

In order to confirm that devulcanization took place, the Horikx function based on the main chain breakage for the GTR was analyzed and compared to the

experimental data (Figure 3.5). It is seen that experimental results lie above the Horikx function. Therefore, it can be concluded that the scCO<sub>2</sub> treatment preferentially cleaved the crosslink network with some breakage of the main chain.

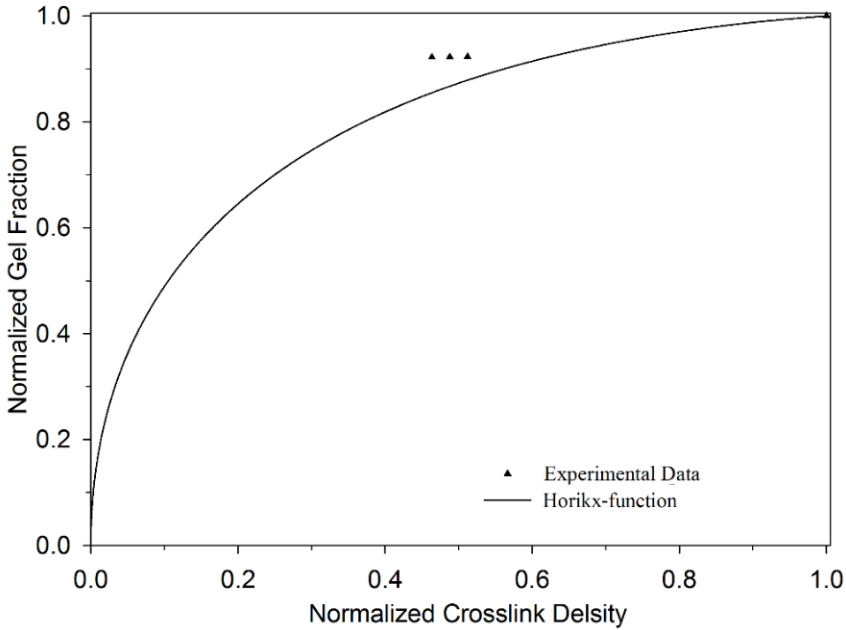


FIGURE 3.5: NORMALIZED GEL FRACTION AS A FUNCTION OF NORMALIZED CROSSLINK DENSITY COMPARED TO THE HORIKX FUNCTION.

Furthermore, the dependence of experimental normalized gel fraction  $GF_f/GF_i$  versus the normalized crosslink density  $v_f/v_i$  was analyzed using the following model [11,19-21]:

$$\frac{GF_f}{GF_i} = \left(1 + \zeta * \frac{v_f}{v_i}\right) * H * \left\{\left(\frac{v_f}{v_i}\right) - e^{(-1/\zeta)}\right\} \quad (\text{EQUATION 3.9})$$

where H represents the Heaviside step function [22].

A good fit ( $R^2 = 0.99$ ) between the experimental data and Equation 3.9 was obtained with  $\zeta = 0.108$ . The  $\zeta$  parameter represents the change of normalized gel fraction with respect to change in normalized crosslink density that is affected by the relative amounts of intermolecular bond breakage and main chain bond breakage [22]. It can be seen that a decrease in the normalized crosslink density

by about 50 %, corresponds to a decrease in the gel fraction by only 10 %, confirming that the treatment preferentially generated the rupture of the crosslink network.

These results support the hypothesis that crosslink network scission occurred during the devulcanization and that the DD mainly reacted with the crosslink network rather than with the main chain.

Both E-GTR and TE-GTR were investigated through ATR; the spectra are shown in Figure 3.6. The two absorption peaks at  $1450\text{ cm}^{-1}$  and  $1375\text{ cm}^{-1}$ , assigned to  $\delta\text{CH}_2$  and  $\delta\text{CH}_3$  deformation in the rubber backbone did not show any difference between the two samples. Nevertheless, the absorption peak at  $2920\text{ cm}^{-1}$ , assigned to CH saturated stretching vibration, was strengthened in the TE-GTR spectra [23,24]. Two new peaks appeared at  $730$  and at  $690\text{ cm}^{-1}$ . These peaks have been assigned to the CH bending in the monosubstituted benzene and a weak peak at  $1580\text{ cm}^{-1}$ , assigned to the aromatic C=C stretching vibration, appeared. Moreover, in the TE-GTR spectrum (Figure 3.6) the peak at  $960\text{ cm}^{-1}$ , assigned to the  $-\text{CH}=\text{CH}-$  (trans) bending, was strengthened [25].

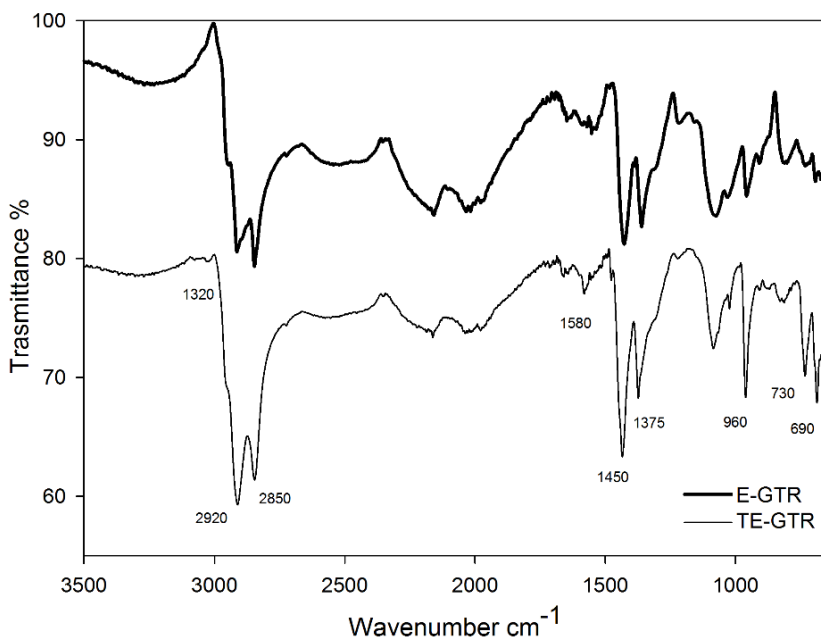


FIGURE 3.6: ATR SPECTRA OF E-GTR AND TE-GTR.

These peaks confirmed that the DD exhibits a radical addition mechanism, which provide the crosslink cleavage with the incorporation of the benzene

sulfide radical into the rubber structure. Moreover, the increase of sulfur observed in the TE-GTR (Table 3.6) seems to confirm this crosslink cleavage mechanism [4,6].

In order to understand this peak variation, the hot acetone and cold toluene extracts of T-GTR were analyzed in GC-MSD. The presence of thiophenols supports the proposed reaction mechanism for NR [26]. This mechanism foresees an initial thermal decomposition of the DD to give benzene sulfide radicals that can abstract the allylic hydrogen from the natural rubber chain to form benzenethiol or give addition reaction to the double bonds. After that, the polymer radical can undergo the crosslink network scission, but also the main-chain degradation. This process and the high temperature explain the observed increase in C=C groups. Figure 3.7 shows a simplified scheme for the radical reactions between the NR and the DD. The same reactions could be observed for the synthetic rubber.

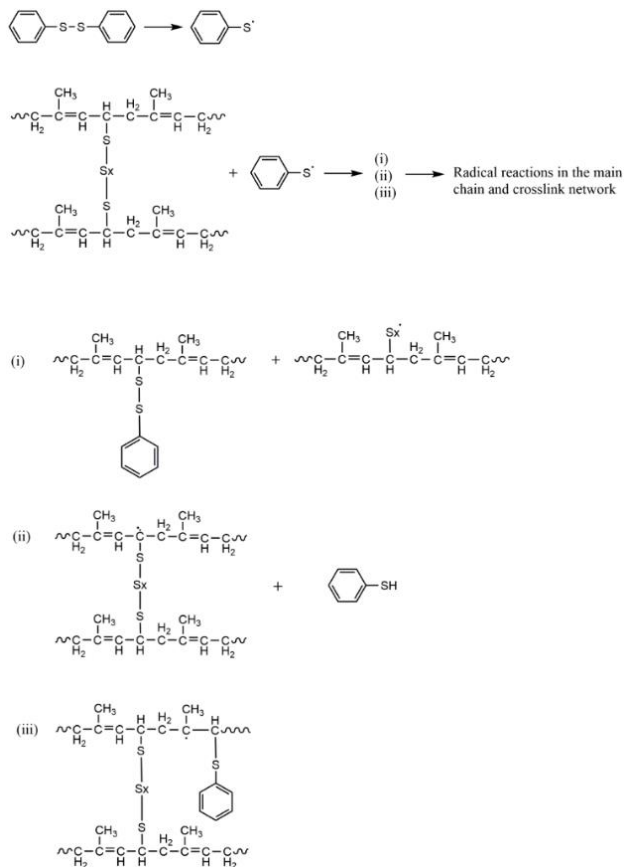


FIGURE 3.7: REACTION SCHEME FOR THE DD AND NR.

### 3.2.3 MECHANICAL PROPERTIES OF VULCANIZED COMPOUNDS (VULCANIZATES)

Stress-strain curves of different vulcanizates are shown in Figure 3.8.

Figure 3.9 shows the moduli at 100 % and at 300 %, the tensile strength and the elongation at break as a function of the devulcanized rubber content (phr) in the vulcanizates.

These mechanical properties displayed that vulcanizates with various amounts of GTR exhibited worse properties than the reference one with NR, as already observed [27-29]. Only the elongation at break of T-GTR was higher than the reference.

While the tensile strength and the elongation at break of the vulcanizate containing T-GTR were higher than the properties of vulcanizate containing GTR, the opposite was observed for moduli at 100 % and at 300 % of elongation. These results indicated that the devulcanization treatment affected the mechanical properties.

In order to evaluate the influence of the devulcanizing agent on the mechanical properties of the vulcanizates, both GTR and T-GTR were extracted with hot acetone, dried and then compounded. From the comparison between the vulcanizates containing GTR and E-GTR at various phr, it can be seen that the extraction process adversely affected all the mechanical properties of the vulcanizates. This is probably due to the removal of most additives from the tire rubber.

To evaluate the effect of residual DD during the revulcanization reaction on mechanical properties, the vulcanizate containing T-GTR was compared to the vulcanizate with TE-GTR. While the tensile strength and the elongation at break of the vulcanizate containing T-GTR were higher than the properties of vulcanizate containing TE-GTR, the opposite was observed for moduli at 100 % and at 300 % of elongation (Figure 3.9). Therefore, the treatment partially balanced the worsening of mechanical properties due to the removal of additives. Indeed, all mechanical properties of vulcanizate containing TE-GTR were higher than the properties of vulcanizate containing E-GTR (Figure 3.9). These results showed that the treatment with DD increases the compatibility of the gel fraction with the rubber.

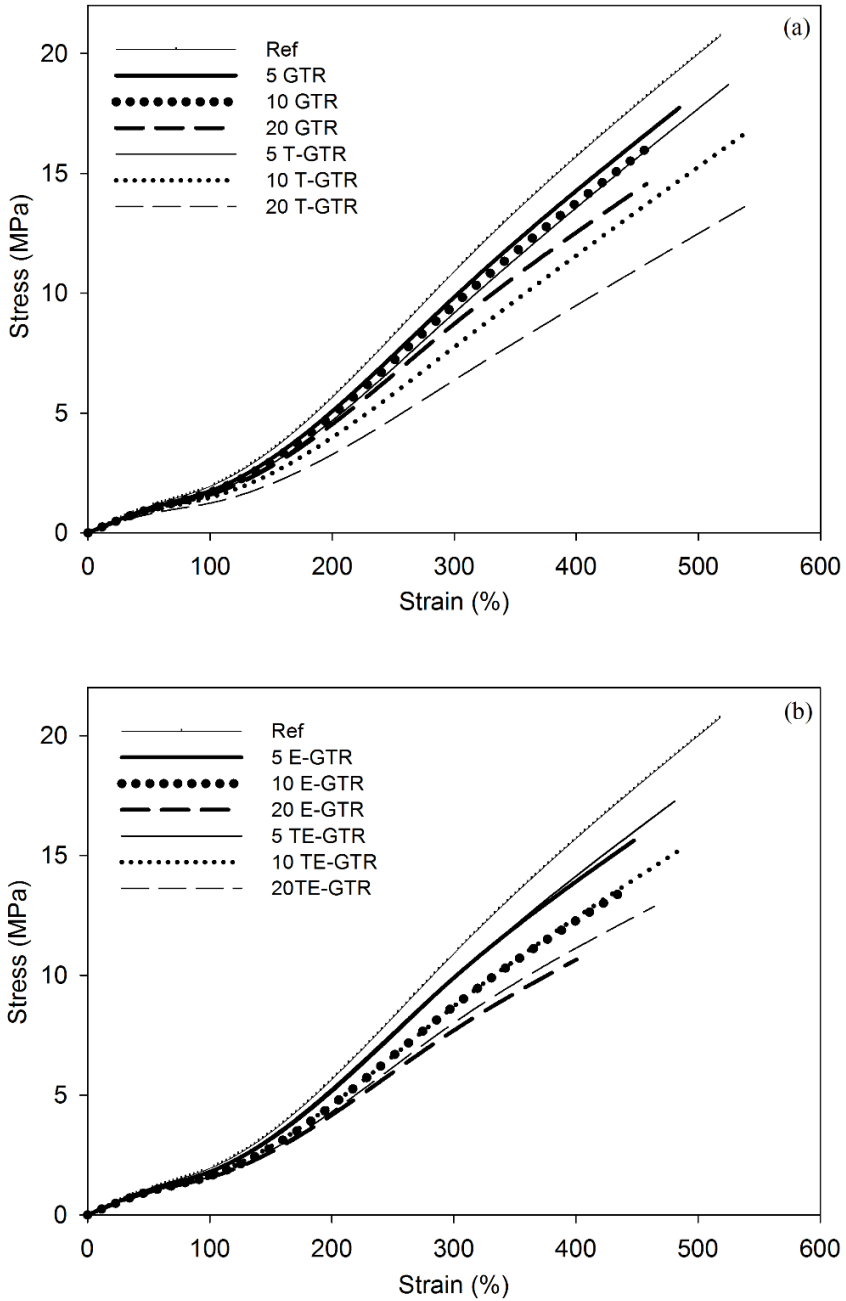


FIGURE 3.8: STRESS-STRAIN CURVES FOR NR VULCANIZATE COMPOUND AND VULCANIZED COMPOUNDS CONTAINING VARIOUS AMOUNTS OF (a) GTR / T-GTR AND (b) E-GTR / TE-GTR.

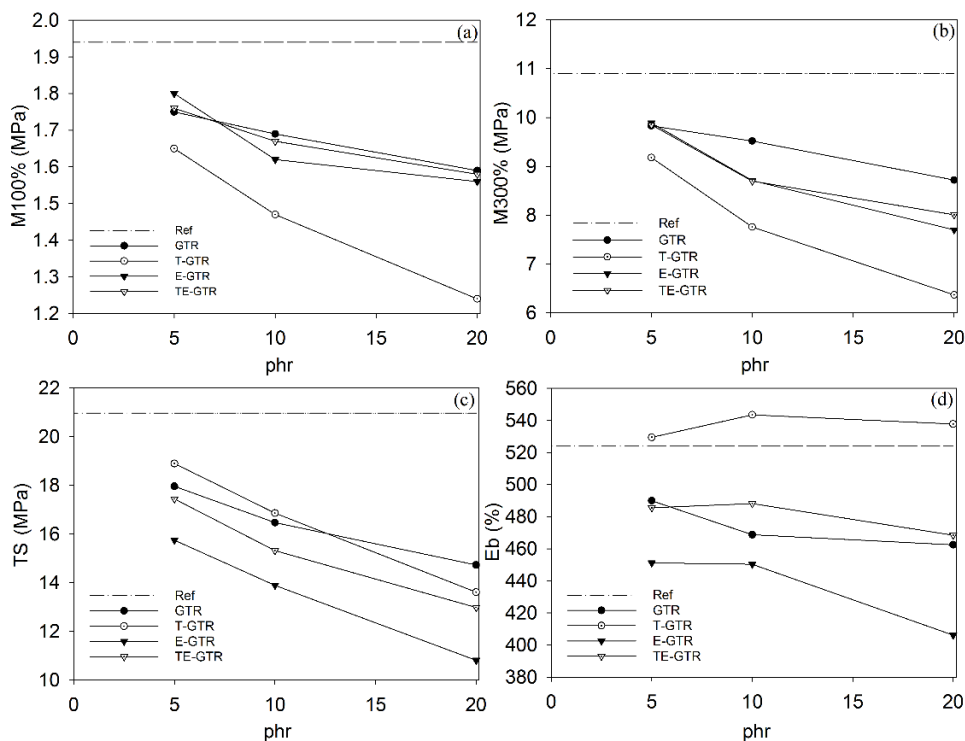


FIGURE 3.9: MODULI AT (A) 100% AND AT (B) 300% ELONGATION, (C) TENSILE STRENGTH AND (D) ELONGATION AT BREAK AS A FUNCTION OF THE DEVULCANIZED RUBBER CONTENT (PHR).

### 3.2.4 CURING BEHAVIOR OF COMPOUNDS

The curing behavior was also analyzed in order to investigate the effect of the DD on the revulcanization process. The maximum ( $M_H$ ), minimum torque ( $M_L$ ) and the differences between them ( $\Delta M$ ) were considered. Figure 3.10 and Figure 3.11 show that  $M_H$  and  $\Delta M$  were strongly influenced by two factors: the amount of GTR and the presence of DD.

The hot acetone extraction of the devulcanized rubber influenced the revulcanization behavior by decreasing the  $M_H$  and the  $\Delta M$  (Figure 3.11). Moreover,  $M_H$  and  $\Delta M$  decreased with the increase of the amount of GTR due to the presence of the crosslinked network hindering the revulcanization process [30]. Comparing the behavior of E-GTR and TE-GTR, the two samples exposed to the same extraction treatment, it can be seen that  $M_H$  and the  $\Delta M$  resulted higher for the compound containing TE-GTR rather than for the compound containing E-GTR. This represents an evidence that the gel fraction of the TE-GTR contained more active sites than E-GTR that could be cured. Moreover, the low



amount of sol fraction obtained with this process did not have any influence on the torque and therefore on the revulcanization process. As a result, it is clear that the DD had a strong influence on the revulcanization as well as on the mechanical properties.

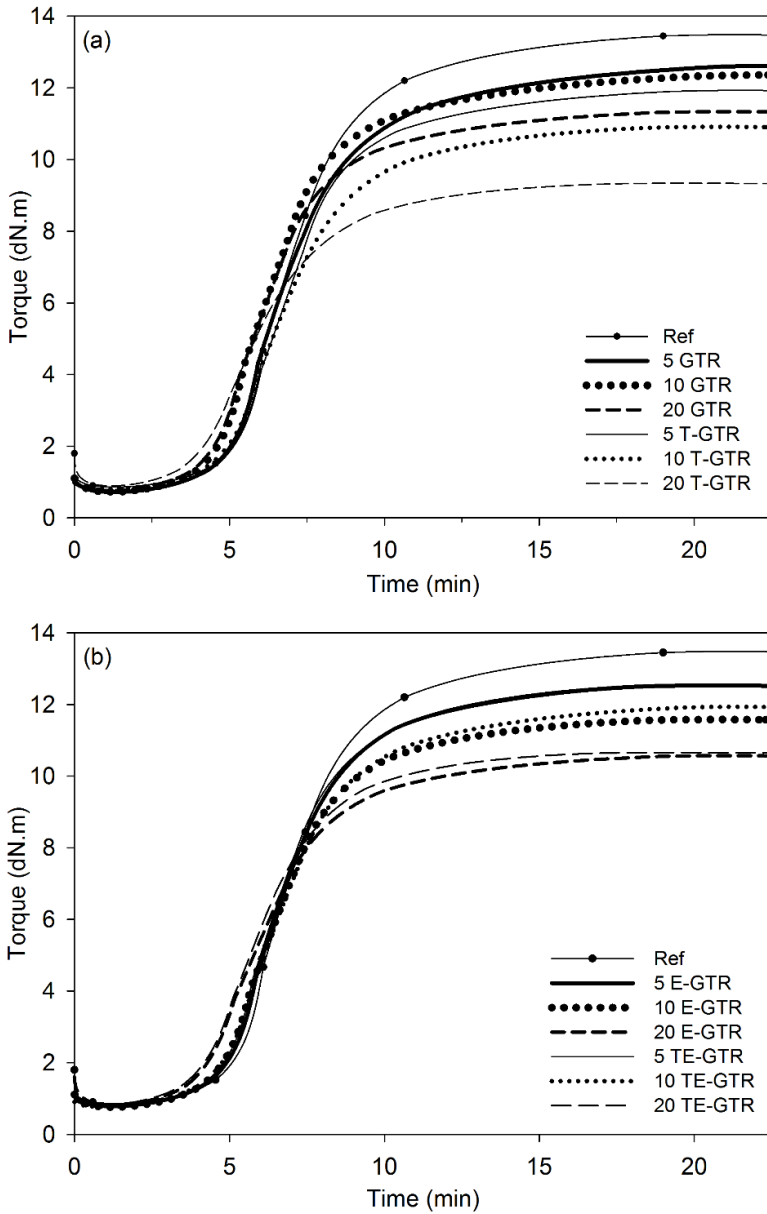


FIGURE 3.10: CURING CURVES FOR NR COMPOUND AND COMPOUNDS CONTAINING VARIOUS AMOUNTS OF (a) GTR / T-GTR AND (b) E-GTR / TE-GTR.

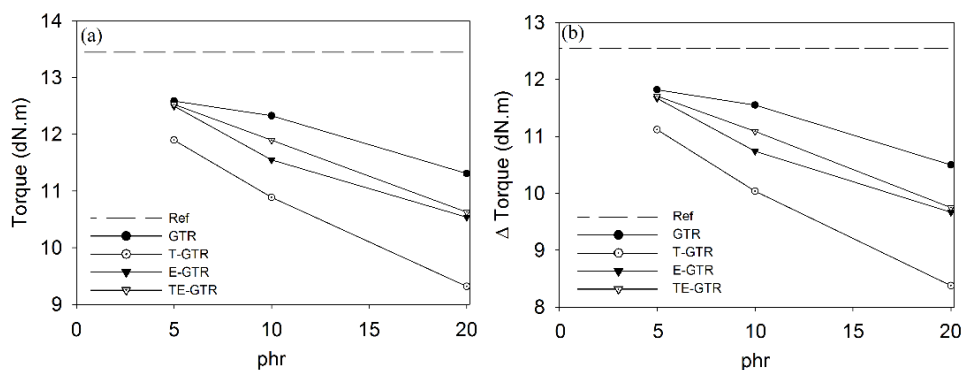


FIGURE 3.11: (a) MAXIMUM TORQUE ( $M_H$ ) AND (b)  $\Delta M$  AS A FUNCTION OF THE DEVULCANIZED RUBBER CONTENT (PHR).

Rajan et al. [29] analyzed the effect of disulfide used as a devulcanizing agent on the revulcanization process. They observed that the presence of an excess of a diphenyl disulfide deteriorates the tensile strength and the elongation at break, but at the same time increases the moduli values. In this study, the large deterioration observed on properties is probably due to the large amount of the DD used in the GTR scCO<sub>2</sub> devulcanization process. At the same time, the effect of the DD on the reduction of maximum torque and on the revulcanization process observed in our experiments was lower than the effect observed on the butyl rubber by Jang et al. [6]. This is probably due to the different chemical structure of the rubber, indeed the NR contains higher unsaturation than butyl rubber.

### 3.3 CONCLUSIONS

In this chapter, the GTR was characterized and subsequently devulcanized using scCO<sub>2</sub> as a solvent and DD as a devulcanizing agent.

The results support the idea that the crosslink network scission occurred during the treatment and that the DD mainly reacts with the crosslink network rather than with the main chain. Nevertheless, the unreacted DD can affect the process of revulcanization and the mechanical properties of the vulcanizates containing the devulcanized GTR, in particular increasing the elongation at break and decreasing the modulus. For this reason, the mechanical properties of the vulcanizates containing devulcanized GTR and unreacted DD cannot be compared with the original material, even though the resulting material undergoes a preferential breakage of crosslink network. The most limiting factor for this devulcanization process is the amount of DD left in the devulcanized GTR.

## REFERENCES

1. I. Mangili, E. Collina, M. Anzano, D. Pitea, M. Lasagni; Characterization and supercritical CO<sub>2</sub> devulcanization of cryo-ground tire rubber: Influence of devulcanization process on reclaimed material. *Polymer Degradation and Stability* 2014;102:15–24.
2. M. Kojima, S. Kohjiya, Y. Ikeda; Role of supercritical carbon dioxide for selective impregnation of decrosslinking reagent into isoprene rubber vulcanizate. *Polymer* 2005;46:2016-2019.
3. M. Kojima, M. Tosaka, Y. Ikeda; Chemical recycling of sulfur-cured natural rubber using supercritical carbon dioxide. *Green Chemistry* 2004;6:84-89.
4. M. Kojima, M. Tosaka, Y. Ikeda, S. Kohjiya; Devulcanization of carbon black filled natural rubber using supercritical carbon dioxide. *Journal of Applied Polymer Science* 2005;95:137-143.
5. M. Kojima, K. Ogawa, H. Mizushima, M. Tosaka, S. Kohjiya, Y. Ikeda; Devulcanization of sulfur-cured isoprene rubber in supercritical carbon dioxide. *Rubber Chemistry and Technology* 2003;76:957-968.
6. K. Jiang, J. Shi, Y. Ge, R. Zou, P. Yao, X. Li, L. Zhang; Complete devulcanization of sulfur-cured butyl rubber by using supercritical carbon dioxide. *Journal of Applied Polymer Science* 2012;127:2397-2406.
7. J. Shi, K. Jiang, D. Ren, H. Zou, Y. Wang, X. Lv, L. Zhang; Structure and performance of reclaimed rubber obtained by different methods. *Journal of Applied Polymer Science* 2013;129:999–1007.
8. P.J. Flory, J.Jr. Rehner; Statistical mechanics of cross-linked polymer networks, I and II. *The Journal of Chemical Physics* 1943;11:512-520 and 521-526.
9. J.L. Valentín, J. Carretero-González, I. Mora-Barrantes, W. Chassé, K. Saalwächter; Uncertainties in the determination of crosslink density by equilibrium swelling experiments in Natural Rubber. *Macromolecules* 2008;41:4717-4729.
10. G. Kraus; Swelling of filler-reinforced vulcanizates. *Journal of Applied Polymer Science* 1963;7:861-871.
11. E. Bilgili, H. Arastoopour, B. Bernstein; Pulverization of rubber granulates using the solid state shear extrusion process Part II. Powder characterization. *Powder Technology* 2001;115:277–289.
12. H. Yazdani, I. Ghasemi, M. Karrabi, H. Azizi, G.R. Bakhshandeh; Continuous devulcanization of waste tires by using a co-rotating twin screw extruder:

- Effects of screw configuration, temperature profile, and devulcanization agent concentration. *Journal of Vinyl Additives Technology* 2013;19:65-72.
13. G.K. Jana, R.N. Mahaling, C.K. Das; A novel devulcanization technology for vulcanized natural rubber. *Journal of Applied Polymer Science* 2006;99:2831-2840.
  14. G. Jiang, S. Zhao, W. Li, J. Luo, Y. Wang, Q. Zhou, C. Zhang; Microbial desulfurization of SBR ground rubber by *Sphingomonas* sp. and its utilization as filler in NR compounds. *Polymer for Advanced Technologies* 2010;22:2344-2351.
  15. K. Huang, A.I. Isayev; Ultrasonic decrosslinking of crosslinked high-density polyethylene: Effect of degree of crosslinking. *RSC Advances* 2014; 4:38877–38892.
  16. M.M. Horikx; Chain scissions in a polymer network. *Journal of Polymer Science* 1956;19:445-454.
  17. M.R. Islam, H. Haniu, J. Fardoushi; Pyrolysis kinetics behavior of solid tire wastes available in Bangladesh. *Waste Management* 2009;29:668–677.
  18. N. Delaunay-Bertoncini, F.W.M. van der Wielen, P. de Voodt, B. Erlandsson, P.J. Schoenmakers; Analysis of low-molar-mass materials in commercial rubber samples by Soxhlet and headspace extractions followed by GC-MS analysis. *Journal of Pharmaceutical and Biomedical Analysis* 2004;35:1059-1073.
  19. X. Sun, A.I. Isayev; Ultrasound devulcanization: Comparison of synthetic isoprene and natural rubbers. *Journal of Material Science* 2007;42:7520-7529.
  20. S. Ghose, A.I. Isayev; Ultrasonic devulcanization of carbon black filled polyurethane rubber. *Journal of Elastomers Plastics* 2004;36:213-239.
  21. V.V. Yashin, A.I. Isayev; A model for rubber degradation under ultrasonic treatment: PartII. Rupture of rubber network and comparison with experiments. *Rubber Chemistry and Technology* 2000;73:325-338.
  22. A.I. Isayev, S.P. Yushanov, S.H. Kim, V.L. Levin; Ultrasonic devulcanization of waste rubbers: Experimentation and modeling. *Rheologica Acta* 1996; 35:616-630.
  23. Y. Li, S. Zhao, Y. Wang; Microbial desulfurization of ground tire rubber by *Thiobacillus ferrooxidans*. *Polymer Degradation and Stability* 2011;96:1662-1668.

24. S. Mitra, A. Ghanbari-Siahkali, P. Kingshott, H.K. Rhemeier, H. Abildgaard, K. Almdal; Chemical degradation of crosslinked ethylene-propylene-diene rubber in an acidic environment. Part I. Effect on accelerated sulfur crosslinks. *Polymer Degradation and Stability* 2006;91:69-80.
25. H. Si, T. Chen, Y. Zhang; Effects of high shear stress on the devulcanization of ground tire rubber in a twin-screw extruder. *Journal of Applied Polymer Science* 2013;128:2307–2318.
26. V.V. Rajan, W.K. Dierkes, R. Joseph, J.W.M. Noordermeer; Science and technology of rubber reclamation with special attention to NR-based waste latex products. *Progress in Polymer Science* 2006;31:811-834.
27. S. Li, J. Lamminmäki, K. Hanhi; Effect of ground rubber powder on properties of natural rubber. *Macromolecular Symposia* 2004;216:209-216.
28. A.K. Naskar, S.K. De, A.K. Bhowmick, P.K. Pramanik, R. Mukhopadhyay; Characterization of ground rubber tire and its effect on natural rubber compound. *Rubber Chemistry and Technology* 2000;73:902-911.
29. V.V. Rajan, W.K. Dierkes, R. Joseph, J.W.M. Noordermeer; Recycling of NR based cured latex material reclaimed with 2,2'-dibenzamidodiphenyldisulphide in a truck tire tread compound. *Journal of Applied Polymer Science* 2006;102:419-426.
30. G.K. Jana, R.N. Mahaling, T. Rath, A. Kozolowska, M. Kozolowski, C.K. Das; Mechano-chemical recycling of sulfur cured natural rubber. *Polimery* 2007;52:131-136.



## 4 MODELING AND INVESTIGATION OF SUPERCRITICAL CO<sub>2</sub> DEVULCANIZATION

---

As shown in Chapter 3, the scCO<sub>2</sub> devulcanization process in presence of DD has been found to be active and selective. Therefore, a 2<sup>4</sup> factorial design is employed in the present chapter both to investigate the scCO<sub>2</sub> devulcanization process behavior in a wider experimental domain and to investigate the influence of temperature, pressure, amount of devulcanizing agent, treatment time and their interactions on the devulcanization process. The obtained results shown in this chapter has been published in The Journal of Supercritical Fluids (2014) [1].

---

### 4.1 INTRODUCTION

For process improvement, it is usually necessary to consider how a number of input variables, such as temperature, feed rate, concentration, etc. can simultaneously influence the experimental responses. The use of statistical experimental design allows to get a clear picture of how these process variables behave separately and together on the experimental responses and how it is possible to control them in order to make the process more effective [2].

The present chapter presents a statistical approach for studying the GTR devulcanization using a *green* devulcanization process employing scCO<sub>2</sub> as a reaction medium and diphenyl disulfide (DD) as a devulcanizing agent.

Most of the previous studies were carried out in order to find the best devulcanizing conditions, analyzing the process variables just considering one variable at a time (OVAT) [3-6]. In OVAT approach, the variables that could possibly affect the performance of the process are kept at a fixed level except for one, which is varied until the best conditions are reached. These studies showed that temperature (T), pressure (P), amount of DD and treatment time (rt) were the variables that can mainly affect the devulcanization process, especially decreasing the crosslink density and increasing the sol fraction of the devulcanized rubber. However, this approach does not allow exploring the influence of the interaction among variables on the responses.

Thus, an experimental design approach is implemented in the present chapter in order to investigate the devulcanization process.

## 4.2 MATERIALS AND METHODS

### 4.2.1 DESIGN OF EXPERIMENTS

A two-level full factorial experimental design [2,7,8] has been chosen to investigate the effect of each single variable and the interactions among them. The number of experiments necessary to carry out this design is  $N=L^k$ , where  $L$  represents the number of levels for the investigation (two in our case) and  $k$  represents the number of variables, or factors (four in our case).

Table 4.1 shows maximum (+1), minimum (-1) and central (0) levels for each variable used in the present study. These levels were chosen considering the type and properties of GTR, the maximum operating level for the equipment (400 °C and 70 MPa) and the CO<sub>2</sub> supercritical conditions (31.1 °C and 7.38 MPa [9]).

TABLE 4.1: FACTORS AND LEVELS OF THE EXPERIMENTAL DESIGN.

Factor Code	Min level -1	Max level 1	Central level 0
Temperature (°C)	70	190	130
Pressure (MPa)	8	24	16
Treatment time (min)	60	240	150
DD/rubber (wt%)	1	25	13

Sixteen experiments were carried out in order to investigate the experimental domain; three experiments were added to investigate the performance in the center of the experimental domain and to estimate the model validity, reproducibility and experimental error. A fully randomized execution of the nineteen experiments was carried out in order to minimize the error due to the planning of the experiments.

The crosslink density (CD), sol fraction (SF), gel fraction (GF) and sulfur content (SC) were chosen as experimental responses. The CD, SF and GF give information on the degree of devulcanization. SC is an important quantitative indicator of the reaction between DD and GTR.



The dependence of each experimental response,  $y$ , on the factors was modeled applying the following equation [2]:

$$y = \beta_0 + \sum_{i=1}^n \beta_i x_i + \sum_{i=1}^{n-1} \sum_{j=i+1}^n \beta_{ij} x_i x_j + \varepsilon \quad (\text{EQUATION 4.1})$$

where  $\beta_0$  is the constant term,  $\beta_i$  and  $\beta_{ij}$  are the regression coefficients,  $\varepsilon$  is the error,  $x_i$  and  $x_j$  are the variables and  $n$  is their number. The coefficients were determined by multiple linear regression.

The analysis of variance (ANOVA) is normally used to determine which factors and which interactions have a significant influence on the process. In our  $2^4$  factorial designs, the use of ANOVA is questionable to discriminate whether the factors and interactions are real [2]. Therefore, the relevance of the effects for the factors and two-factor interactions was also evaluated comparing each computed effect with the standard error (SE) through a t-test. The main and the interactive effects were calculated according to Box et al. [2].

The three central experiments were used to evaluate the experimental error and therefore the standard error for the effects through the following equation:

$$SE(\text{effect}) = \frac{2\sigma}{\sqrt{n}} \quad (\text{EQUATION 4.2})$$

where  $n$  is the total number of runs of the two-level factorial design and  $\sigma$  is the standard deviation of the central experiments. Moreover, under the assumption that higher-order interactions are largely due to noise, the effect of these interactions ( $b_k$ ) can provide a reference set for the estimation of the standard error. The standard error for main effects and two-factor interactions was also calculated applying following equation:

$$SE(\text{effect}) = \sqrt{\frac{\sum_{k=1}^5 (b_k)^2}{5}} \quad (\text{EQUATION 4.3})$$

In order to point out the best fitting model and to confirm the significant parameters for each experimental response, the step-wise approach was used to find the best combination of factors and interactions considering the

coefficient of determination ( $R^2$ ), the adjusted  $R^2$  and the coefficient of determination for prediction ( $Q^2$ ) [8,10].  $Q^2$  represents the leave-one-out cross-validated  $R^2$  in which the residual sum of squares is substituted by the predicted sum of squares.

The PRESS is calculated using the following equation:

$$PRESS = \sum_{i=1}^n (y_i - \hat{y}_{i\setminus i}) \quad (\text{EQUATION 4.4})$$

where  $\hat{y}_{i\setminus i}$  represents the predicted response estimated using a regression model calculated without the  $i$ -th observation.

The linear regression models (Equation 4.1), ANOVA and response surfaces were calculated by MODDE 6.0 (Umetrics, Umeå, Sweden) and MATLAB R2013 (The MathWorks Inc., Natick, USA).

#### 4.2.2 EXPERIMENTAL AND ANALYTICAL PROCEDURES

The GTR used in the present study was a cryo-ground rubber from truck tires, the same used and characterized in Chapter 3. The chemical reagents were the same used in Chapter 3.

A pre-treatment of GTR was necessary to remove all chemicals that could affect experimental determinations. Thus, GTR was first extracted in a Büchi Extraction System B-811 automatic Soxhlet with acetone for 16 h and then with chloroform for 4 h, according to ISO 1407 and ASTM D 297 standard methods. After the extraction, the powder was vacuum dried at 50 °C for 24 h.

The obtained GTR was mixed with DD and then treated in  $scCO_2$  at several conditions as planned in the experimental design (Table 4.2), in the same reactor shown in Figure 3.1.

TABLE 4.2: FULL FACTORIAL DESIGN AND EXPERIMENTAL RESPONSES.

Experiment	Factor					Response				
	rt (min)	DD/rubber (wt%)	T (°C)	P (MPa)	CD (mmol/cm <sup>3</sup> )	SF (wt%)	GF (wt%)	SC (wt%)		
E1	60	1	70	8	0.073	2.3	98.2	2.43		
E2	240	1	70	8	0.070	2.6	97.8	2.40		
E3	60	25	70	8	0.073	1.8	99.1	2.45		
E4	240	25	70	8	0.068	2.6	98.2	2.37		
E5	60	1	190	8	0.046	9.8	91.6	2.43		
E6	240	1	190	8	0.042	10.9	91.1	2.53		
E7	60	25	190	8	0.035	14.8	85.9	2.79		
E8	240	25	190	8	0.019	22.6	79.8	2.84		
E9	60	1	70	24	0.070	3.2	97.8	2.37		
E10	240	1	70	24	0.067	1.7	98.4	2.36		
E11	60	25	70	24	0.073	5.8	97.1	2.39		
E12	240	25	70	24	0.076	2.3	97.9	2.43		
E13	60	1	190	24	0.046	11.8	89.6	2.43		
E14	240	1	190	24	0.036	8.5	91.8	2.35		
E15	60	25	190	24	0.021	15.4	83.0	2.87		
E16	240	25	190	24	0.033	23.5	79.2	3.17		
Center 1	150	13	130	16	0.043	4.6	95.4	2.24		
Center 2	150	13	130	16	0.039	6.8	93.6	2.43		
Center 3	150	13	130	16	0.046	6.3	94.4	2.51		

After the devulcanization, each sample was extracted in acetone for 24 h to remove the excess of unreacted DD, dried again under vacuum and finally pressed in a two-roll mill at 40 °C keeping conditions constant in order to obtain 1-mm-thick sheets (TE-GTR). These sheets were suitable to be characterized avoiding loss of material, especially during swelling measurements. The crosslink density, sol fraction, gel fraction and sulfur content were determined on the TE-GTR. Every measurement was repeated at least three times.

Figure 4.1 shows the schematic of the procedure used for the treatment and characterization.

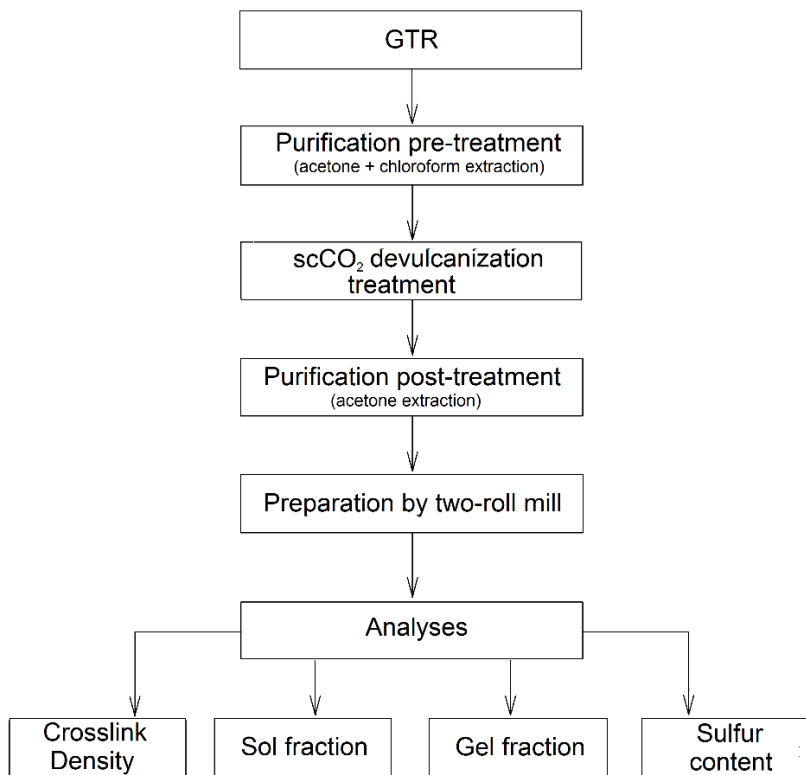


FIGURE 4.1: PROCEDURE USED FOR THE TREATMENT AND CHARACTERIZATION.

The crosslink density was determined according to ASTM D 6814-02 as shown in Chapter 3. Flory-Rehner equation and Kraus correction were applied considering the content of carbon black (Table 3.3) and the same parameters used in Chapter 3 [11-14].

Sol and gel fractions were evaluated through a 24-hour Soxhlet extraction using toluene as a solvent [15] and about 1 g of TE-GTR ( $W_i$ ). After this period of

time, the toluene extract was dried and weighed ( $W_{SF}$ ). The rubber sample was dried in vacuum oven for 24 h and weighed again ( $W_{GF}$ ). Sol and gel fraction were calculated as in Equation 3.4 and Equation 3.5.

Sulfur content was determined by CHNS elemental analysis as in Chapter 3.

## 4.3 RESULTS AND DISCUSSION

### 4.3.1 REGRESSION MODELS

The experimental conditions and the obtained responses are summarized in Table 4.2.

A preliminary regression model, evaluated for each response, was an interaction model including the four factors and all two-factor interactions [8]. Higher-order interactions were omitted since in real phenomena, the relevance of the effect decreases with the increase of the interaction order [2]. This assumption allowed excluding three- and four-factor interactions to privilege the quality of the model and to avoid over-fitting. Although not advisable, the ANOVA was carried out on this model, thus it was possible to point out which factors and interactions were statistically significant [7]. Table 4.3 shows the ANOVA for the four responses containing all the factors and two-factor interactions. The P-values of T, DD and their interaction (T \* DD) were lower than 0.05 and therefore these parameters proved to be significant [7].

The standard error, estimated by both the central points (Equation 4.2) and higher-order interactions (Equation 4.3), was also used to evaluate whether the effect of either factors or two-factor interactions were significant. Table 4.4 and Table 4.5 show the estimated effects, their standard error (SE) evaluated using the three central points and the higher-order interactions, respectively.

TABLE 4.3: ANALYSIS OF VARIANCE FOR THE INTERACTION MODEL.

Variable	DF <sup>a</sup>	CD		SF		GF		SC	
		S.S.	P-value	S.S.	P-value	S.S.	P-value	S.S.	P-value
Constant	1		<0.001		<0.001		<0.001		<0.001
rt	1	0.0422E-03	0.419	60.020E-01	0.360	41.010E-01	0.258	0.526E-02	0.596
DD	1	0.0169E-02	0.127	90.250	0.005	81.4510	<0.001	0.253	0.005
T	1	0.0533E-01	<0.001	56.406	<0.001	53.477E+01	<0.001	0.305	0.003
P	1	0.0100E-04	0.899	14.400E-01	0.647	29.760E-01	0.33	0.106E-02	0.811
rt * DD	1	0.0123E-03	0.659	17.222	0.138	88.510E-01	0.111	0.681E-02	0.547
rt * T	1	0.0625E-04	0.752	19.360	0.119	43.060E-01	0.247	0.127E-01	0.416
rt * P	1	0.0562E-03	0.354	65.020E-01	0.341	37.060E-01	0.280	0.276E-02	0.700
DD * T	1	0.0324E-02	0.046	66.423	0.012	82.3560	<0.001	0.214	0.008
T * P	1	0.0400E-04	0.800	42.200E-02	0.803	45.600E-02	0.695	0.681E-02	0.547
DD * P	1	0.025E-030	0.531	19.600E-01	0.594	13.810E-01	0.500	0.298E-01	0.225
Residuals	8	0.0465E-02		50.827		22.0910		0.138	
Total	18	0.0643E-01		82.447E+01		74.6437E+01		0.975	

<sup>a</sup> Degrees of freedom.

TABLE 4.4: ESTIMATED EFFECTS AND STANDARD ERROR (SE) CALCULATED THROUGH THE THREE CENTRAL EXPERIMENTS (EQUATION 4.2).

Effect	CD	SE	$t_{(2,0.05)} * SE$	SF	SE	$t_{(2,0.05)} * SE$	GF	SE	$t_{(2,0.05)} * SE$	SC	SE	$t_{(2,0.05)} * SE$
Average	0.053	± 0.002	± 0.009	8.7	± 0.6	± 2.6	92.3	± 0.5	± 2.2	2.54	± 0.07	± 0.30
rt	-0.003	± 0.002	± 0.009	1.2	± 0.6	± 2.6	-1.0	± 0.5	± 2.2	0.04	± 0.07	± 0.30
DD	-0.007	± 0.002	± 0.009	4.8	± 0.6	± 2.6	-4.5	± 0.5	± 2.2	0.25	± 0.07	± 0.30
T	-0.037	± 0.002	± 0.009	11.9	± 0.6	± 2.6	-11.6	± 0.5	± 2.2	0.28	± 0.07	± 0.30
P	-0.001	± 0.002	± 0.009	0.6	± 0.6	± 2.6	-0.9	± 0.5	± 2.2	0.02	± 0.07	± 0.30
rt * DD	0.002	± 0.002	± 0.009	2.1	± 0.6	± 2.6	-1.5	± 0.5	± 2.2	0.04	± 0.07	± 0.30
rt * T	-0.001	± 0.002	± 0.009	2.2	± 0.6	± 2.6	-1.0	± 0.5	± 2.2	0.06	± 0.07	± 0.30
rt * P	0.004	± 0.002	± 0.009	-1.3	± 0.6	± 2.6	1.0	± 0.5	± 2.2	0.03	± 0.07	± 0.30
DD * T	-0.009	± 0.002	± 0.009	4.1	± 0.6	± 2.6	-4.5	± 0.5	± 2.2	0.23	± 0.07	± 0.30
T * P	-0.001	± 0.002	± 0.009	-0.3	± 0.6	± 2.6	-0.3	± 0.5	± 2.2	0.04	± 0.07	± 0.30
DD * P	0.003	± 0.002	± 0.009	0.7	± 0.6	± 2.6	-0.6	± 0.5	± 2.2	0.09	± 0.07	± 0.30

TABLE 4.5: ESTIMATED EFFECTS AND STANDARD ERROR (SE) CALCULATED THROUGH HIGHER ORDER INTERACTIONS (EQUATION 4.3).

Effect	CD	SE	$t_{(5,0.05)} * SE$	SF	SE	$t_{(5,0.05)} * SE$	GF	SE	$t_{(5,0.05)} * SE$	SC	SE	$t_{(5,0.05)} * SE$
Average	0.053	± 0.003	± 0.008	8.7	± 1.2	± 3.1	92.3	± 0.6	± 1.5	2.54	± 0.05	± 0.13
rt	-0.003	± 0.003	± 0.008	1.2	± 1.2	± 3.1	-1.0	± 0.6	± 1.5	0.04	± 0.05	± 0.13
DD	-0.007	± 0.003	± 0.008	4.8	± 1.2	± 3.1	-4.5	± 0.6	± 1.5	0.25	± 0.05	± 0.13
T	-0.037	± 0.003	± 0.008	11.9	± 1.2	± 3.1	-11.6	± 0.6	± 1.5	0.28	± 0.05	± 0.13
P	-0.001	± 0.003	± 0.008	0.6	± 1.2	± 3.1	-0.9	± 0.6	± 1.5	0.02	± 0.05	± 0.13
rt * DD	0.002	± 0.003	± 0.008	2.1	± 1.2	± 3.1	-1.5	± 0.6	± 1.5	0.04	± 0.05	± 0.13
rt * T	-0.001	± 0.003	± 0.008	2.2	± 1.2	± 3.1	-1.0	± 0.6	± 1.5	0.06	± 0.05	± 0.13
rt * P	0.004	± 0.003	± 0.008	-1.3	± 1.2	± 3.1	1.0	± 0.6	± 1.5	0.03	± 0.05	± 0.13
DD * T	-0.009	± 0.003	± 0.008	4.1	± 1.2	± 3.1	-4.5	± 0.6	± 1.5	0.23	± 0.05	± 0.13
T * P	-0.001	± 0.003	± 0.008	-0.3	± 1.2	± 3.1	-0.3	± 0.6	± 1.5	0.04	± 0.05	± 0.13
DD * P	0.003	± 0.003	± 0.008	0.7	± 1.2	± 3.1	-0.6	± 0.6	± 1.5	0.09	± 0.07	± 0.13

Both this approach and the ANOVA, applied to each experimental response, identified the same significant factors and interactions. Temperature, content of DD and their interaction resulted the only significant parameters, while the other factors and interactions resulted negligible. The DD resulted unimportant only for the crosslink density, whereas T and their interaction resulted significant. However, even for this experimental response, the DD was considered in the final reduced model in order to preserve the hierarchy among factors.

A model is considered hierarchical if the presence of significant higher-order interactions or higher-order terms requires the inclusion of the lower-order terms within the higher-order ones.

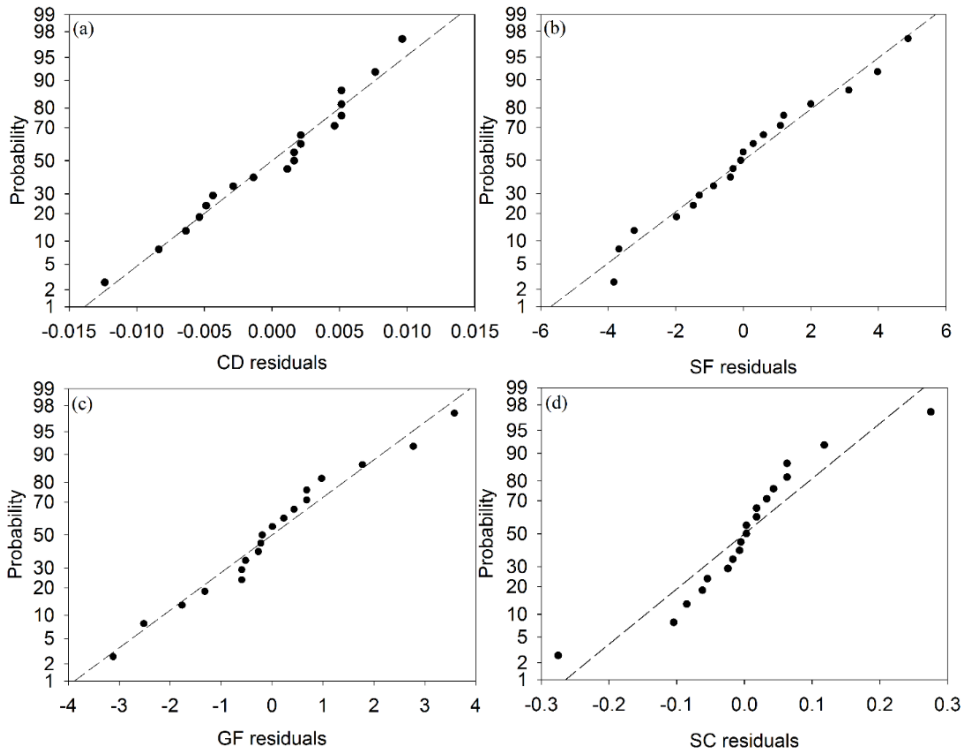
The effect of pressure was negligible; as a result, the treatment can be conducted at relatively low pressure. Nevertheless, pressure must be at least equal to the one of scCO<sub>2</sub>, since scCO<sub>2</sub> acts as the solvent media for the devulcanization reaction. Treatment time resulted the least important factor, indeed the devulcanization reaction employing DD involves radical reactions, resulting very fast in comparison to the tested treatment times. Therefore, a final reduced model was calculated by multiple linear regression for each experimental response, considering only significant factors and interactions. In order to confirm that the obtained models were the optimal ones, a stepwise approach was used to find the best combination of factors and interactions by evaluating the coefficient of determination for prediction ( $Q^2$ ).

Table 4.6 shows the regression coefficients and the coefficients of determination for each experimental response referred to the scaled and centered variables. The model obtained for the gel fraction exhibits the highest  $R^2$ ,  $Q^2$  and the smallest difference between these two coefficients, resulting in the best model. All final reduced regression models were statistically significant at 95 % and without any lack of fit considering the same probability [2]. Moreover, for a sound evaluation of models, the residuals distribution was studied. Figure 4.2 shows the normal probability plots of the residuals for each response. No evident anomalies are present for crosslink density (a), sol (b) and gel fractions (c). For sulfur content (d), two runs appear to be highly discrepant. Nevertheless, the normal distribution for residuals was confirmed by the Shapiro-Wilk normality test for 95 % confidence interval [16] for each response.



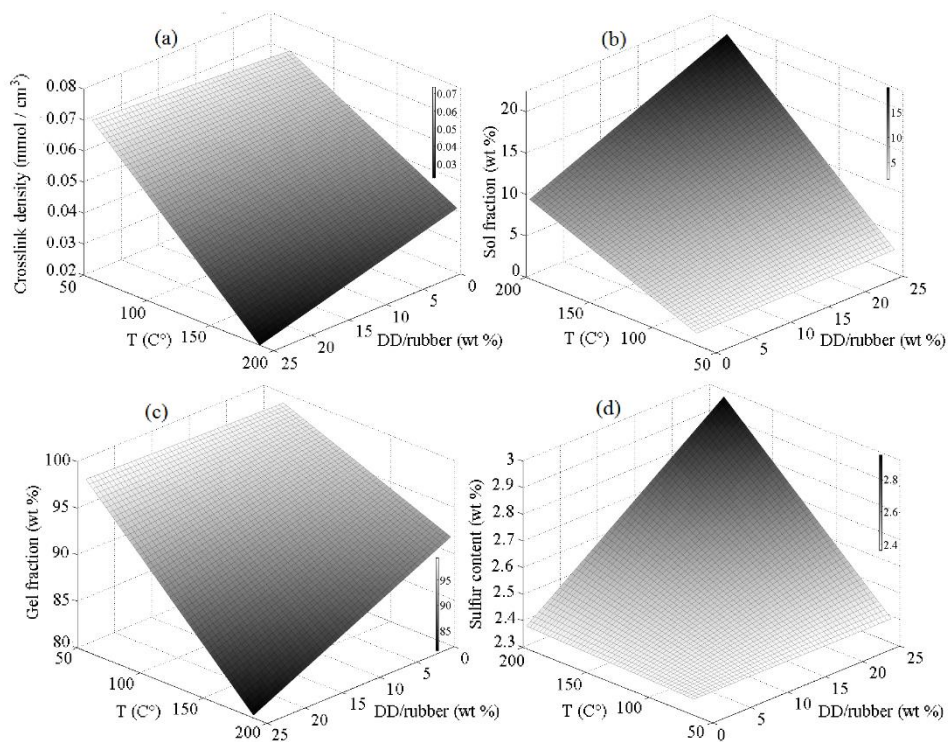
**TABLE 4.6: REGRESSION COEFFICIENTS WITH STANDARD ERROR (SE) AND COEFFICIENTS OF DETERMINATION FOR EACH EXPERIMENTAL RESPONSE REFERRED TO THE SCALED AND CENTERED VARIABLES.**

	Response			
	CD	SF	GF	SC
Constant	0.051	8.3	92.6	2.52
SE	0.001	0.6	0.4	0.03
DD	-0.003	2.4	-2.3	0.13
SE	0.002	0.7	0.4	0.03
T	-0.018	5.9	-5.8	0.14
SE	0.002	0.7	0.4	0.03
DD * T	-0.005	2.0	-2.3	0.12
SE	0.002	0.7	0.4	0.03
R <sup>2</sup>	0.91	0.87	0.94	0.79
R <sup>2</sup> adj	0.89	0.85	0.92	0.75
Q <sup>2</sup>	0.86	0.80	0.90	0.69



**FIGURE 4.2: NORMAL PROBABILITY PLOT OF RESIDUALS FOR (a) CROSSLINK DENSITY, (b) SOL FRACTION, (c) GEL FRACTION AND (d) SULFUR CONTENT.**

In order to visualize the influence of T and DD on the devulcanization process, a 3-D graph (Figure 4.3) was plotted for each experimental response using the reduced models. The plotted surfaces do not show any maximum. Temperature proved to be the most important factor for this devulcanization process, since high temperatures cause the degradation of the rubber network. A significant variation of responses was observed. Increasing the temperature, especially at high amounts of DD. Indeed, at high T values the decomposition of DD generates more benzene sulfide radicals [5,17,18], leading to the chain scission and crosslinks rupture, reducing the crosslink density, the gel fraction and increasing the sol fraction as shown in Figure 4.3 (a-c) [17]. These radicals react with the rubber chain and with the crosslink network increasing the sulfur content (Figure 4.3 d).



**FIGURE 4.3: 3-D PLOT FOR THE FOUR EXPERIMENTAL RESPONSES AS A FUNCTION OF DD AND T. (a) CROSSLINK DENSITY, (b) SOL FRACTION, (c) GEL FRACTION AND (d) SULFUR CONTENT. IN ORDER TO SHOW CLEARLY THE SURFACES TRENDS, FIGURES (c) AND (d) SHOW AXES WITH OPPOSITE DIRECTIONS.**

## 4.3.2 VALIDATION

A validation was carried out in order to test the reduced models predictive power within the studied domain. Indeed, for the optimization procedure and for future predictions, both a good descriptive and good predictive capacities of models are required.

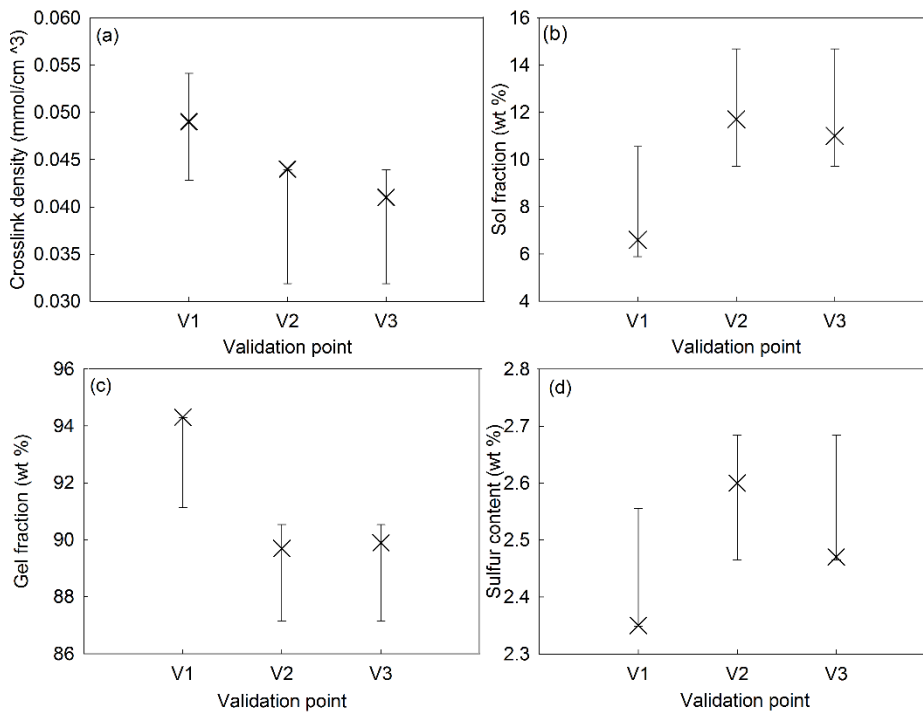
The leave-one-out cross validation was used for internal validation. In this procedure, each observation is predicted by the model without including that observation. The predictive power of the reduced regression models is given by  $Q^2$  (Table 4.6) which is based on this procedure [8,10] and it had already been used to select the best models.

In addition to the internal validation, a set of new experimental runs within the experimental domain (V1, V2 and V3 in Table 4.7) was predicted and compared to the experimental results. These experiments were chosen varying either the significant parameters for the final reduced models (T and DD) or the negligible ones (rt and P).

TABLE 4.7: VALIDATION EXPERIMENT CONDITIONS WITHIN THE STUDIED DOMAIN.

Experiment	Treatment time (min)	DD (wt%)	Temperature (°C)	Pressure (MPa)
V1	60	5	150	24
V2	60	10	180	24
V3	120	10	180	15

Figure 4.4 shows the experimental crosslink density, sol and gel fraction and sulfur content obtained for these validation points compared to the predicted values. It can be seen that each experimental value is contained within the models error bars, resulting in accordance with the predicted ones.



**FIGURE 4.4: VALIDATION EXPERIMENT RESULTS WITHIN THE MODELS ERROR BARS AT 99 % OF CONFIDENCE LEVEL.**

#### 4.4 CONCLUSIONS

The aim of the present chapter was to investigate the scCO<sub>2</sub> devulcanization process of a GTR by varying treatment time, temperature, percentage of devulcanizing agent DD and CO<sub>2</sub> pressure. A full factorial experimental design was used to define the experimental conditions within the variables domain and a set of four responses was used to characterize the devulcanized GTR. The experimental dataset was modeled by multiple linear regression. The most significant variables were temperature, amount of DD and their interaction. Regression models developed in the study resulted in a reliable prediction of devulcanization indicators within the experimental domain. Treatment time resulted the least important factor and the influence of pressure resulted negligible. The same evidence was not observed in previous studies performed on natural rubber and butyl rubber where pressure, treatment time, temperature and amount of devulcanizing agent had strong influence on the devulcanization reaction.

Indications regarding the reaction mechanism were also obtained. High T and decomposition of DD generate radicals that react with the rubber chain and with the crosslink network increasing the sulfur content of the TE-GTR.

These results have an important outcome since this devulcanization process can be carried out in a short time and at relatively low pressure, with subsequent energy saving.

## REFERENCES

1. I. Mangili, M. Oliveri, M. Anzano, E. Collina, D. Pitea, M. Lasagni; Full factorial experimental design to study the devulcanization of ground tire rubber in supercritical carbon dioxide. *The Journal of Supercritical Fluids* 2014;92:249-256.
2. G.P.E. Box, W.G. Hunter, J.S. Hunter; *Statistics for experimenters*, 2nd ed., Hoboken: Wiley, 1978.
3. M. Kojima, M. Tosaka, Y. Ikeda; Chemical recycling of sulfur-cured natural rubber using supercritical carbon dioxide. *Green Chemistry* 2004;6:84–89.
4. M. Kojima, M. Tosaka, Y. Ikeda, S. Kohjiya; Devulcanization of carbon black filled natural rubber using supercritical carbon dioxide. *Journal of Applied Polymer Science* 2005;95:137–143.
5. K. Jiang, J. Shi, Y. Ge, R. Zou, P. Yao, X. Li, L. Zhang; Complete devulcanization of sulfur-cured butyl rubber by using supercritical carbon dioxide. *Journal of Applied Polymer Science* 2012;127:2397-2406.
6. J. Shi, K. Jiang, D. Ren, H. Zou, Y. Wang, X. Lv, L. Zhang; Structure and performance of reclaimed rubber obtained by different methods. *Journal of Applied Polymer Science* 2013;129:999–1007.
7. P. Sutanto, F. Picchioni, L.P.B.M. Janssen; The use of experimental design to study the responses of continuous devulcanization processes. *Journal of Applied Polymer Science* 2006;102:5028-5038.
8. L. Eriksson, E. Johansson, N. Kettaneh-Wold, C. Wikström, S. Wold; *Design of experiments principles and applications*, 3rd ed., Umeå: Umetrics Academy, 2008.
9. M. Kojima, S. Kohjiya, Y. Ikeda; Role of supercritical carbon dioxide for selective impregnation of decrosslinking reagent into isoprene rubber vulcanizate. *Polymer* 2005;46:2016-2019.
10. I.E. Frank, R. Todeschini; *The data analysis handbook*, Amsterdam: Elsevier, 1994.

11. P.J. Flory, J.Jr. Rehner; Statistical mechanics of cross-linked polymer networks, I and II. *The Journal of Chemical Physics* 1943;11:512-520 and 521-526.
12. J.L. Valentín, J. Carretero-González, I. Mora-Barrantes, W. Chassé, K. Saalwächter; Uncertainties in the determination of crosslink density by equilibrium swelling experiments in Natural Rubber. *Macromolecules* 2008;41:4717-4729.
13. E. Bilgili, H. Arastoopour, B. Bernstein; Pulverization of rubber granulates using the solid state shear extrusion process Part II. Powder characterization. *Powder Technology* 2001;115:277–289.
14. G. Kraus; Swelling of filler-reinforced vulcanizates. *Journal of Applied Polymer Science* 1963;7:861-871.
15. X. Zhang, C. Lu, M. Liang; Properties of natural rubber vulcanizates containing mechanochemically de-vulcanized ground tire rubber. *Journal of Polymer Research* 2009;16:411–419.
16. S.S. Shapiro; M.B. Wilk; An analysis of variance test for normality (complete samples). *Biometrika* 1965;52:591-611.
17. V.V. Rajan, W.K. Dierkes, R. Joseph, J.W.M. Noordermeer; Science and technology of rubber reclamation with special attention to NR-based waste latex products. *Progress in Polymer Science* 2006;31:811-834.
18. G.K. Jana, R.N. Mahaling, T. Rath, A. Kozolowska, M. Kozolowski, C.K. Das; Mechano-chemical recycling of sulphur cured natural rubber. *Polimery* 2007;52:131-136.

## 5 MODELING AND INVESTIGATION OF ULTRASONIC DEVULCANIZATION

---

As shown in Chapter 2, both ultrasonic and twin-screw extrusion are well-known devulcanization techniques for tire rubber. In the present chapter, these techniques are combined, investigated and optimized. The process variables considered are those relevant for the two technologies, in particular the ultrasonic amplitude, screw speed, flow rate and temperature. Several responses, including crosslink density, gel fraction, complex viscosity of devulcanizates, tensile strength, modulus and elongation at break of revulcanizates are analyzed. A multi-response optimization is carried out through a desirability function approach in order to define the combination of factors that maximize the overall level of satisfaction with respect to the responses under study.

---

### 5.1 INTRODUCTION

The last decade gave birth to a green devulcanization process, employing ultrasound [1]. This process is carried out without involving any chemical, since ultrasound can generate cavitation leading to the rupture of three-dimensional network in the rubber matrix within a time of several seconds. Most of the previous studies investigated this devulcanization process using an ultrasonic single-screw extruder on several types of rubber, in particular, GTR, NR and various synthetic rubber. GTR represents an ideal raw material for the ultrasonic devulcanization, since it can be fed directly into the extruder. Recently, the incorporation of an ultrasonic device in a twin-screw extruder made the process more efficient [2]. The resulting devulcanized tire rubber can be directly compounded with curatives without adding virgin rubber and the revulcanized showed good mechanical properties [1,2].

Several researches have also investigated a devulcanization process based only on shear stress and high temperature produced in twin-screw extruders at several conditions and varying several screw configurations [3-8]. Most of these devulcanization studies were carried out in order to find the best devulcanization

conditions by analyzing the process parameters just considering one variable at a time [9]. Moreover, the devulcanization process on GTR in a twin-screw extruder was investigated using the response surface methodology (RSM) [10-13]. These studies mainly pointed out that temperature, screw shape, screw speed and flow rate have significant effect on the devulcanization process. Nevertheless, no ultrasonic devulcanization study was carried out by means of RSM.

Simulations of ultrasonic devulcanization based on physical modeling were performed in [14-16]. The complex nature of ultrasonic devulcanization of GTR, only led to a qualitative agreement between experimental and simulation results, indicating that the process model reported in Isayev et al. [14-16] was insufficient for the process optimization.

Another possibility to develop a process model of ultrasonic devulcanization of GTR is to carry out statistical modeling. The use of statistical experimental design and responses surfaces allows to get a clear picture of how the process variables behave both separately and cooperatively on the experimental responses and how it is possible to control them in order to make the process more effective [9]. Since all the previous physical approaches used to describe, predict and optimize the ultrasonic rubber devulcanization process resulted in complex systems, this statistical approach offers a useful tool for the optimization of this process within the studied domain for a multi-response situation.

The aim of the chapter is to investigate and optimize a multi-response ultrasonic devulcanization process of a GTR in co-rotating twin-screw extruder using the RSM based on central composite face-centered design (CCFD) [17,18]. A similar study using a more classical OVAT approach would require many more experiments, necessary to cover the experimental domain, without estimating the interaction effects among the variables and with the risk to locate the wrong optimum for each response [19,20].

The process variables considered in the present study were those that resulted to be significant in the aforementioned studies with the addition of the ultrasonic amplitude. Several responses, including crosslink density, gel fraction, complex viscosity of devulcanizates, tensile strength, modulus and elongation at break of revulcanizates were analyzed. A multi-response optimization was carried out through a desirability function approach.



## 5.2 MATERIALS AND METHODS

### 5.2.1 MATERIALS AND EQUIPMENT

The GTR used for the ultrasonic devulcanization was the same characterized in Chapter 3.

The devulcanization process was carried out in an ultrasonic co-rotating twin-screw extruder (Prism USALAB 16, Thermo Electron Co., UK) [2]. A water-cooled ultrasonic horn with an 800 W power supply (Branson 2000 bdc, Branson Ultrasonic Co., CT) was operating at 40 kHz, providing a longitudinal ultrasonic wave perpendicular to the flow direction of the material. The cross section of the horn had dimensions of 28x28 mm<sup>2</sup>. The gap between the horn tip and the screws was 2.5 mm and the volume of ultrasonic treatment zone was 1.54 cm<sup>3</sup>. Energy from a power supply was converted into mechanical energy for the devulcanization. The barrel temperature was monitored by several thermocouples inserted in the barrel. The flow rate was regulated by varying the material feeding rate.

The configuration of the screw elements is shown in Figure 5.1. Both screws were single-flighted with diameter of 16 mm and L/D ratio of 24. One reverse element was introduced after the ultrasonic zone to guarantee the complete filling of the ultrasonic treatment zone and to increase pressure and residence time of the GTR in this zone. The addition of more reverse elements resulted in extremely high torque.



FIGURE 5.1: SCHEMATIC OF THE SCREW CONFIGURATION.

### 5.2.2 DESIGN OF EXPERIMENTS

A central composite face-centered experimental design [17,18] has been chosen in the present study to model and optimize the ultrasonic devulcanization process and to analyze the effect of each variable, their interactions and second order terms. It is generated by combining a two-level full factorial design with axial experiments requiring a number of experiments equal to  $N = L^k + 2*k + N_c$ .  $L$  represents the number of levels for the investigation (two in our case),  $k$  represents the number of process variables, or factors (four in our case) and  $N_c$  is the number of central experiments.

Table 5.1 shows maximum (coded as +1), minimum (coded as -1) and central (coded as 0) levels for each process variable, including the ultrasonic amplitude (US), screw speed (SS), flow rate (FR) and temperature (T). Each level was chosen by carrying out several trial experiments, considering the type of GTR and the maximum operating level for the equipment in term of maximum torque, screw speed and temperature.

TABLE 5.1: FACTORS AND LEVELS OF THE EXPERIMENTAL DESIGN.

Factor, Units Code	Min level -1	Max level +1	Central level 0
Ultrasonic amplitude (US), $\mu\text{m}$	5	12	8.5
Screw speed (SS), rpm	150	250	200
Flow rate (FR), g/min	4	8	6
Temperature (T), $^{\circ}\text{C}$	130	210	170

Although just one or two center runs are required for central composite designs [18], four center runs were introduced in the experimental design considering one of the criteria reported by Draper [21]. He suggested to add at least four center runs for a face-centered central composite design. This number is required to achieve adequate pure error degrees of freedom and a reasonably sensitive lack of fit test [21]. The rotatability of central composite designs [17] was sacrificed in the present study by choosing the distance of axial experiments at  $\pm 1$ , due to the experimental complexity to carry out the axial experiments at different levels. Twenty-eight experiments were carried out to investigate the experimental domain. A fully randomized execution of experiments was carried out in order to minimize the error due to the planning of experiments.

The complex viscosity ( $\eta^*$ ), crosslink density (CD) and gel fraction (GF) were chosen as experimental responses in order to study the devulcanized GTR (D-GTR). The modulus at 100 % of elongation (M100), tensile strength (TS) and elongation at break (Eb) were chosen as experimental responses in order to study the properties of the revulcanized GTR (R-GTR).

A preliminary regression model, evaluated for each response, was a second order model containing the four factors, their squares and two-factor interactions. The dependence of each experimental response,  $y$ , on the factors was modeled by applying the following equation [17,18]:

$$y = \beta_0 + \sum_{i=1}^n \beta_i x_i + \sum_{i=1}^n \beta_{ii} x_i^2 + \sum_{i=1}^{n-1} \sum_{j=i+1}^n \beta_{ij} x_i x_j + \varepsilon \quad (\text{EQUATION 5.1})$$

where  $\beta_0$  is the constant term,  $\beta_i$ ,  $\beta_{ii}$  and  $\beta_{ij}$  are the coefficients,  $\varepsilon$  is the error,  $x_i$  and  $x_j$  are the variables (US, SS, FR and T) and  $n$  is the number of variables. The coefficients were determined by multiple linear regression.

The three-factor interaction terms were considered in case the experimental observations were not adequately fitted by the second order model (Equation 5.1), resulting in a poor model with low coefficients of determination or serious lack of fit. In these cases, the response surface could be more complex than the one defined by the second order approximation model given by Equation 5.1 [22-24].

Model term P-values from ANOVA and the coefficient of determination in prediction ( $Q^2$ ) were considered to achieve the best subset model.  $Q^2$  represents the leave-one-out cross-validated  $R^2$ , where the residual sum of square is replaced by the predicted residual sum of square (Equation 4.4) [25-27]. The terms whose P-value was higher than 0.1 were sequentially and systematically eliminated. The terms whose P-value was between 0.1 and 0.05 were kept in the model only if they contributed to an increase of the  $Q^2$  value. The best reduced model containing only the significant factors, interactions and second order terms was thus calculated for each experimental response. A validation was carried out in order to test the reduced models predictive power.

### 5.2.3 RESPONSES FOR THE DEVULCANIZED GTR (D-GTR)

The crosslink density, gel fraction and complex viscosity were determined on D-GTR. These measurements gave information on the degree of devulcanization. Each measurement was repeated at least three times.

Advanced Polymer Analyzer (APA 2000, Alpha Technologies, Akron, OH) was used to determine the dynamic properties of the D-GTR, in particular the complex viscosity. The frequency sweep analysis was carried out at 120 °C within a frequency range between 0.15 rad/s and 200 rad/s and a strain amplitude of 0.042.

The crosslink density was determined through swelling measurements. 1 g D-GTR ( $W_i$ ) was extracted for 24 h in standard Soxhlet using toluene as a solvent. After this period of time, the excess of solvent on the sample surface was removed with a paper towel and the swollen sample was weighed. Finally, the sample was dried in vacuum oven for 24 h and weighed again ( $W_{GF}$ ). Flory-Rehner equation and Kraus correction were calculated as in Chapter 3, considering the content of carbon black (Table 3.3) and the same parameters considered in Chapter 3 [28-31]. The gel fraction was also evaluated by the same Soxhlet extraction and it was calculated using Equation 3.5.

#### 5.2.3.1 HORIKX FUNCTION

In order to investigate in more detail the relative effect of degradation of the main chain and of the crosslink network, the dependence of experimental normalized gel fraction versus normalized crosslink density was analyzed and compared to the Horikx function for the main chain degradation (Equation 3.6).

#### 5.2.4 RESPONSES FOR THE REVULCANIZED GTR (R-GTR)

In order to investigate the mechanical properties, the D-GTR was homogenized and compounded with curatives using a two-roll mill (Reliable Rubber & Plastic Machinery Co., North Bergen, NJ) for 10 and 30 passes, respectively. The chemicals used for the compounding recipe were courteously donated by Akrochem Corporation (Akron, OH, USA) and were added as follows: 1 part per hundred of rubber (phr) powder N-cyclohexyl-2-benzothiazole sulfenamide, 1 phr rubbermakers sulfur, 1.25 phr RGT-M zinc oxide and 0.25 phr rubber grade stearic acid, based on 100 phr of D-GTR.

The curing behavior of the D-GTR samples at 160 °C was studied using the APA 2000 by performing a time sweep, at a frequency of 10 rad/s and a strain amplitude of 0.042. The resulting curves were used to evaluate the optimal curing time for the tensile test. R-GTR sheets of 15x15 cm<sup>2</sup> with thickness varying from 2.2 to 3.5 mm were prepared using a compression-molding press (Carver, Wabash, IN) at the optimum cure time ( $t_{95}$ ). The dumbbell shape specimens for tensile test (type C in the ASTM D 412 standard method) were cut out from those sheets. Mechanical properties were measured at room temperature using tensile testing machine (Instron tensile tester, Model 5567, Instron), following the ASTM D 412 standard method, at an elongation rate of 500 mm/min. Tensile strength, modulus at 100 % of elongation and elongation at break were evaluated on at least five R-GTR samples.

## 5.2.5 OPTIMIZATION

Desirability functions were used to define the optimum condition for the treatment [32]. The desirability function approach ( $d_i$ ) assigns numbers ranging between 0 and 1 for each response  $y_i(x)$ . The individual desirability functions are then combined in order to find the most desirable condition with respect to all the responses. Two different desirability functions were employed to maximize the overall level of satisfaction with respect to all the responses.

## 5.2.5.1 DERRINGER AND SUICH DESIRABILITY FUNCTIONS

Three different types of desirability functions exist according to the response characteristics [33]. Each of them transforms the response for each combination of experimental conditions into a value lying between 0 and 1, where 1 is the best condition and 0 represents the worst one. The nominal-the-best (NTB), the larger-the-best (LTB) and the smaller-the-best (STB) desirability functions, are respectively calculated as:

$$d_i(x) = \begin{cases} \left( \frac{\hat{y}_i(x) - y_i^{\min}}{T_i - y_i^{\min}} \right)^s, & y_i^{\min} < \hat{y}_i(x) < T_i \\ \left( \frac{\hat{y}_i(x) - y_i^{\max}}{T_i - y_i^{\max}} \right)^t, & T_i < \hat{y}_i(x) < y_i^{\max} \\ 0, & (\text{otherwise}) \end{cases} \quad \text{NTB} \quad (\text{EQUATION 5.2})$$

$$d_i(x) = \begin{cases} 0, & \hat{y}_i(x) \leq y_i^{\min} \\ \left( \frac{\hat{y}_i(x) - y_i^{\min}}{y_i^{\max} - y_i^{\min}} \right)^r, & y_i^{\min} < \hat{y}_i(x) < y_i^{\max} \\ 1, & \hat{y}_i(x) \geq y_i^{\max} \end{cases} \quad \text{LTB} \quad (\text{EQUATION 5.3})$$

$$d_i(x) = \begin{cases} 1, & \hat{y}_i(x) \leq y_i^{\min} \\ \left( \frac{\hat{y}_i(x) - y_i^{\max}}{y_i^{\min} - y_i^{\max}} \right)^r, & y_i^{\min} < \hat{y}_i(x) < y_i^{\max} \\ 0, & \hat{y}_i(x) \geq y_i^{\max} \end{cases} \quad \text{STB} \quad (\text{EQUATION 5.4})$$

where  $y_i^{\max}$  and  $y_i^{\min}$  represent the maximum and minimum tolerance limits and  $(\hat{y}_i(x))$  are the estimated responses;  $s$ ,  $t$  and  $r$ , having positive values, represent the weights. The NTB desirability function, reported in Equation 5.2, is used for responses that need to reach a specific target ( $T_i$ ). The LTB, reported in Equation 5.3, is used when the value of the estimated response is expected to be larger than a lower tolerance limit. The STB, reported in Equation 5.4 is used when the value of the estimated response is expected to be smaller than an upper tolerance limit.

In a multi-response situation, the overall desirability function ( $D$ ) is maximized and represented by a geometric mean obtained by combining the individual desirability functions ( $d_i$ ) defined as:

$$\max_{x \in \Omega} D = \left( \prod_{i=1}^n d_i^{w_i} \right)^{\frac{1}{\sum_{i=1}^n w_i}} \quad (\text{EQUATION 5.5})$$

where  $d_i$  is the individual desirability function of the  $i$ -th response,  $x$  represents the combination of experimental conditions within the experimental domain  $\Omega$  and  $w_i$  are the weights assigned to each response. A high  $w_i$  implies that the desirability value is close to 0, unless the response gets very close to its target value. Higher  $w_i$  values assign more importance to the  $d_i$ . The objective of this approach is to find the experimental conditions, maximizing the  $D$  value within the experimental domain.

#### 5.2.5.2 KIM AND LIN DESIRABILITY FUNCTIONS

In this approach [34], the individual desirability function of  $i$ -th response,  $d_i$ , has an exponential form and it is defined as:

$$d'(z) = \begin{cases} \frac{\exp(\tau') - \exp(\tau'|z|)}{\exp(\tau') - 1}, & \tau = 0 \\ 1 - |z|, & \tau \neq 0 \end{cases} \quad (\text{EQUATION 5.6})$$

where  $\tau' = \tau + (1 - R^2)(\tau^{max} - \tau)$  and  $\tau^{max}$  is a sufficient large value of  $\tau$  (constant,  $-\infty < \tau < \infty$ ) such that  $d'(z)$  with  $\tau^{max}$  is a concave curve assuming virtually no effect in the optimization process. Realistic values of  $\tau$  lies between -10 and 10. For  $\tau < 0$  the function is convex, for  $\tau = 0$  the function is linear and for  $\tau > 0$  the function is concave.  $R^2$  is the coefficient of determination and  $z$  is a standardized parameter representing the distance of the estimated response from its target in units of the maximum allowable deviation. This parameter ( $z$ ) depends on the response type and is defined as:

$$z_i(x) = \begin{cases} \frac{\hat{y}_i(x) - T}{y_i^{max} - T}, & (\text{for NTB}) \\ \frac{\hat{y}_i(x) - y_i^{min}}{y_i^{max} - y_i^{min}}, & (\text{for STB}) \\ \frac{y_i^{max} - \hat{y}_i(x)}{y_i^{max} - y_i^{min}}, & (\text{for LTB}) \end{cases} \quad \text{with } y_i^{min} \leq \hat{y}_i(x) \leq y_i^{max} \quad (\text{EQUATION 5.7})$$

where  $y_i^{max}$  and  $y_i^{min}$  represent the maximum and minimum values of the estimated response ( $\hat{y}_i(x)$ ). Equation 5.7 ranges between  $-1$  and  $1$  for NTB-type responses and between  $0$  and  $1$  for STB and LTB ones.

In the present study, in order to consider the predictive ability of each response model,  $R^2$  was substituted by the coefficient of determination in prediction ( $Q^2$ ).  $\tau^{max}$  was fixed equal to  $10$ . The values of  $\tau$  for each model were chosen considering the importance of the response.

In this approach, the overall minimal level of satisfaction is reached following the formulation:

$$\max_{x \in \Omega} (\min [d_1 \{(\hat{y}_1(x))\}, d_2 \{(\hat{y}_2(x))\}, \dots, d_n \{(\hat{y}_n(x))\}]) \quad (\text{EQUATION 5.8})$$

where  $x$  represents the combination of experimental conditions within the experimental domain  $\Omega$ .

In the present study, only LTB and STB response types were considered for both approaches. The minimum and maximum values for each responses ( $y_i^{max}$  and  $y_i^{min}$ ) were set at the extreme values of each estimated response.

The linear regression models, ANOVA, response surfaces and desirability functions were calculated by Modde 6.0 (Umetrics, Umeå, Sweden) and MATLAB R2013 (The MathWorks Inc., Natick, USA).

## 5.3 RESULTS AND DISCUSSION

### 5.3.1 REGRESSION MODELS

The results of the experiments are summarized in Table 5.2. As a response for the model, the value of  $\eta^*$  was uniquely taken at the frequency of  $200$  rad/s, since the analysis was more stable at this frequency.

For each experimental response, a reduced subset model was obtained considering the only terms that resulted significant. Table 5.3 shows regression coefficients for each experimental response related to the scaled and centered variables. In order to achieve the best subset model, some terms were included even if they did not result significant to preserve the principal of hierarchy.

TABLE 5.2: CENTRAL COMPOSITE DESIGN AND EXPERIMENTAL RESPONSES.

Experiment	Factor				Response						
	US ( $\mu\text{m}$ )	SS (rpm)	FR (g/min)	T ( $^{\circ}\text{C}$ )	$\eta^*$ (kPa.s)	CD (mmol/cm <sup>3</sup> )	GF (wt%)	M100 (MPa)	TS (MPa)	Eb (elongation %)	
Experiments based on a full factorial design at two level											
E1	5.0	150	4	130	3.26	0.043	83.0	3.22	4.52	132	
E2	12.0	150	4	130	1.90	0.028	75.5	2.71	5.37	169	
E3	5.0	250	4	130	3.53	0.040	85.0	3.43	4.21	117	
E4	12.0	250	4	130	1.34	0.020	74.0	2.53	5.88	179	
E5	5.0	150	8	130	4.03	0.043	84.2	3.49	4.43	127	
E6	12.0	150	8	130	2.23	0.032	77.0	3.01	4.71	136	
E7	5.0	250	8	130	3.79	0.031	83.2	3.50	3.86	112	
E8	12.0	250	8	130	1.63	0.024	76.5	2.56	6.52	196	
E9	5.0	150	4	210	3.09	0.027	81.3	3.19	4.02	124	
E10	12.0	150	4	210	1.70	0.028	76.1	2.48	4.70	161	
E11	5.0	250	4	210	1.75	0.028	79.1	3.12	6.10	159	
E12	12.0	250	4	210	1.00	0.018	74.4	2.86	6.13	179	
E13	5.0	150	8	210	3.35	0.035	83.6	3.19	3.52	112	
E14	12.0	150	8	210	2.07	0.027	77.7	2.62	4.89	162	
E15	5.0	250	8	210	2.01	0.023	77.8	2.89	6.06	170	
E16	12.0	250	8	210	1.28	0.020	74.8	2.60	6.22	189	
Axial experiments (distance $\pm 1$ from the center)											
E17	5.0	200	6	170	3.77	0.037	84.1	3.38	4.11	116	
E18	12.0	200	6	170	2.16	0.026	77.4	3.05	5.65	160	
E19	8.5	150	6	170	3.01	0.033	80.7	3.10	4.27	133	
E20	8.5	250	6	170	1.81	0.023	77.4	3.03	6.02	163	
E21	8.5	200	4	170	2.09	0.029	77.7	2.83	5.92	174	
E22	8.5	200	8	170	2.54	0.030	79.3	2.90	4.96	152	
E23	8.5	200	6	130	2.62	0.038	80.5	3.20	4.97	150	
E24	8.5	200	6	210	1.58	0.027	77.8	2.87	6.35	178	
Central experiments											
C1	8.5	200	6	170	2.37	0.033	79.1	2.97	5.42	160	
C2	8.5	200	6	170	2.59	0.028	78.6	2.84	5.09	158	
C3	8.5	200	6	170	2.48	0.027	78.6	3.13	5.39	142	
C4	8.5	200	6	170	2.51	0.027	77.9	3.19	5.00	140	



TABLE 5.3: REGRESSION COEFFICIENTS AND STANDARD ERROR (SE) FOR EACH EXPERIMENTAL RESPONSE RELATED TO THE SCALED AND CENTERED VARIABLES.

Experimental response	$\eta^*$	SE	CD	SE	GF	SE	M100	SE	TS	SE	Eb	SE
Constant	2.45	0.05	0.0295	0.0004	79.0	0.2	3.05	0.03	5.3	0.1	153	3
US	-0.74	0.04	-0.0047	0.0005	-3.2	0.2	-0.28	0.02	0.51	0.09	20	2
SS	-0.36	0.04	-0.0038	0.0005	-0.9	0.2	-0.03	0.02	0.59	0.09	12	2
FR	0.18	0.04	0.0002	0.0005	0.4	0.2	0.02	0.02	-	-	-2	2
T	-0.36	0.04	-0.0037	0.0005	-0.9	0.2	-0.10	0.02	0.20	0.09	6	2
US*US	0.40	0.09	-	-	1.1	0.4	0.13	0.05	-0.3	0.1	-14	5
SS*SS	<sup>a</sup>	-	-	-	-	-	-	-	-	-	-	-
FR*FR	-	-	-	-	-1.1	0.4	-0.22	0.05	-	-	-	-
T*T	-0.47	0.09	-	-	-	-	-	-	-	-	12	5
US*SS	-0.02E-05	0.04	-0.0004	0.0005	0.2E-01	0.2	-0.01	0.02	0.08	0.09	3	2
US*FR	-	-	0.0009	0.0005	0.3	0.2	-	-	-	-	-	-
US*T	0.21	0.04	0.0021	0.0005	0.8	0.2	0.06	0.02	-0.20	0.09	-4	2
SS*FR	-	-	-0.0012	0.0005	-0.4	0.2	-0.07	0.02	-	-	5	2
SS*T	-0.19	0.04	-	-	-0.7	0.2	0.03	0.02	0.37	0.09	6	2
FR*T	-	-	0.0003	0.0005	-	-	-0.06	0.02	-	-	-	-
US*SS*FR	-	-	0.0016	0.0005	0.4	0.2	-	-	-	-	-	-
US*SS*T	0.15	0.04	-	-	0.4	0.2	0.10	0.02	-0.32	0.09	-9	2
US*FR*T	-	-	-0.0012	0.0005	-	-	-	-	-	-	-	-
SS*FR*T	-	-	-	-	-	-	-	-	-	-	-	-

<sup>a</sup> The character ‘\_’ represents the coefficient removed from the reduced model.

All the obtained reduced regression models were statistically significant at 95 %, without showing any lack of fit at the same probability [9,18]. The residual distributions, as shown in Figure 5.2, do not reveal evident anomalies. The normal distribution for the residuals was confirmed by the Shapiro-Wilk normality test at 99 % confidence level [35].

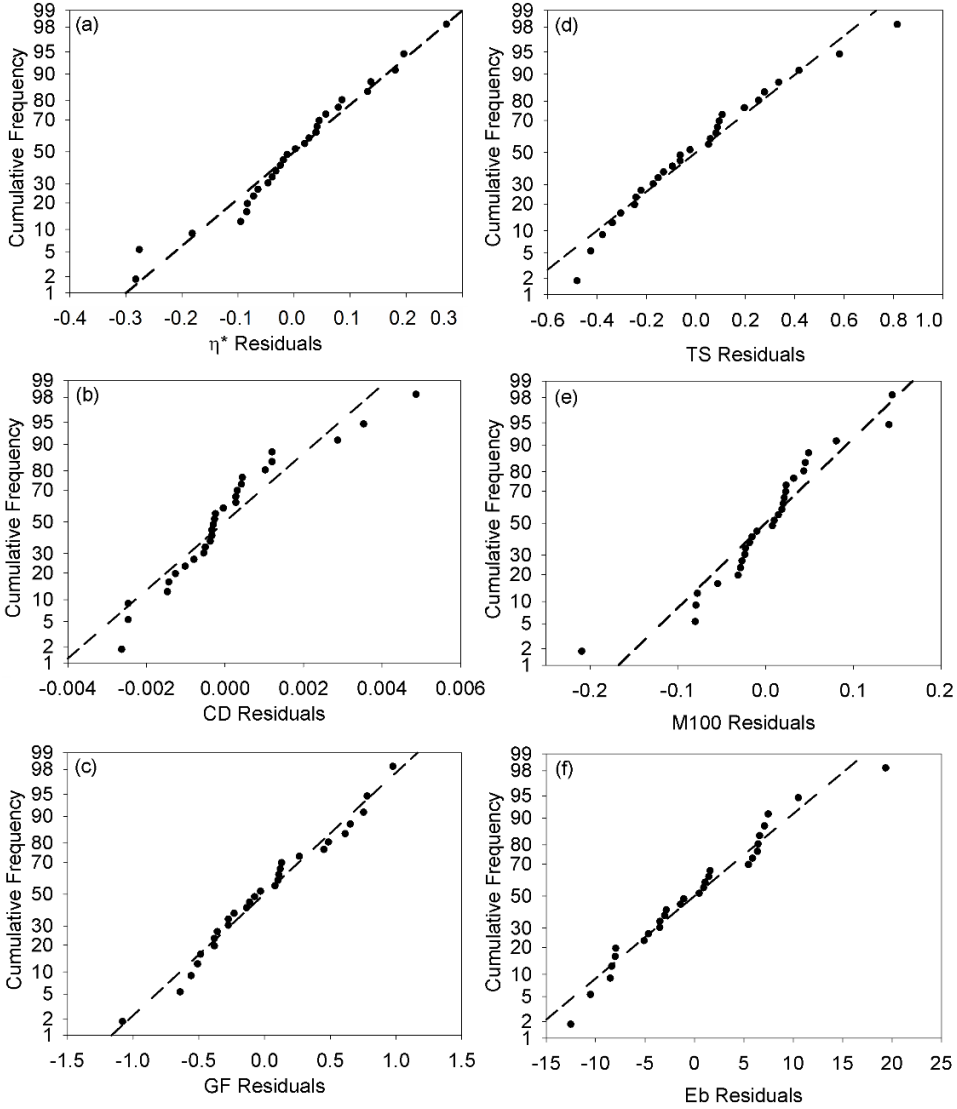


FIGURE 5.2: NORMAL PROBABILITY PLOT OF RESIDUALS FOR (a)  $\eta^*$ , (b) CD, (c) GF, (d) TS, (e) M100 AND (f) Eb.

$Q^2$  was used to select the best subset model for each response. Therefore, this statistic results in the highest power prediction for each model (Table 5.4).

Moreover, each model shows relatively high  $R^2$  and  $R^2$  adjusted ( $R^2$  adj), offering an acceptable explanation of the total variance.

TABLE 5.4: COEFFICIENTS OF DETERMINATIONS OF REDUCED MODELS.

Response	$R^2$	$R^2$ adj	$Q^2$
$\eta^*$	0.98	0.96	0.94
CD	0.93	0.89	0.86
GF	0.98	0.95	0.88
M100	0.94	0.90	0.88
TS	0.87	0.81	0.74
EB	0.91	0.85	0.72

### 5.3.2 D-GTR

$\eta^*$  was determined as a function of the angular frequency and followed the power law behavior. Therefore, the experimental data were fitted according to the following equation:

$$\eta^* = K\omega^{n-1} \quad (\text{EQUATION 5.9})$$

where  $\omega$  represents the frequency and  $K$  and  $n$  are empirical constants ( $n < 1$ ).

The constant  $K$  in Equation 5.9, representing a measure of flow resistance, could have been used as an additional experimental response for the model. This parameter allowed us to consider the behavior of the rubber in the entire region of the studied frequencies. Figure 5.3 shows the dependence of  $\eta^*$  on the frequency  $\omega$  and the power law fit for three samples chosen as representative ones.

Nevertheless, this additional response ( $K$ ) showed an analogous behavior as  $\eta^*$  at 200 rad/s with the same significant terms for the fitted reduced model. For this reason, it was decided to uniquely consider  $\eta^*$  during the optimization process.

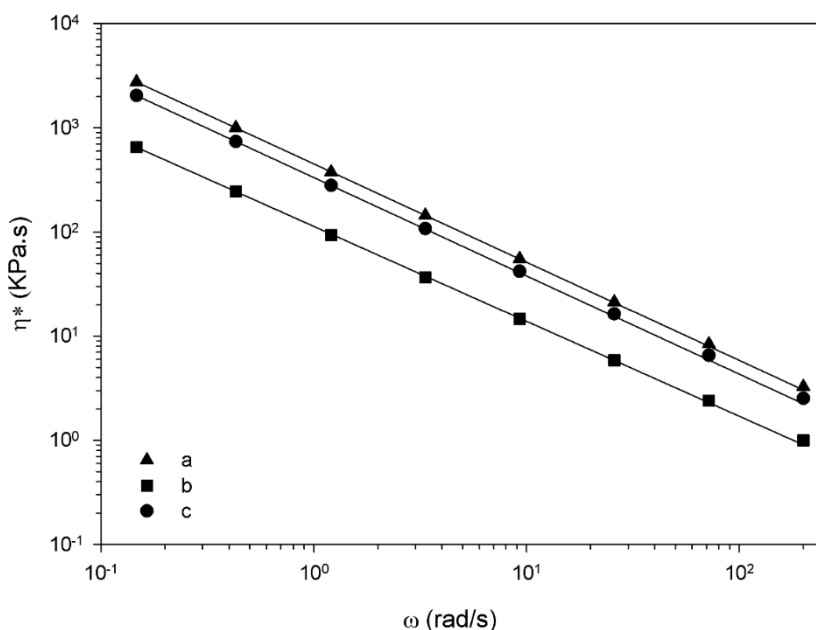


FIGURE 5.3: POWER LAW FITTING EXAMPLES ON SAMPLES (a) E1, (b) E12 AND (c) C4 CORRESPONDING TO TABLE 5.2.

The analysis of the  $\eta^*$ , GF and CD were performed directly on the material after the devulcanization, since these values give information on the rupture of the crosslink network.

The  $\eta^*$ , as function of angular frequency, is a measure of the resistance to flow. In particular  $\eta^*$  decreases with a decrease of molecular weight, crosslink density and gel fraction.

The GF represents the insoluble fraction after removing the sol fraction. It decreases with the increase of network breakage and with the increase of polymeric soluble fraction. Similarly, the CD represents the effective number of chains per unit of volume and it decreases with the increase of devulcanization.

From the reduced models (Table 5.3) it can be observed that all process variables had influence on the devulcanization process. The ultrasonic amplitude showed the highest effect, acting with a negative trend on D-GTR properties. Indeed, as already observed in [1], the ultrasonic devulcanization increases with the ultrasonic amplitude. The effects of screw speed and temperature were found to be less important despite the fact that these process variables acted in the same direction as the ultrasonic amplitude. Indeed these two process

variables are responsible for thermal and mechanical degradation and decrosslinking [5,6]. The effect of flow rate was observed to be less important and acting in opposite direction, since the flow rate enhance decreases the residence time of the material within the extruder, decreasing the devulcanization treatment time.

### 5.3.2.1 HORIKX FUNCTION

In Figure 5.4, the line indicates the Horikx function based on the main chain breakage. Experimental data are indicated by symbols. It is seen that experimental results lie above the Horikx function [36]. Therefore, it can be concluded that the ultrasonic treatment preferentially cleaved the crosslink network with some breakage of the main chain. However, it is impossible from this plot to define types of crosslink breakage (monosulfidic, disulfidic and polysulfidic). In addition, it was difficult to experimentally measure the amount of different type crosslink breakage on D-GTR. In that regard, a previous study [37] (conducted on a model SBR rubber) indicated that the ultrasonic devulcanization causes a significant decrease of polysulfidic and monosulfidic crosslinks indicating that ultrasonic devulcanization takes place indeed.

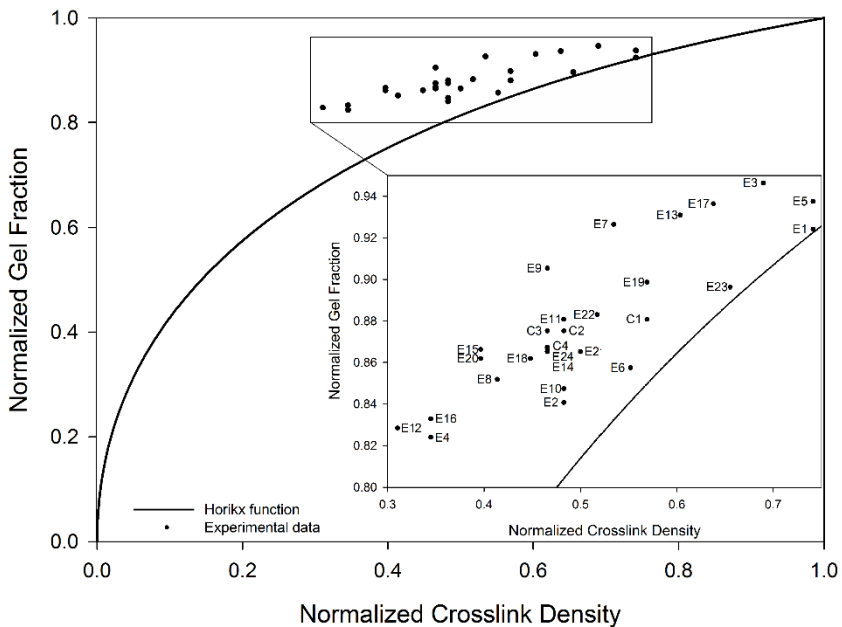


FIGURE 5.4: NORMALIZED GEL FRACTION AS A FUNCTION OF NORMALIZED CROSSLINK DENSITY COMPARED TO THE HORIKX FUNCTION.

### 5.3.3 R-GTR

The analysis of M100, TS and Eb were performed on the material R-GTR after compounding and revulcanization. Generally, the compound recipe and crosslink network type are the main parameters influencing all these mechanical properties [38]. However, in our case, the filler content and recipe of the R-GTR were kept constant. Therefore, the mechanical properties were strictly correlated to the devulcanization effect induced by the ultrasonic treatment.

M100 is a measure of the tensile properties at 100 % of elongation. TS and Eb represent the final mechanical properties. They define the failure point of the vulcanizates.

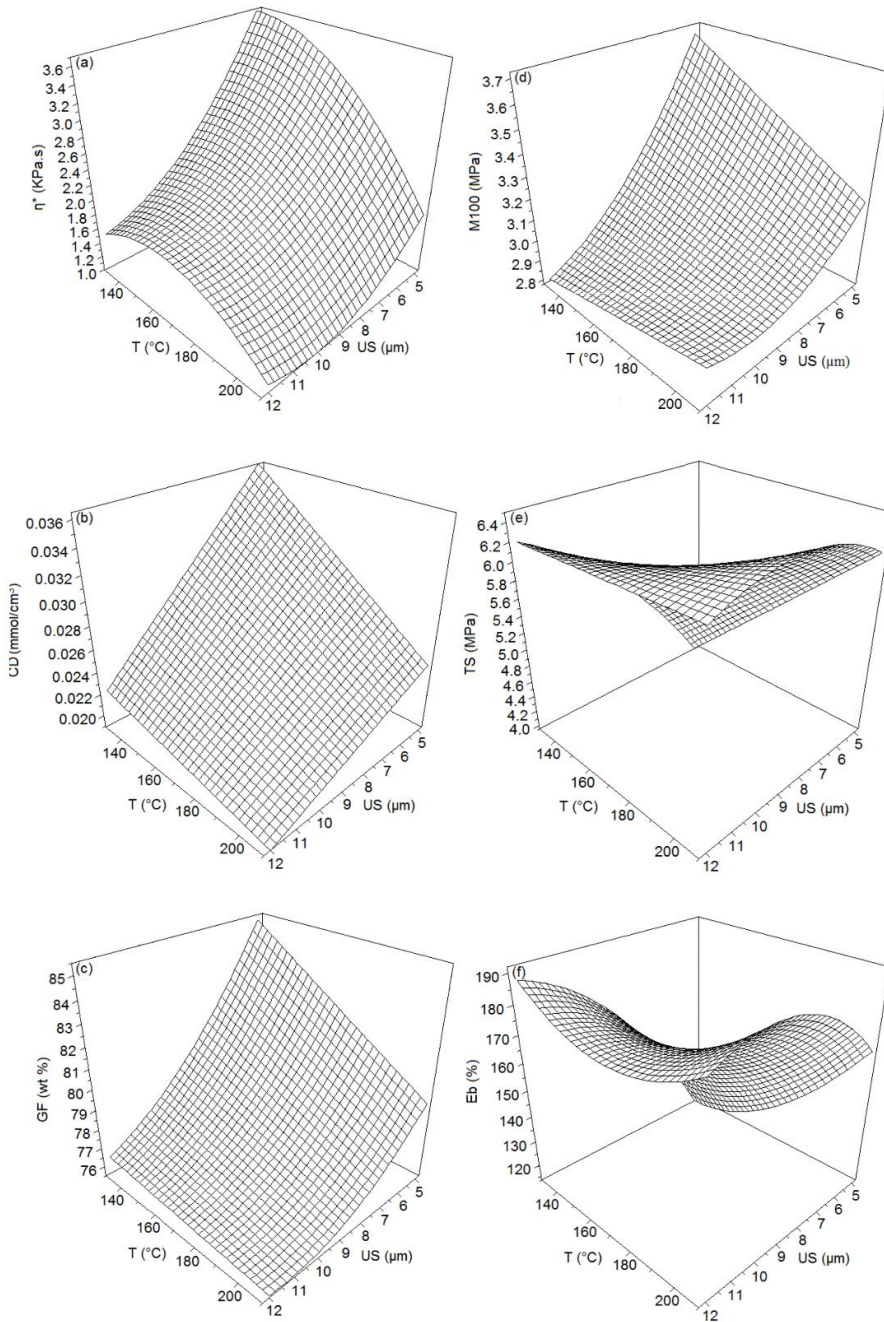
As seen from Table 5.3, M100 followed a reduced model similar to the one observed for all the responses evaluated on the D-GTR. The increase of the ultrasonic amplitude, screw speed and temperature and the decrease of the flow rate led to lower values of M100. Several researches had already observed that the modulus increases with the crosslink density and gel fraction of the material. Furthermore, the crosslink density and gel fraction of revulcanizates are highly correlated with the correspondent devulcanizates, as long as the curing recipe is kept constant [2,39]. Also in this study higher values of gel fraction and crosslink density of D-GTR led to higher values of R-GTR.

Although M100 of R-GTR resulted being correlated with the crosslink density and gel fraction of the D-GTR, it is clear that TS and Eb behaved differently. Indeed, the main significant process variables had a completely opposite influence on these two properties. These final mechanical properties were strongly influenced by the degree of devulcanization. More breakage of the three-dimensional network can generate more active sites that can be cured during the revulcanization process, increasing the compatibility among the D-GTR particles.

In order to better understand the trend of the response surfaces, 3D plots are shown in Figure 5.5. In these surfaces each response was plotted as a function of US and T, fixing the values of FR at center level (0) and SS at the highest one (+ 1).

In Figure 5.5 it is clear that the mechanical properties are strongly dependent on the structure properties. Namely, the CD, GF and  $\eta^*$  showed similar behaviors, since their decrease was observed with an increase of T and US. On the other hand, the mechanical properties did not show a unique behavior. The M100 showed significant decrease at high T and US, while the opposite was

observed for TS and Eb. As already observed in [2], this different behavior of the mechanical properties of the R-GTR can be explained by considering their correlation with the structure of the D-GTR. The reduction of CD and GF is generally associated to an increase of the sol fraction. This soluble polymeric fraction, along with the gel of lower crosslink density, provides enough active sites that can be re-cured, increasing the compatibility among various D-GTR particles, resulting in better final properties of R-GTR. On the other hand, the M100 behaves in opposite manner since this property shows higher values at higher values of CD and GF.



**Figure 5.5: RESPONSES SURFACES OF (a)  $\eta^*$ , (b) CD, (c) GF, (d) M100, (e) TS AND (f) Eb AS A FUNCTION OF T AND US AT HIGHEST VALUE OF SS (250 rpm) AND MIDDLE VALUE OF FR (6 g/min).**



## 5.3.4 VALIDATION

A validation was carried out in order to test the reduced models predictive power within the studied domain. In addition, some experiments were carried out to evaluate the applicability of the model outside the studied domain.

The conditions used for validation experiments are reported in Table 5.5.

TABLE 5.5: VALIDATION EXPERIMENT CONDITIONS.

Experiment	US ( $\mu\text{m}$ )	SS (rpm)	FR (g/min)	T ( $^{\circ}\text{C}$ )
Experiments out of the experimental domain				
v1	0	250	8	130
v2	0	200	8	170
Experiments within the experimental domain				
v3	8.5	250	6	170
v4	8.5	200	6	170
v5	12	250	6	130
v6	12	200	6	170
v7	12	150	8	130

These experiments were fixed by selecting combinations of independent variables within the experimental domain. Moreover, the predictive power of the models was tested outside the experimental region, removing the most influential process variable. Therefore, two experiments (v1 and v2) were carried out without applying any ultrasonic treatment.

Figure 5.6 shows the experimental responses compared to the predicted values. It can be seen that the experimental values are in good agreement with the predicted ones within the experimental domain (v3 to v7). Moreover, some models show an acceptable predictive capacity outside the experimental range (v1 and v2).

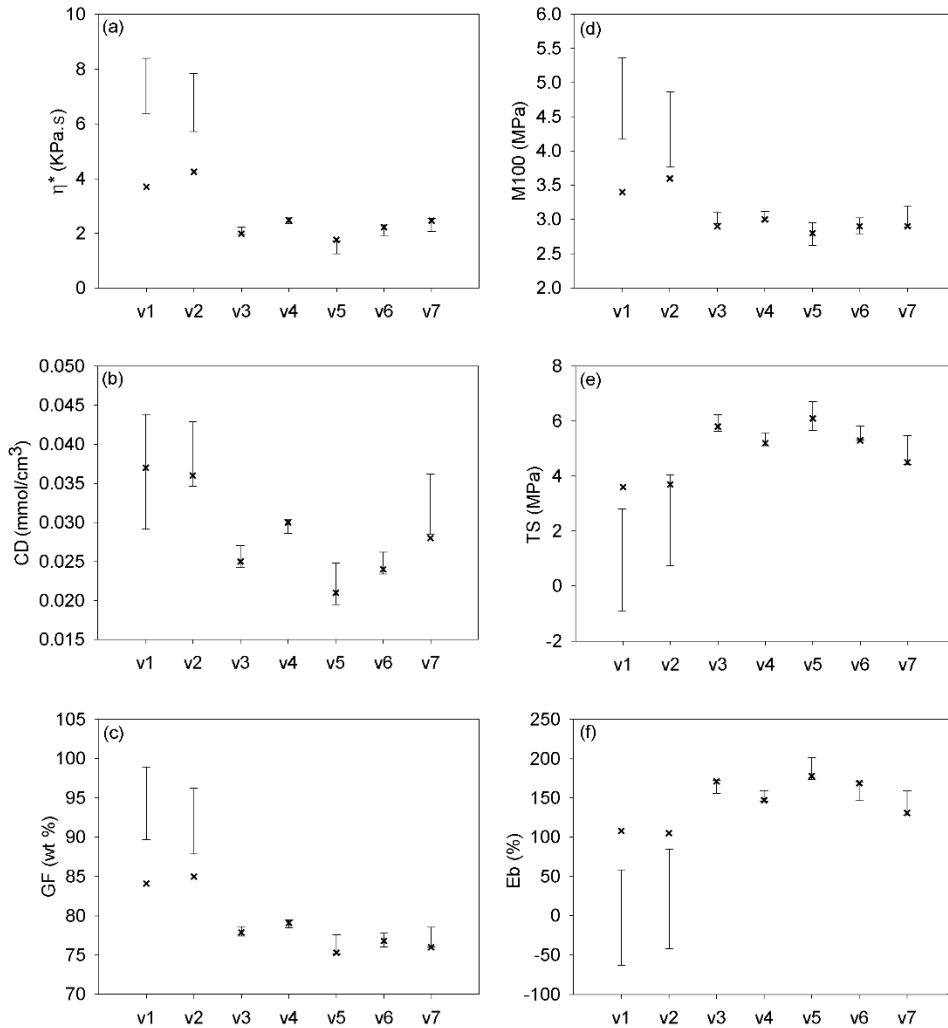


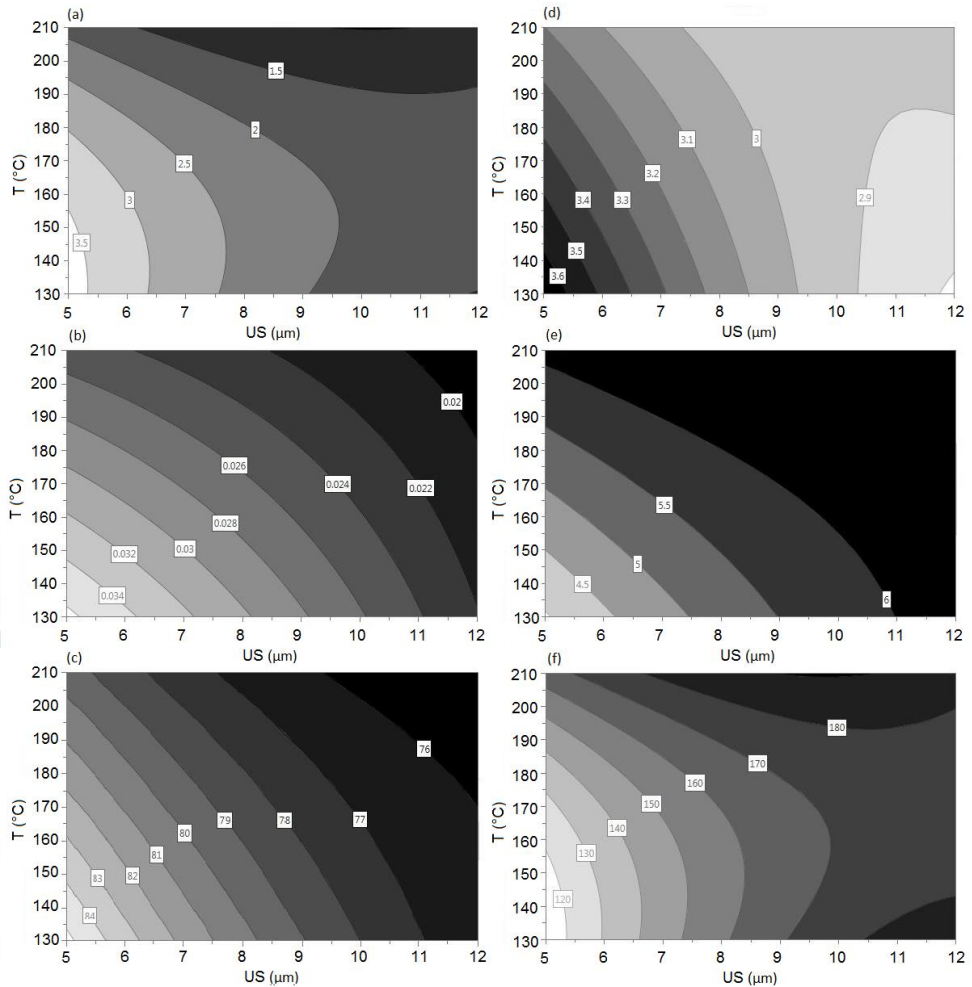
FIGURE 5.6: RESULTS OF VALIDATION EXPERIMENTS WITH THE MODELS ERROR BARS AT 95 % CONFIDENCE LEVEL.

### 5.3.5 OPTIMIZATION

In the previous sections, our attention was focused on modeling each response as a function of the input process variables. Two different behaviors were generally observed, as seen in Figure 5.5. In addition, in Figure 5.7 it can be observed that the optimal condition as a function of US and T is different for each response.

Although, for practical applications, the process variables could be varied in order to achieve the optimal conditions for a desired property, in the present

study a multiple response optimization approach was performed. In particular, this optimization was carried out considering a possible application of the D-GTR in new tires. Therefore, it was decided to assign more importance to the M100 and TS.



**FIGURE 5.7: CONTOUR PLOTS OF (a)  $\eta^*$ , (b) CD, (c) GF, (d) M100, (e) TS AND (f) Eb AS A FUNCTION OF T AND US FIXING SS=250 rpm AND FR = 6 g/min. The optimal conditions are shown in black color.**

The weights and parameters used for the two different desirability function approaches are shown in Table 5.6. The results of the optimization are listed in Table 5.7.

Although the two desirability function approaches gave different overall degree of satisfaction, the two approaches gave comparable results in term of optimal process conditions. In order to maximize the value of M100 and TS, it is necessary to keep a relatively low value of US, sufficient to reduce the network density and to increase the number of active sites so D-GTR can be revulcanized, without introducing an excessive degradation.

TABLE 5.6: PARAMETERS FOR DESIRABILITY FUNCTIONS.

Response	Type of desirability function	$y_i^{min}$ <sup>a</sup>	$y_i^{max}$ <sup>a</sup>	w <sup>b</sup>	$\tau$ <sup>c</sup>
$\eta^*$	STB	0.80	4.16	1	-1
CD	STB	0.018	0.044	1	-1
GF	STB	73.8	85.3	1	-1
M100	LTB	2.52	3.67	3	-3
TS	LTB	3.69	6.46	3	-3
Eb	LTB	194	102	1	-1

<sup>a</sup> The value of  $y_i^{min}$  and  $y_i^{max}$  were computed for each response, using the reduced subset models reported in Table 5.3.

<sup>b</sup> Weights for the Derringer and Suich approach.

<sup>c</sup> Value of  $\tau$  parameter for the Kim and Lin approach.

TABLE 5.7: DESIRABILITY FUNCTIONS OPTIMIZATION RESULTS.

Parameter	Derringer and Suich	Kim and Lin
Optimal Conditions (US, SS, FR, T)	(7.2, 250, 5.5, 210)	(5, 250, 5.6, 202)
Predicted responses ( $\eta^*$ , CD, GF, M100, TS, Eb)	(1.22, 0.023, 77.4, 3.03, 6.39, 183)	(2.16, 0.027, 80.2, 3.27, 5.87, 155)
Desirability function value optimal conditions d ( $\eta^*$ , CD, GF, M100, TS, Eb)	(0.87, 0.79, 0.69, 0.09, 0.93, 0.88) <sup>a</sup>	(0.55, 0.73, 0.48, 0.48, 0.82, 0.80) <sup>a</sup>
Overall degree of satisfaction	0.71	0.48

<sup>a</sup> Each d ( $\eta^*$ , CD, GF, M100, TS, Eb) was already weighed considering the parameters in Table 5.6.

## 5.4 CONCLUSIONS

The aim of the present study was to investigate a green and continuous ultrasonic devulcanization process that could be carried out in a short time adjusting the process variables in order to optimize specific required conditions. Ultrasonic-assisted devulcanization in a twin-screw extruder was studied and modeled using a face-centered central composite design and desirability functions. Several responses on the D-GTR and on R-GTR were chosen as responses and reduced regression models were obtained by regression analysis. The properties of the D-GTR and R-GTR were influenced by all the process variables as well as interaction effects between them. However, the US was found to be the most influencing process variable for the described screw configuration. Different behaviors were observed for the various responses. For this reason, an optimization was performed in order to maximize the TS and M100, considered the most important parameters for reuse of D-GTR. A relatively low value of US was required to reduce the network density without introducing an excessive degradation of the tire rubber.

## REFERENCES

1. A.I. Isayev; In J.E. Mark, B. Erman, M. Roland, editors. The science and technology of rubber, 4th ed., Boston: Elsevier Academic Press, 2014, p. 697-764.
2. A.I. Isayev, T. Liang, T.M. Lewis; Effect of particle size on ultrasonic devulcanization in twin-screw extruder. *Rubber Chemistry and Technology* 2014;87:86-102.
3. K. Formela, M. Cysewska, J. Haponiuk, A. Stasiak; The influence of feed rate and shear forces on the devulcanization process of ground tire rubber (GTR). *Polimery* 2013;58:906-912.
4. K. Formela, M. Cysewska, J. Haponiuk; The influence of screw configuration and screw speed of co-rotating twin screw extruder on the properties of products obtained by thermomechanical reclaiming of ground tire rubber. *Polimery* 2014;59:170-177.
5. J. Shi, K. Jiang, D. Ren, H. Zou, Y. Wang, X. Lv, L. Zhang; Structure and performance of reclaimed rubber obtained by different methods. *Journal of Applied Polymer Science* 2013;129:999-1007.
6. G. Tao, Q. He, Y. Xia, G. Jia, H. Yang, W. Ma; The effect of devulcanization level on mechanical properties of reclaimed rubber by thermal-mechanical

- shearing devulcanization. *Journal of Applied Polymer Science* 2013;129:2598-2605.
7. B. Maridass; Cure modeling and mechanical properties of counter rotating twin screw extruder devulcanized ground rubber tire-natural rubber blends. *Journal of Polymer Research* 2009;16:133-141.
  8. H. Si, T. Chen, Y. Zhang; Effects of high shear stress on the devulcanization of ground tire rubber in a twin-screw extruder. *Journal of Applied Polymer Science* 2013;128:2307-2318.
  9. G.P.E. Box, W.G. Hunter, J.S. Hunter; *Statistics for experimenters*, 2nd ed., Hoboken: Wiley, 1978.
  10. B. Maridass, B.R. Gupta; Effect of extruder parameters on mechanical properties of revulcanized ground rubber tire powder. *Polimery* 2007;52:456-460.
  11. B. Maridass, B.R. Gupta; Process optimization of devulcanization of waste rubber powder from syringe stoppers by twin screw extruder using response surface methodology. *Polymer Composite* 2008;29:1350-1357.
  12. H. Yazdani, I. Ghasemi, M. Karrabi, H. Azizi, G.R. Bakhshandeh; Continuous devulcanization of waste tires by using a co-rotating twin screw extruder: Effects of screw configuration, temperature profile, and devulcanization agent concentration. *Journal of Vinyl Additives Technology* 2013;19:65-72.
  13. B. Maridass, R.B. Gupta; Performance optimization of a counter rotating twin screw extruder for recycling natural rubber vulcanizates using response surface methodology. *Polymer Testing* 2004;23:377-385.
  14. A.I. Isayev, S.P. Yushanov, J. Chen; Ultrasonic devulcanization of rubber vulcanizates. I. Process model. *Journal of Applied Polymer Science* 1996;59:803-813.
  15. A.I. Isayev, S.P. Yushanov, J. Chen; Ultrasonic devulcanization of rubber vulcanizates. II. Simulation and experiment. *Journal of Applied Polymer Science* 1996;59:815-824.
  16. S.P. Yushanov, A.I. Isayev, S.H. Kim; Ultrasonic Devulcanization of SBR Rubber: Experimentation and Modeling Based on Cavitation and Percolation Theories; *Rubber Chemistry and Technology* 1998;71:168-190.
  17. I. Khuri, J.A. Cornell; *Response surfaces: Designs and analyses*, 2nd ed., New York: Marcel and Dekker Inc, 1996.

18. R.H. Myers, D.C. Montgomery; Response surface methodology: Process and product optimization using designed experiments. 2nd ed., New York: Wiley, 2002.
19. P.J. Brandvik; Statistical simulation as an effective tool to evaluate and illustrate the advantage of experimental designs and response surface methods. *Chemometrics and Intelligent Laboratory Systems* 1998;42:51–61.
20. R. Leardi; Experimental design in chemistry: A tutorial. *Analytica Chimica Acta* 2009;652:161–172.
21. N.R. Draper; Center points in second-order response surface designs. *Technometrics* 1982;24:127-133.
22. J.A. Dec, M.N. Thornblom; Autonomous aerobraking: Thermal analysis and response surface development. *Advances in Astronautical Science* 2012;142:483-498.
23. L.A. Dillon, V.N. Stone, L.A. Croasdell, P.R. Fielden, N.J. Goddard, C.L. Thomas; Optimisation of secondary electrospray ionisation (SESI) for the trace determination of gas-phase volatile organic compounds. *Analyst* 2010;135:306-314.
24. E. Cagigal, L. González, R.M. Alonso, R.M. Jiménez; Experimental design methodologies to optimise the spectrofluorimetric determination of Losartan and Valsartan in human urine. *Talanta* 2001;54:1121-1133.
25. L. Eriksson, E. Johansson, N. Kettaneh-Wold, C. Wikström, S. Wold, Design of experiments principles and applications, 3rd ed., Umeå: Umetrics Academy.
26. I.E. Frank, R. Todeschini, *The Data analysis handbook*, Amsterdam: Elsevier, 1994.
27. I. Batmaz, S. Tunali; Second-order experimental designs for simulation metamodeling. *Simulation* 2002;78:699-715.
28. P.J. Flory, J.Jr. Rehner; Statistical mechanics of cross-linked polymer networks, I and II. *The Journal of Chemical Physics* 1943;11:512-520 and 521-526.
29. J.L. Valentín, J. Carretero-González, I. Mora-Barrantes, W. Chassé, K. Saalwächter; Uncertainties in the determination of crosslink density by equilibrium swelling experiments in Natural Rubber. *Macromolecules* 2008;41:4717-4729.



30. E. Bilgili, H. Arastoopour, B. Bernstein; Pulverization of rubber granulates using the solid state shear extrusion process Part II. Powder characterization. *Powder Technology* 2001;115:277–289.
31. G. Kraus; Swelling of filler-reinforced vulcanizates. *Journal of Applied Polymer Science* 1963;7:861-871.
32. N.R. Costa, J. Lourenço, Z.L. Pereira; Desirability function approach: A review and performance evaluation in adverse conditions. *Chemometrics and Intelligent Laboratory Systems* 2011;107:234-244.
33. G. Derringer, R. Suich; Simultaneous optimization of several response variables. *Journal of Quality Technology* 1980;12:214-219.
34. K.J. Kim, D. Lin; Simultaneous optimization of multiple responses by maximizing exponential desirability functions. *Journal of Royal Statistical Society C-App.* 2000;49:311-325.
35. S.S. Shapiro, M.B. Wilk; An analysis of variance test for normality (complete samples). *Biometrika* 1965;52:591-611.
36. M.M. Horikx; Chain scissions in a polymer network. *Journal of Polymer Science* 1956;19:445-454.
37. W. Feng, A.I. Isayev; In-situ ultrasonic compatibilization of unvulcanized and dynamically vulcanized PP/EPDM blends. *Polymer Engineering Science* 2006;46:8-16.
38. A.Y. Coran. In J.E. Mark, B. Erman, M. Roland, editors. *The science and technology of rubber*, 4th ed., Boston: Elsevier Academic Press, 2014.
39. V. Yu Levin, S. H. Kim, and A. I. Isayev; Effect of Crosslink Type on the Ultrasound Devulcanization of SBR Vulcanizates. *Rubber Chemistry and Technology* 1997;70:641-649.



## 6 MODELING AND INVESTIGATION OF BIOLOGICAL DEVULCANIZATION

---

A biological devulcanization process of a vulcanized ground natural rubber model system (VGNR) is investigated by a two-level full factorial design of experiments. In particular, the devulcanization ability of *Gordonia desulfuricans* 213E is evaluated as a function of several parameters influencing the bacterial growth, such as the glucose concentration, dibenzothiophene concentration and initial biomass concentration. The complex viscosity is chosen as experimental response. Furthermore, the automated ribosomal intergenic spacer analysis (ARISA) method is proposed to investigate the persistence of the inoculated strain during the experiments.

The author is grateful to research group led by Prof. Bestetti (DISAT, University of Milano-Bicocca) and in particular to Dr. Valeria Tatangelo for the microbiological analyses.

---

### 6.1 INTRODUCTION

Last decades gave birth to a microbial desulfurization process as an alternative to the known traditional methods that require hazardous chemicals or energetic operative conditions.

Just few researchers have investigated the biodesulfurization of ground rubber [1-3] and few aspects of the process have been taken into consideration, for example an important parameter such as the effect of growth medium composition on desulfurization activity has never been investigated. Another important point never studied so far regards the evaluation of the persistence of bacterial inoculum during the treatment. Since GTR is a complex material, the sterilization process may not be completely efficient and other bacterial strains can over compete the inoculated strain.

In the present chapter, *Gordonia desulfuricans* 213E with known desulfurization ability [3] is employed to study the devulcanization process of a vulcanized ground natural rubber (VGNR) in order to reproduce a vulcanized system similar to the GTR.

In [3], *G. desulfuricans* 213E has already been employed for the desulfurization of vulcanized rubber. In this patent, it was reported a selective desulfurization mechanism leading to a decrease in the sulfur content between

23 % and 35 %, keeping the growth parameters at the optimal conditions, in presence of a swelling agent and of benzothiophene as a degradation pathway inducer.

In the present chapter, a statistical approach based on experimental design is used to investigate how some process parameters, influencing the bacterial growth but not considered in [3], could affect the complex viscosity ( $\eta^*$ ) and therefore the desulfurization or degradation process of the rubber structure. In particular, the concentration of glucose as a source of carbon, of DBT as desulfurization pathway inducer and the *G. desulfuricans* 213E initial biomass in the culture medium were considered as variables.

The choice to analyze the process on a VGNR model system, instead directly on GTR was carried out since tire rubber is an extremely complex system to control and monitor in case of a biological process. However, although the VGNR is a model system, less complex than a GTR, it is still porous and difficult to sterilize. Therefore, the fingerprinting method ARISA (automated ribosomal intergenic spacer analysis) was used to characterize the microbiological community and to evaluate the persistence of the inoculated bacterium [4].

Moreover, since the purpose of the thesis work is to study *green* processes, the experiments were conducted avoiding all the chemical aids reported by Christofi et al. [3], such as swelling agents. Indeed, although these chemicals are useful to increase the devulcanization efficiency, they might have a toxic effect for the microorganisms and for the environment.

## 6.2 MATERIALS AND METHODS

### 6.2.1 REAGENTS

The biological devulcanization was carried out on a model system of vulcanized ground natural rubber (VGNR). NR was mixed in a two-roll mill as follows: 1 part per hundred of rubber (phr) powder N-cyclohexylbenzothiazole-2-sulfenamide, 1 phr sulfur, 5 phr zinc oxide and 2 phr stearic acid, based on 100 phr of NR. After mixing, the rubber sheet was cured for 18 min at 150 °C. After the curing process, the NR was ground at room temperature in order to reach particle dimensions between 250  $\mu\text{m}$  and 500  $\mu\text{m}$ . All the reagents were the same as in Chapter 3.

The strain *G. desulfuricans* 213E (NCIMB 40816) was purchased from Lebeniz Institut DSMZ-“German Collection of Microorganisms and Cell Culture”

(Germany). Constituents of mineral salt medium (MSM) were purchased from Sigma Aldrich (Germany).

#### 6.2.1.1 BIOLOGICAL MEDIUM

Sulfur-free MSM (pH 7.0) [5] was prepared by dissolving, 4.5 g/l of  $K_2HPO_4$ , 1.5 g/l of  $NaH_2PO_4$ , 2 g/l of  $NH_4Cl$  and autoclaved at 121 °C for 30 min. Then, the following chemicals were added after sterilization by filtration: 0.2 g/l of  $MgCl_2$ ; 0.02 g/l of  $CaCl_2 \cdot 2H_2O$ ; 10 ml/l vitamin (RPMI 1640 Vitamins Solution (100×)-Sigma Aldrich- Germany); 5 mg/l  $MnCl_2 \cdot 6H_2O$ ; 0.5 mg/l  $H_3BO_3$ ; 0.5 mg/l  $ZnCl_2$ ; 0.5 mg/l  $CoCl_2 \cdot 6H_2O$ ; 0.46 mg/l  $NiCl_2 \cdot 6H_2O$ ; 0.3 mg/l  $CuCl_2$ , 0.1 mg/l  $NaMoO_4 \cdot 2H_2O$ ; 1.49 mg/l  $FeCl_2 \cdot 4H_2O$ ; 0.003 mg/l  $Na_2SeO_3$ ; 0.008 mg/l  $Na_2WO_4$  [6]. Glucose and DBT were added after sterilization by filtration.

#### 6.2.2 DESIGN OF EXPERIMENTS

##### 6.2.2.1 EXPERIMENTAL PROCEDURE

VGNR was extracted with acetone for 72 h at room temperature, using a volume of 10 ml/g of rubber. Acetone was changed every 24 h. After that, VGNR was dried under vacuum for 24 h at 50 °C. This step was necessary to remove unreacted sulfur and vulcanizing agents.

Each experiment of the experimental design was carried out in a flask with 10 g of VGNR, in 50 ml of final biological medium volume. All flasks were incubated under stirring at 30 °C for 14 days. At the end of the treatment, the treated VGNR was recovered and dried under vacuum for 24 h at 50 °C.

VGNR complex viscosity ( $\eta^*$ ) was chosen as experimental response, since it is influenced by the NR structure and its change may result from both decrosslinking and degradation of main polymer chain.

The samples showing the lowest viscosity were tested with crosslink density and molecular analysis (ARISA).

##### 6.2.2.2 FULL FACTORIAL DESIGN

A  $2^3$  full factorial experimental design [7,8] was chosen to investigate the devulcanization process.

Table 6.1 shows the maximum (+1), minimum (-1) and central (0) levels for each variable used in the present study. Glucose was used as a carbon source (Gc) and dibenzothiophene (DBT) was added as a desulfurization pathway inducer. The third variable considered was the initial bacterial biomass

concentration in the culture medium and it was evaluated in terms of optical density at 600 nm (OD). Highest absorbance corresponds to the maximum concentration of bacteria and vice versa. These variables were chosen since they were considered the most important parameters influencing the growth of microorganisms.

TABLE 6.1: FACTORS AND LEVELS OF THE EXPERIMENTAL DESIGN.

Factor Code	Min level	Max level	Central level
	-1	1	0
Gc (g/l)	10	20	15
DBT (mg/l)	0.00	3.12	1.56
OD <sub>600</sub> (AU)	0.10	1.00	0.55

Eight experiments were carried out in order to investigate the experimental domain (Table 6.2). Three experiments were added to assess the performance in the center of the experimental domain (Table 6.2). Three experiments were added as control samples without the bacterial inoculum (Table 6.3) to investigate the effect of the VGNR bacterial community lasting even after the sterilization. A fully randomized execution of the experiments was carried out in order to minimize the error due to the planning of experiments.

TABLE 6.2: FULL FACTORIAL DESIGN AND EXPERIMENTAL RESPONSE.

Experiment	Factor			Response
	Gc (g/l)	DBT (mg/l)	OD <sub>600</sub> (AU)	$\eta^*$ (Kpa.s)
E1	10	0.00	0.10	3.01
E2	20	0.00	0.10	3.70
E3	10	3.12	0.10	2.76
E4	20	3.12	0.10	3.02
E5	10	0.00	1.00	2.40
E6	20	0.00	1.00	2.92
E7	10	3.12	1.00	3.11
E8	20	3.12	1.00	3.05
Center1	15	1.56	0.55	3.02
Center2	15	1.56	0.55	3.05
Center3	15	1.56	0.55	2.78

TABLE 6.3: CONTROL SAMPLES WITHOUT BACTERIAL INOCULUM.

Experiment	Factor			Response
	Gc (g/l)	DBT (mg/l)	OD600 (AU)	$\eta^*$ (Kpa.s)
Control1	15	1.56	0.00	3.25
Control2	15	1.56	0.00	3.19
Control3	15	1.56	0.00	2.98

The dependence of  $\eta^*$  on the factors was modeled applying an interaction model containing the variables and their interactions [7,8], the same used in Equation 4.1. The coefficients were determined by multiple linear regression.

The ANOVA is normally used to determine which factors and which interactions have a significant influence on the process. In our  $2^3$  factorial design, the use of ANOVA is questionable to discriminate whether the factors and interactions are real [7]. Therefore, the relevance of the effects for the factors and interactions was also evaluated comparing each computed effect with the standard error (SE) through a t-test. The main and the interactive effects were calculated according to Box et al. [7].

The three central and three control samples were used to evaluate the experimental error and therefore the standard error for the effects by the following equations:

$$\sigma = \sqrt{\frac{N_C \cdot \sigma_{N_C}^2 + N_A \cdot \sigma_{N_A}^2}{N_C + N_A}} \quad (\text{EQUATION 6.1})$$

$$SE(\text{effect}) = \frac{2\sigma}{\sqrt{n}} \quad (\text{EQUATION 6.2})$$

where  $\sigma$  is the standard deviation of the experiments,  $N_C$  and  $N_A$  are the number of central and control samples and  $n$  is the total number of runs of the two-level factorial design.

The linear regression models, ANOVA and response surfaces were calculated by MODDE 6.0 (Umetrics, Umeå, Sweden).

#### 6.2.2.3 COMPLEX VISCOSITY

Rheological characterization was performed by Rubber Process Analyzer (RPA 2000, Monsanto). The frequency sweep tests were carried out at a temperature of 100 °C at a strain amplitude of 20 % and within a frequency range between 0.1 Hz and 30 Hz.

As a response for the model, the value of complex viscosity ( $\eta^*$ ) was uniquely taken at the frequency of 30 Hz as shown in Table 6.2, since the analysis was more stable at this frequency. Moreover, all the models obtained with the others frequencies gave the same significant factors and interactions with lower  $R^2$  and  $Q^2$ .

#### 6.2.3 HORIKX FUNCTIONS

In order to confirm that the devulcanization process took place, samples E3, E4, E5, E6 (Table 6.2) and Control1 (Table 6.3) were swollen in toluene and the crosslink density and gel fraction were calculated as in Chapter 3. In this case, the Kraus correction was not necessary since the VGNR did not contain any carbon black.

In order to investigate in more detail the relative effect of degradation of the main chain and of the crosslink network, the dependence of experimental normalized gel fraction versus normalized crosslink density was analyzed and compared to the Horikx functions described in Chapter 3 [9,10].

The value of  $M_n$  is available for the natural rubber STR-20 and therefore it was possible to calculate both Horikx curves for the main chain and crosslink scission of VGNR [11].

Equation 3.6 was used to plot the relationship between the normalized gel fraction and the normalized crosslink density of VGNR devulcanization in case of the only main chain breakage. Equation 3.7 was used in case of the only crosslink cleavage. By these equations, it was possible to describe the type of preferential bond breakage during the devulcanization process.

#### 6.2.4 AUTOMATED RIBOSOMAL INTERGENIC SPACER ANALYSIS (ARISA)

In order to apply ARISA analysis, total DNA was extracted from 0.5 g of VGNR (experiments E3, E4, E5, E6 and Control1) and from 0.5 g of the autoclaved VGNR samples by using the FastDNA\_SPIN for Soil Kit (MP Biomedicals, Solon, OH, USA). Moreover, total DNA was extracted from a pure culture of *G. desulfuricans*



213E, with ZR Soil Microbe DNA Miniprep kit (Zymo Research Corporation, Irvine, CA).

ARISA is a Polymerase Chain Reaction (PCR)-based technique for the analysis of bacterial community structure and is based on amplification sizing of the 16S-23S intergenic region [4].

Ribosomal intergenic spacer was amplified by using both primer ITSF (5'-GTCGTAACAAGGTAGCCGTA-3') and primer ITSReub (5'-GCCAAGGCATCCACC-3') with a fluorescent probe [4]. PCR was performed in 40  $\mu$ l containing 20  $\mu$ l of 2X GoTaq Green Master Mix (Promega Corporation, Madison, WI), 5  $\mu$ l of each primer (10  $\mu$ M), 2  $\mu$ l of DNA template and 8  $\mu$ l of water. PCR program was as follows: 94 °C for 3 min followed by 30 cycles at 94 °C for 45 s, 55 °C for 1 min, 72 °C for 2 min and a final extension at 72 °C for 7 min [4]. An aliquot of PCR reaction was analyzed by capillary electrophoresis using 2500 ROX (Applied Biosystems) as size standard for Peak Scanner (Applied Biosystems) analysis. Capillary electrophoresis results in an electropherogram where each peak represents an operative taxonomic unit (OTU).

The signed area of each peak was used to estimate the OTU relative abundance. A normalization was carried out to compare the OTU in different samples setting the sum of the all OTU in every sample equal to 10000. Finally, OTU with a relative abundance minor than 1.5 % were removed to reduce the noise.

## 6.3 RESULTS AND DISCUSSION

### 6.3.1 REGRESSION MODEL

The experimental conditions and the obtained results are summarized in Table 6.2.

A preliminary considered regression model was an interaction model including the three factors and all two-factor interactions [7,8].

Although not advisable, the ANOVA was carried out on this model, thus it was possible to point out which factors and interactions were statistically significant. Table 6.4 shows the ANOVA for the response containing all the factors and two-factor interactions.

Moreover, the significance of factors and interactions was evaluated by estimation of effects and the standard error (SE) calculated as in Equations 6.2 and shown in Table 6.5.

In both cases, the terms whose P-value was higher than 0.05 were sequentially and systematically eliminated. The terms whose P-value was lower than 0.05 were kept in the model since considered significant. Both these approaches identified the same significant factors and interactions.

TABLE 6.4: ANALYSIS OF VARIANCE FOR THE INTERACTION MODEL.

Variable	Degrees of Freedom	S.S.	P-value
Constant	1		<0.001
Gc	1	0.249	0.012
DBT	1	0.101E-02	0.793
OD	1	0.128	0.034
Gc*DBT	1	0.128	0.034
Gc*OD	1	0.300E-01	0.201
DBT*OD	1	0.392	0.005
Residuals	4	0.513E-01	
Total	10	0.977	

TABLE 6.5: ESTIMATED EFFECTS AND STANDARD ERROR (SE) CALCULATED THROUGH THE THREE CENTRAL EXPERIMENTS AND THREE CONTROL SAMPLES (EQUATION 6.2).

Variable	Estimated Effect	SE	P-value
Average	3.0	±0.1	<0.001
Gc	0.4	±0.1	0.016
DBT	-0.02	±0.1	0.851
OD	-0.3	±0.1	0.040
Gc*DBT	-0.3	±0.1	0.040
Gc*OD	-0.1	±0.1	0.374
DBT*OD	0.4	±0.1	0.016

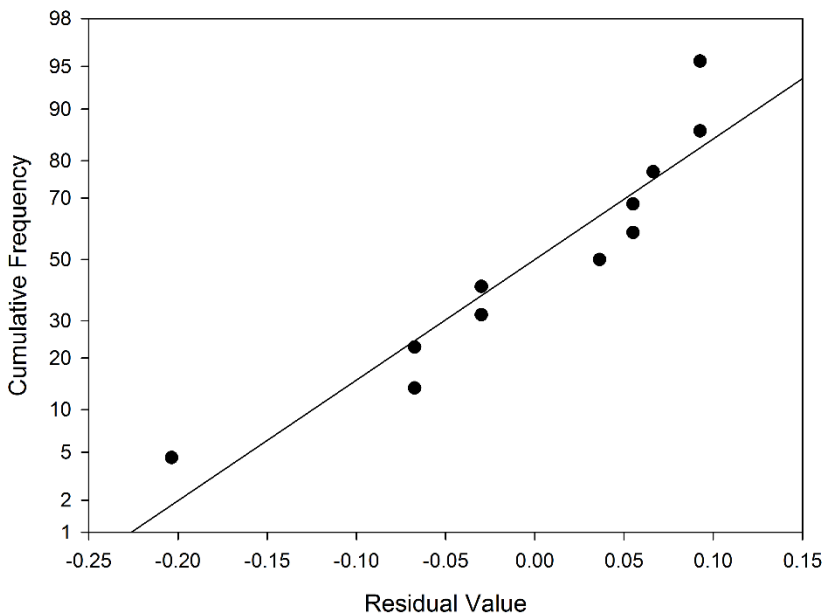
A final reduced model was calculated by multiple linear regression considering only significant factors and interactions. Table 6.6 shows the scaled and centered regression coefficients and the coefficients of determination for the reduced model. The reduced regression model was statistically significant at 95 % and without any lack of fit, considering the same probability [12]. It can be observed that DBT\*OD and Gc resulted the most important variables, acting with a positive effect on the  $\eta^*$ , on the other hand Gc\*DBT and OD act with a negative effect (Table 6.6). The DBT did not result significant, however it was kept in the

final model to preserve the hierarchy, since it is contained within significant higher-order interactions.

**TABLE 6.6: REGRESSION COEFFICIENTS WITH THE STANDARD ERROR (SE) AND COEFFICIENTS OF DETERMINATION REFERRED TO THE SCALED AND CENTERED VARIABLES.**

Variable	Coefficient	SE	R <sup>2</sup>	R <sup>2</sup> adj	Q <sup>2</sup>
Constant	2.98	0.04			
Gc	0.16	0.04			
DBT	-0.01	0.04	0.92	0.83	0.58
OD	-0.11	0.04			
Gc*DBT	-0.10	0.04			
DBT*OD	0.18	0.04			

Moreover, the residual distribution, as shown in Figure 6.1, do not show evident anomalies. The normal distribution for the residuals was confirmed by the Shapiro-Wilk normality test at 95 % confidence level [13].



**FIGURE 6.1: NORMAL PROBABILITY PLOT OF RESIDUALS.**

In order to display the influence of the factors and interactions on the  $\eta^*$ , 3D-plot surfaces were analyzed and are shown in Figure 6.2 and Figure 6.3. In particular, Figure 6.2 shows a  $\eta^*$  decrease alongside with a decrease of glucose

as source of carbon from 20 g/l to 10 g/l and with a decrease of DBT concentration from 3.12 mg/l to 0 mg/l, especially at high values of OD. An increase in the initial bacterial medium concentration (OD) helped to reduce the rubber  $\eta^*$ . When bacteria were inoculated at high concentration of easily accessible carbon source, they might have preferentially used this compound without breaking the rubber carbon and the  $\eta^*$  remained high. The same behavior can be observed for the DBT concentration. It is even clearer that when bacteria were inoculated with DBT as pathway inducer, they might have preferentially used this compound without breaking the rubber crosslinks and the  $\eta^*$  remained high. Indeed, although the DBT was added at low concentration this effect was evident, since the sulfur is a micronutrient for the microorganisms and even a small amount of DBT is enough to avoid the rubber sulfur degradation.

In Figure 6.3, it can be observed the importance of initial OD related to the DBT concentration. As previously noticed, higher OD is able to enhance the decrease of  $\eta^*$ . Nevertheless, the importance of DBT as inducer of the desulfurization pathway can be observed, independently from the amount of carbon source, especially when OD is lower. Indeed, in this case, the competition is low and bacteria are more stimulated to induce the degradation pathway.

3D-plots and final reduced model (Table 6.6) also show that in order to induce bacteria to decrease the  $\eta^*$ , the carbon source and DBT concentration have to be kept at the lowest level and OD at the highest one. However, in this case the main component for the  $\eta^*$  reduction might be attributed both to the carbon and crosslink degradation. High concentration of carbon source can prevent such reduction of the  $\eta^*$ , since bacteria have enough carbon, limiting the rubber degradation.

However, since bacteria need sulfur to grow up and increase the biomass, a low DBT initial concentration at high OD might lead to a decrease in the  $\eta^*$  due to utilization of sulfur crosslinks. It can be seen that this condition may be the most favorable one for a selective decrosslinking.

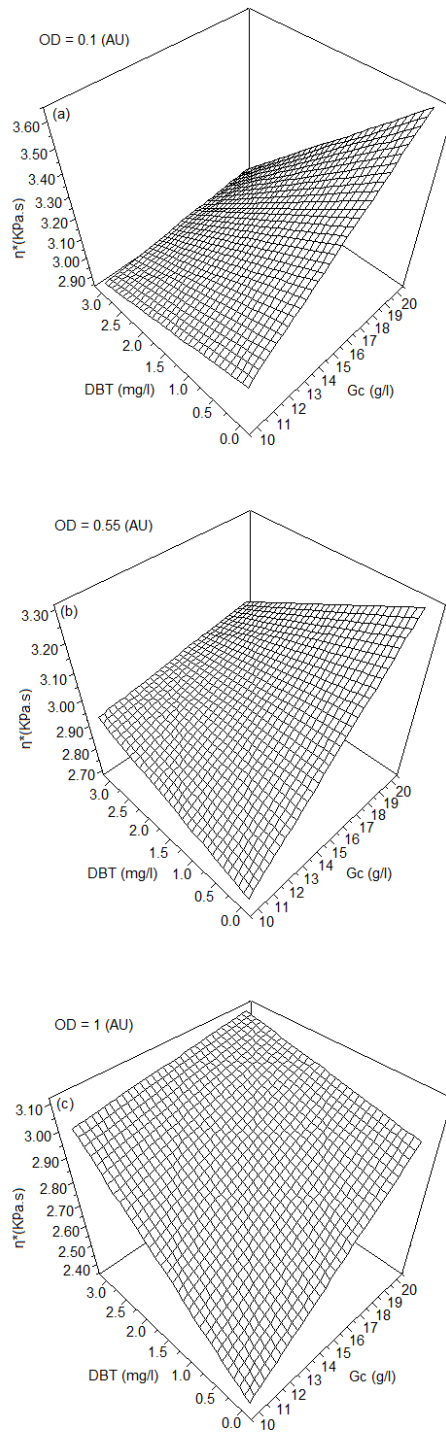


FIGURE 6.2: 3-D PLOT FOR  $\eta^*$  AS A FUNCTION OF DBT AND Gc, FIXING OD AT (a) 0.1, (b) 0.55 AND (c) 1 AU.

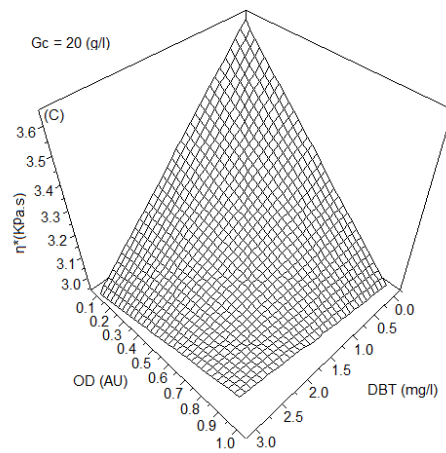
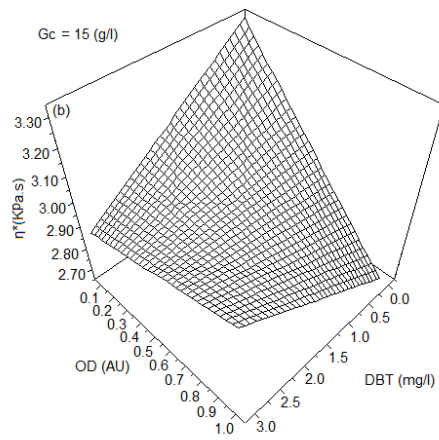
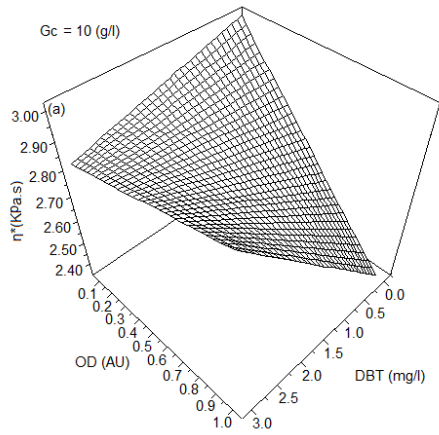


FIGURE 6.3: 3-D PLOT FOR  $\eta^*$  AS A FUNCTION OF OD AND DBT, FIXING Gc AT (a) 10 (b) 15 AND (c) 20 g/l.

## 6.3.2 HORIKX FUNCTIONS

Figure 6.4 shows the normalized gel fraction versus the normalized crosslink density of the VGNR. The solid and dotted lines in Figure 6.4 show the breakage of only main chains and only crosslinks, respectively. It is seen that some devulcanized samples showed a decrease in the crosslink density without showing any decrease in the gel fraction. In particular, it can be observed that E5 and E6 samples showed a slight decrease in the crosslink density, overlapping the dotted Horikx function. In both these experiments the DBT concentration was kept at the lowest value. Therefore, it can be concluded that the biological treatment preferentially cleaved the crosslink network, resulting in a selective process. All the other experiments are located in the point with value 1 for both the normalized crosslink density and normalized gel fraction. However, it is clear from Figure 6.4 that all data points are located in the area close to this point. A similar observation has been reported by Yao et al. [14], indicating that the biological devulcanization is a low yield process limited to the surface due to the bacterial dimensions unable to penetrate the rubber matrix.

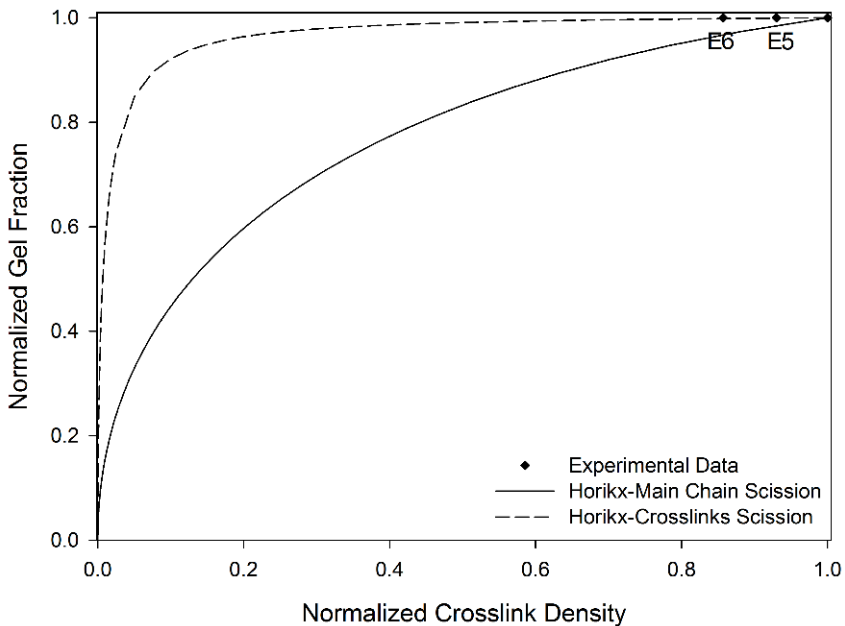


FIGURE 6.4: NORMALIZED GEL FRACTION AS A FUNCTION OF NORMALIZED CROSSLINK DENSITY COMPARED TO THE HORIKX FUNCTIONS.

### 6.3.3 MICROBIAL CHARACTERIZATION

ARISA was carried out on the conditions E3, E4, E5 and E6 (Table 6.2), Control1 (Table 6.3) and on VGNR after acetone extraction and autoclave treatment. Since the ribosomal operon sequences of *G. desulfuricans* 213E had never been reported in literature and the number and the length of 16S-23S intergenic region is unknown, ARISA was also conducted on a pure culture strain. The 16S-23S intergenic region has a heterogeneity in length and sequence. Every strain is characterized by the combination of fragments of different length, usually more than one, due to the presence of multiple ribosomal operons in the bacterial genomes.

In the present study, this technique was used as a technique to assess the presence of the inoculated strain in the experiments.

VGNR is complex porous material and it might be colonized by microbial populations during storage and grinding. Therefore an effective treatment should be necessary to assure the persistence of the inoculated bacteria and microbial monitoring should be used to observe the survival of inoculated strain during the competition with the bacterial populations naturally hosted on VGNR.

Some ARISA fragments were detected in the VGNR sample after acetone and autoclave treatment (Figure 6.5). Although we cannot exclude that these fragments are due to the amplification of DNA from dead organisms, the fingerprinting profile of the uninoculated sample (control1) after incubation revealed that alive microbial populations actually resisted to chemical and thermal treatments on VGNR. Particularly, the fragment 596 bp was shared between VGNR and Control1.

Furthermore, in Figure 6.5 a difference between the communities of samples VGNR and Control1 was observed. This indicates a change in the community during the experiment confirming the presence of bacterial survival to the sterilization treatments.



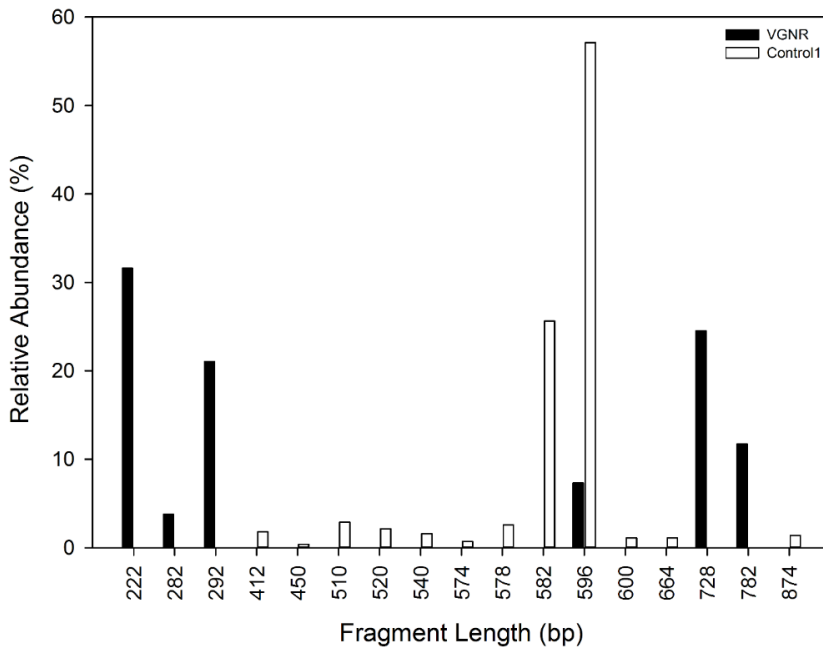


FIGURE 6.5: CONTROL1 AND VGNR ARISA PROFILES.

The characteristic fragments of *G. desulfuricans* 213E are reported in Figure 6.6. These fragments were found in samples E3, E4, E5 and E6 (Figure 6.7). This demonstrates that the *G. desulfuricans* 213E persisted under the four tested conditions of the experimental design. However, in E4 and E6 samples the 596 bp fragment, typical of the autochthonous rubber microbial community, was also detected. In Figure 6.7, it can be also observed that 582 bp fragment is the second abundant fragment in Control1 sample and it was also found at 35 % in all other treated samples (Figure 6.7). This demonstrate that other bacterial populations grew up despite the inoculum addition.

Therefore, the community fingerprinting analysis showed that *G. desulfuricans* 213E persisted in all experiments.

It is clear the need to monitor the bacterial community in the experiments and sample without inoculum to observe the persistence of inoculated strain.

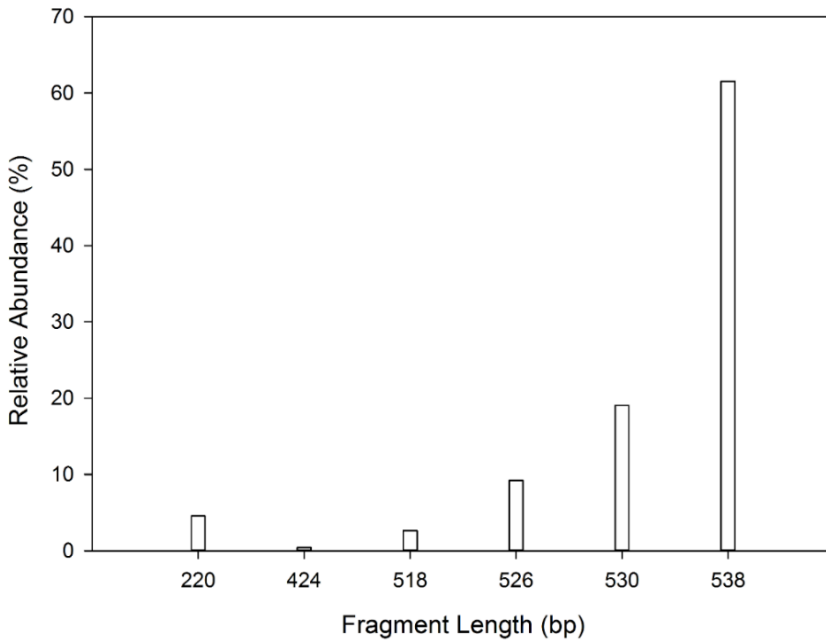


FIGURE 6.6: *G. desulfuricans* 213E ARISA PROFILE.

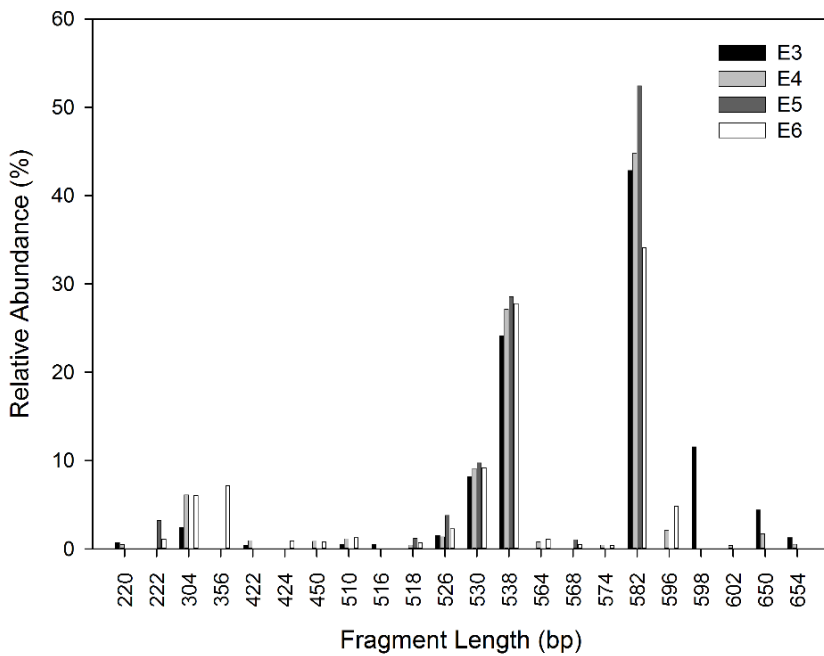


FIGURE 6.7: ARISA PROFILES OF THE EXPERIMENTS E3, E4, E5 AND E6 IN TABLE 6.2.

### 6.3.4 CONCLUSIONS

In the present chapter, VGNR bio-devulcanization was studied by a full factorial experimental design in order to test the parameters and conditions that could affect the bacterial growth on this material. Bio-devulcanization process was carried out using *G. desulfuricans* 213E strain, which had previously been described by Christofi et al in 2010. In their patent, the growth conditions had not been reported in details, therefore this strain has been deeply studied in this research in order to obtain more information on its growth condition for the devulcanization of vulcanized rubber. The  $\eta^*$  was used as response and it was supported by an investigation of the crosslink density and gel fraction to evaluate the selectivity of the process and by a microbiological analysis to assess the persistence of the inoculated strain during the experiments.

A regression model was used to fit the experimental observation and a final reduced model, containing the significant factors and interaction, was obtained. The model indicated that the lowest  $\eta^*$  can be reached keeping the carbon source at the minimum level (10 g/l), without DBT and when the initial biomass is high (OD equal to 1). However, in this case the  $\eta^*$  reduction might be attributed both to the carbon and crosslink degradation. For future experiments, it is advisable to use a high concentration of carbon source, absence of DBT and a high OD. This condition might be the most favorable one for a selective decrosslinking.

Despite the fact that microbiological analysis confirmed that initial bacterial population naturally hosted on VGNR resisted to thermal and chemical pre-treatment and grew up, the community fingerprinting analysis showed that *G. desulfuricans* 213E persisted in all the experiments, leading to a decrease of  $\eta^*$ .

### REFERENCES

1. Y. Li, S. Zhao, Y. Wang; Microbial desulfurization of ground tire rubber by *Sphingomonas* sp.: A novel technology for crumb rubber composites. *Journal of Polymer and Environment* 2012;20:372–380.
2. G. Jiang, S. Zhao, J. Luo, Y. Wang, W. Yu, C. Zhang; Microbial desulfurization for NR ground rubber by *Thiobacillus ferrooxidans*. *Journal of Applied Polymer Science* 2010;116:2768–2774.
3. N. Christofi, J. Geoffrey, D. Edward; US 7737191 B2, 2010.
4. M. Cardinale, L. Brusetti, P. Quatrini, S. Borin, A.M. Puglia, A. Rizzi, E. Zanardini, C. Sorlini, C. Corselli, D. Daffonchio; Comparison of different

- primer sets for use in automated ribosomal intergenic spacer analysis of complex bacterial communities. *Applied and Environmental Microbiology* 2004;70:6147–6156.
5. J.H. Chang, S.K. Rhee, Y.K. Chang, H.N. Chang; Desulfurization of diesel oils by a newly isolated dibenzothiophene-degrading *Nocardia* sp. strain CYKS2. *Biotechnology Progress* 1998;14:851-855.
  6. F. Widdel, F. Bak; In A. Balows, H.G. Trüper, M. Dworkin, W. Harber, K.H. Schleifer, editors. *The prokaryotes*, Berlin: Springer-Verlag, 1992, p. 3352–3378.
  7. G.P.E. Box, W.G. Hunter, J.S. Hunter; *Statistics for experimenters*, 2nd ed., Hoboken: Wiley, 1978.
  8. L. Eriksson, E. Johansson, N. Kettaneh-Wold, C. Wikström, S. Wold; *Design of experiments principles and applications*, 3rd ed., Umeå: Umetrics Academy, 2008.
  9. M.M. Horikx; Chain scissions in a polymer network. *Journal of Polymer Science* 1956;19:445-454.
  10. K. Huang, A.I. Isayev; Ultrasonic decrosslinking of crosslinked high-density polyethylene: Effect of degree of crosslinking. *RSC Advances* 2014;4:38877–38892.
  11. O. Chaikumpollert, K. Sae-Heng, O. Wakisaka, A. Mase, Y. Yamamoto, S. Kawahara; Low temperature degradation and characterization of natural rubber. *Polymer Degradation and Stability* 2011;96:1989–1995.
  12. R.H. Myers, D.C. Montgomery; *Response surface methodology: Process and product optimization using designed experiments*, 2nd ed., New York: Wiley, 2002.
  13. S.S. Shapiro, M.B. Wilk; An analysis of variance test for normality (complete samples). *Biometrika* 1965;52:591–611.
  14. C. Yao, S. Zhao, Y. Wang, B. Wang, M. Wei, M. Hu; Microbial desulfurization of waste latex rubber with *Alicyclobacillus* sp.. *Polymer Degradation and Stability* 2013;98:1724-1730.

## 7 INFLUENCE ON PROPERTIES OF NATURAL RUBBER COMPOUNDS CONTAINING DEVULCANIZED GTRS

---

Supercritical fluid, ultrasonic and biological devulcanization technologies were extensively investigated and optimized in previous chapters, therefore only the best conditions are now considered and compared.

The aim of the present chapter is to provide an extensive comparison among the optimal conditions for these three different devulcanization techniques by blending the devulcanized tire rubber derived from each technique with raw rubber and testing the properties. In particular, GTR and devulcanizates by each technique are compounded into the raw NR at a concentration of 10 phr to find out the rubber providing the highest compatibility for compounding and revulcanization. The rheological and mechanical properties of their vulcanizates are investigated and compared. In addition, a comparison of these results is made with the ones of raw NR compounds and vulcanizates.

---

### 7.1 MATERIALS AND METHODS

The GTR used in the present chapter is the same characterized in Chapter 3 and studied in the entire thesis work.

#### 7.1.1 DEVULCANIZATION TECHNOLOGIES

##### 7.1.1.1 $scCO_2$ DEVULCANIZATION

In Chapter 4 this devulcanization technique was extensively studied on GTR using the experimental design approach. In the same chapter, it was demonstrated that the only significant processing variables are temperature, amount of DD and their interaction and that the devulcanization process can be carried out in a short time at relatively low pressure. Moreover, the obtained results supported the idea that the crosslink network scission occurred during the treatment. However, the unreacted DD can affect the revulcanization process and the mechanical properties of the obtained vulcanizates, in particular increasing the elongation at break and decreasing the modulus.

Considering the results of the full factorial investigation and the reverse influence of DD on the mechanical properties of the revulcanizates, three

different conditions were chosen as the optimal conditions for the comparison carried out in the present chapter. The conditions shown in Table 7.1 were chosen using the crosslink density model reported in Table 4.6, keeping the degree of devulcanization higher than 40 %. Furthermore, the choice was done keeping T at a relatively low level in order not to introduce degradation in the rubber chain and keeping the DD/rubber ratio lower than 5 wt% in order not to deteriorate the mechanical properties of the vulcanizates. Each of these scCO<sub>2</sub> devulcanization experiment was carried out in the static reactor shown in Figure 3.1, with the same reagents described in Chapter 3.

TABLE 7.1: EXPERIMENTAL CONDITIONS FOR THE scCO<sub>2</sub> DEVULCANIZATION.

X-GTR <sup>a</sup> sample name	Time (min)	DD/Rubber (wt%)	Temperature (°C)	Pressure (MPa)
DD0-GTR	60	0	170	24
DD1.5-GTR	60	1.5	160	24
DD5-GTR	60	5	150	24

<sup>a</sup>X-GTR is decrosslinked GTR.

#### 7.1.1.2 ULTRASONIC DEVULCANIZATION

In Chapter 5, this devulcanization technique was extensively studied and optimized on GTR using the response surface methodology. The properties of the devulcanized and revulcanized rubber were influenced by all the process variables. The ultrasonic amplitude (US) was found to be the most influencing process variable. It was also demonstrated that it is necessary to keep a relatively low value of US, sufficient to reduce the network density and to increase the number of active sites. Three different conditions were chosen for the comparison carried out in the present chapter. US5-GTR and US7.2-GTR (Table 7.2) were chosen considering the results of the optimization calculated in Chapter 5. US12-GTR was added since at this condition the highest degree of devulcanization was observed. The devulcanization process was carried out in the ultrasonic co-rotating twin-screw extruder described in Chapter 5 with the same screw configuration (Figure 5.1).

TABLE 7.2: EXPERIMENTAL CONDITIONS FOR THE ULTRASONIC DEVULCANIZATION.

X-GTR sample name	Ultrasonic Amplitude ( $\mu\text{m}$ )	Screw Speed (rpm)	Flow Rate (g/min)	Temperature ( $^{\circ}\text{C}$ )
US5-GTR	5	250	5.6	202
US7.2-GTR	7.2	250	5.5	210
US12-GTR	12	250	4.0	210

## 7.1.1.3 BIOLOGICAL DEVULCANIZATION

Biological devulcanization was carried out in a bioreactor (Biostat B, Sartorius Stedim Biotech S.A) using *Gordonia desulfuricans* 213E as a desulfurizing bacterium. The schematic of bioreactor is shown in Figure 7.1. The culture medium (1.5 l) was the sulfur-free MSM with an initial glucose concentration equal to 20 g/l and 150 g of GTR as sulfur source. The test was executed for ten days at 500 rpm, 30  $^{\circ}\text{C}$  and pH 7. Glucose concentration was monitored every two days and added just in case the concentration was found to be lower than 10 g/l. Sulfur free MSM composition was described in Chapter 6.

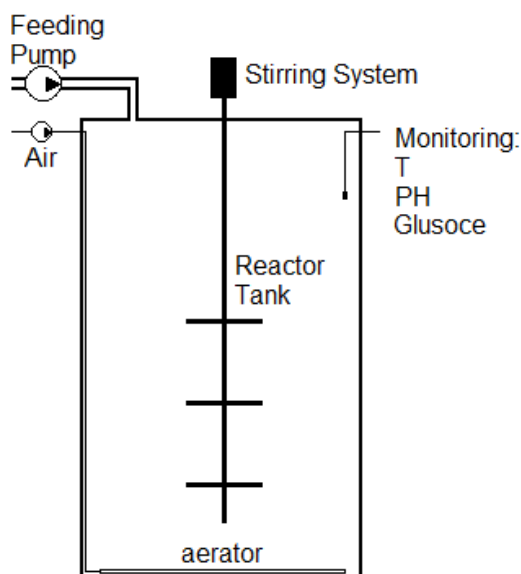


FIGURE 7.1: SCHEMATIC OF THE BIOREACTOR.

The experimental conditions were chosen considering the optimal conditions found in Chapter 6, where *G. desulfuricans* 213E desulfurization activity was investigated and optimized on VGNR. It was shown that the high glucose concentration as a source of carbon, the absence of dibenzothiophene as an

inducer of the desulfurization pathway and high initial bacterial biomass are the most favorable conditions for a selective bio-devulcanization. The sample obtained by this treatment is shown in Table 7.3 as G-GTR.

TABLE 7.3: EXPERIMENTAL CONDITIONS FOR THE BIOLOGICAL DEVULCANIZATION.

X-GTR sample name	Glucose Concentration (g/l)	Initial Bacterial Biomass, OD <sub>600</sub> (AU)	Dibenzothiophene (mg/l)
G-GTR	20	1	0

### 7.1.2 COMPOUNDS

The GTR and all devulcanized samples by each technique (X-GTRs) were compounded into raw NR at a concentration of 10 phr. As a reference, a compound with only natural rubber (Ref-NR) was prepared (Table 7.4). The compounds were formulated considering the composition of the GTR in order to reach the same amount of rubber and CB in each compound. All reagents for compounding were the same used and described in Chapter 3.

A master-batch, containing most of the NR, carbon black and chemicals of the recipe reported in Table 7.4 was prepared using a Pomini Banbury mixer of 1.2 Kg.

The compounds were finished in a two-roll mill (roll diameters 470 mm; working distance 20 mm), adding the GTR/X-GTRs, vulcanizing agents and a small amount of NR and carbon black ingredients as listed in Table 7.5 in order to reach the recipe reported in Table 7.4. Each compound was mixed for 10 min.



TABLE 7.4: COMPOUNDS FORMULATION.

Formulation (phr) <sup>a</sup>	RefNR	GTR	DD0-GTR	DD1.5-GTR	DD5-GTR	US12-GTR	US5-GTR	US7.2-GTR	G-GTR
NR	100.0	95.0	95.0	95.0	95.0	95.0	95.0	95.0	95.0
GTR	0.0	10.0	0.0	0.0	0.0	0.0	0.0	0.0	0.0
DD0-GTR	0.0	0.0	10.0	0.0	0.0	0.0	0.0	0.0	0.0
DD1.5-GTR	0.0	0.0	0.0	10.0	0.0	0.0	0.0	0.0	0.0
DD5-GTR	0.0	10.0	0.0	0.0	10.0	0.0	0.0	0.0	0.0
US12-GTR	0.0	0.0	10.0	0.0	0.0	10.0	0.0	0.0	0.0
US5-GTR	0.0	0.0	0.0	0.0	0.0	0.0	10.0	0.0	0.0
US7.2-GTR	0.0	0.0	0.0	0.0	0.0	0.0	0.0	10.0	0.0
G-GTR	0.0	0.0	0.0	0.0	0.0	0.0	0.0	0.0	10.0
Carbon Black	37.0	34.0	34.0	34.0	34.0	34.0	34.0	34.0	34.0
Silicon Dioxide	15.0	15.0	15.0	15.0	15.0	15.0	15.0	15.0	15.0
Zinc Oxide	3.5	3.5	3.5	3.5	3.5	3.5	3.5	3.5	3.5
Zinc Salts of Fatty Acids	2.0	2.0	2.0	2.0	2.0	2.0	2.0	2.0	2.0
Stearic Acid	2.0	2.0	2.0	2.0	2.0	2.0	2.0	2.0	2.0
Waxes	1.0	1.0	1.0	1.0	1.0	1.0	1.0	1.0	1.0
TMQ-6PPD (25 %-75 %) <sup>b</sup>	4.0	4.0	4.0	4.0	4.0	4.0	4.0	4.0	4.0
Sulfur	1.3	1.3	1.3	1.3	1.3	1.3	1.3	1.3	1.3
CBS <sup>c</sup>	1.2	1.2	1.2	1.2	1.2	1.2	1.2	1.2	1.2
Resin	0.3	0.3	0.3	0.3	0.3	0.3	0.3	0.3	0.3
Silane Coupling Agent	3.0	3.0	3.0	3.0	3.0	3.0	3.0	3.0	3.0

<sup>a</sup> The values are expressed parts per hundred of rubber (phr).

<sup>b</sup> 2,2,4-trimethyl-1,2-dihydroquinoline and N-(1,3-Dimethylbutyl)-N'-phenyl-p-phenylenediamine.

<sup>c</sup> N-Cyclohexylbenzothiazole-2-sulfenamide.

TABLE 7.5: INGREDIENTS ADDED TO THE MASTER-BATCH IN TWO-ROLL MILL.

Ingredient (phr)	Ref-NR	GTR or X-GTR
Ref-NR	15.0	10.0
Carbon Black	13.0	10.0
GTR / X-GTR	0.0	10.0
TMQ-6PPD (25 %-75 %)	4.0	4.0
Resin	0.3	0.3
CBS	1.2	1.2
Sulfur	1.3	1.3

### 7.1.3 CHARACTERIZATION TECHNIQUES

#### 7.1.3.1 GTR AND X-GTRs SOL AND GEL FRACTIONS

Gel fraction was evaluated on GTR and devulcanized X-GTRs samples before compounding with raw NR. It was evaluated through a 24-hour Soxhlet extraction using toluene as a solvent [1] and about 1 g of material ( $W_i$ ). After this period of time the rubber sample was dried in vacuum oven for 24 h and weighed again ( $W_{GF}$ ). Gel fraction was calculated as in Equation 3.5. Sol fraction was calculated as:

$$Sol\ fraction\ (\%) = \left(1 - \frac{gel\ fraction\ (\%)}{100}\right) * 100 \quad (EQUATION\ 7.1)$$

The crosslink density of several X-GTRs samples was impossible to determine due to the powdery nature of the devulcanized material especially for the G-GTR. As a result, the crosslink density was only determined on vulcanized compounds.

#### 7.1.3.2 COMPOUNDS CHARACTERIZATION

The curing behavior of the compounds were measured according to the ISO 6502 standard in a Moving Die Rheometer (MDR 2000, Alpha Technologies) at an oscillation angle of 0.5°, a temperature equal to 150 °C, a pressure equal to 4.3 bar and a frequency of 1.7 Hz. The resulting curves allowed to evaluate the maximum and minimum torque ( $M_H$ ,  $M_L$ ) and were used to evaluate the optimal curing time for the tensile test and for the rheological characterization of the vulcanizates.

Rheological characterization was performed by Rubber Process Analyzer (RPA2000, Alpha Technologies). The frequency sweep tests were carried out at a temperature of 100 °C, at a strain amplitude of 20 % at 120 °C and within a frequency range between 0.1 Hz and 30 Hz. Each sample was first heated at 150 °C (corresponding to the vulcanization temperature) for the optimal curing time and then tested at the same conditions as aforementioned.

All the specimens for MDR and RPA analyses were cut by a Constant Volume Rubber Sample Cutter (CUTTER 2000, Alpha Technologies) from the uncured compounds sheets (diameter = 3.5 cm, thickness = 0.2 cm and weight =  $4.5 \pm 0.3$  g).

Tensile test was carried out according to the ISO 37 standard, using ring as specimens shape. At least three samples were prepared by compression molding at the optimum cure temperature and time for each sample. Mechanical properties were measured at room temperature using a Zwick dynamometer.

The crosslink density was determined according to ASTM D 6814-02 as shown in Chapter 3. Flory-Rehner equation and Kraus correction were applied considering the content of carbon black (Table 3.3) and the same parameters used in Chapter 3 [2-5].

## 7.2 RESULTS AND DISCUSSION

### 7.2.1 GTR AND X-GTRS SOL AND GEL FRACTIONS

The devulcanization was analyzed from the amount of the sol and gel fraction that are shown in Table 7.6. The GTR sample, which had not been subjected to any devulcanization treatment, showed the highest gel fraction and lowest sol fraction. From Table 7.6, it can be observed that under the scCO<sub>2</sub> treatment the sol fraction showed a slight increase, especially increasing the content of DD from 0 wt% to 5 wt%. In the same way, the samples treated with ultrasound showed an increase in the sol fraction content and a decrease in the gel content with an increase in the ultrasonic amplitude. The same behavior had previously been observed in [6,7]. In this second group of samples, the increase was more evident and significant. The G-GTR, which underwent a biological treatment, showed the lowest increase in the sol fraction and the lowest decrease in the gel fraction compared to GTR and to the other X-GTRs. This behavior can be explained considering the nature of the biological desulfurization process that is a superficial treatment, able to give devulcanization only on the GTR surface, therefore unable to produce large amounts of sol fraction [8].

TABLE 7.6: SOL AND GEL FRACTION OF GTR/X-GTRs SAMPLES.

GTR/X-GTR	Gel Fraction wt%	Sol Fraction wt%	SE <sup>a</sup>
GTR	97.7	2.3	0.1
DD0-GTR	96.7	3.3	0.2
DD1.5-GTR	95.9	4.1	0.3
DD5-GTR	94.5	5.5	0.5
US5-GTR	93.6	6.4	0.5
US7.2-GTR	87.3	12.7	0.5
US12-GTR	84.5	15.5	0.5
G-GTR	96.9	3.1	0.5

<sup>a</sup> Standard Error

## 7.2.2 CHARACTERIZATION OF COMPOUNDS CONTAINING GTR AND X-GTRs SAMPLES

The sol and gel fractions and the crosslink density in the reclaimed rubber are two of the most important factors influencing the mechanical and viscoelastic properties of the revulcanizates. Decreases in properties with increasing concentration of reclaimed material and therefore, with respect to the decrease in the molecular weight of the sol fraction and to the presence of the crosslinked gel, were reported by many researchers [9]. Even in the present study, most of the properties of vulcanizates containing either GTR or X-GTRs materials at 10 phr were found to be worse than the ones of reference vulcanized compound containing only NR at 100 phr.

### 7.2.2.1 CURING BEHAVIOR AND CROSSLINK DENSITY

The curing curves of the different compounds were analyzed and the minimum torque ( $M_L$ ), maximum torque ( $M_H$ ), scorch time ( $t_{S2}$ ) and the optimal curing time ( $t_{95}$ ) of each sample are shown in Figure 7.2.

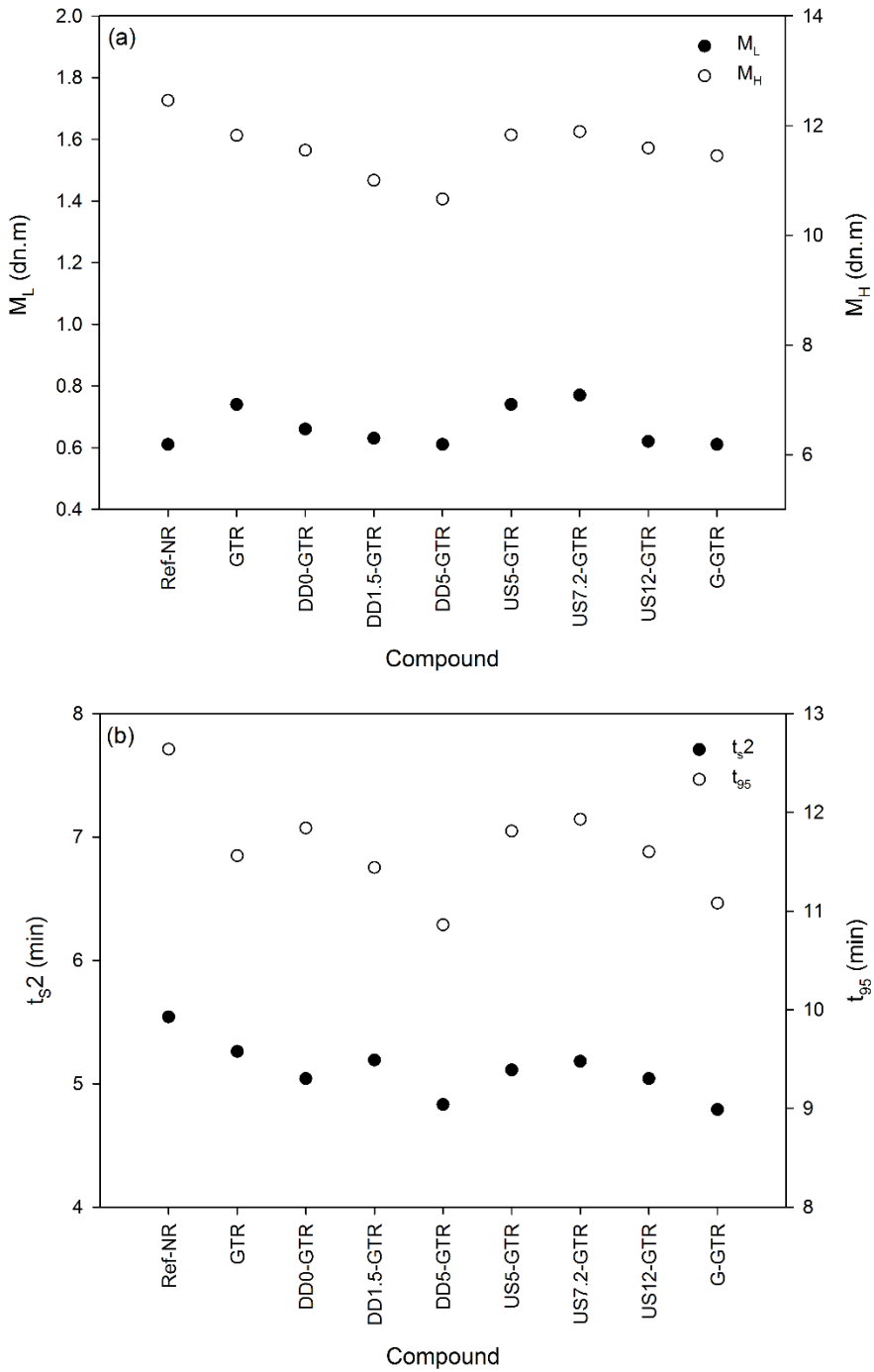


FIGURE 7.2: (a) MAXIMUM TORQUE ( $M_H$ ) AND MINIMUM TORQUE ( $M_L$ ), (b) SCORCH TIME ( $t_{s2}$ ) AND OPTIMAL CUTING TIME ( $t_{95}$ ) FOR THE COMPOUNDS.

In Figure 7.2, it can be seen that compounds containing devulcanized samples treated with different techniques showed different curing behaviors. The Ref-NR compound containing only NR without any GTR or X-GTRs showed the lowest  $M_L$  and the highest  $M_H$ ,  $t_{52}$  and  $t_{95}$ . Indeed, the three-dimensional gel network of crosslinked particles imparts a certain elastic contribution to the unvulcanized sample causing the  $M_L$  to increase. Nevertheless, when the compounds are vulcanized, the gel particles also co-cure with the matrix, hence the mobility and flexibility of particles get lost. At the same time, the Ref-NR compound containing only NR has more active sites that can react during vulcanization, resulting in higher values of  $t_{52}$  and  $t_{95}$  [9].

The compound containing DD5-GTR showed the most significant difference if compared to the GTR and to the other DD-GTRs compounds. An increase in the DD content from 0 wt% to 5 wt% led to a decrease in all the curing parameters. This behavior had been observed in Chapter 3 and in [9-12]. Residual DD seriously impedes the curing process, also contributing to decrease the value of the crosslink density of the vulcanizate as shown in Figure 7.3. The same trend can be observed for the values of moduli ( $M_{100}$  and  $M_{300}$  in Figure 7.4) and storage modulus curves (Figure 7.5).

The compounds containing US5-GTR and US7.2-GTR showed similar curing behavior to the one containing GTR (Figure 7.2). On the other hand, it can be observed that the compound containing US12-GTR showed lower  $M_L$  due to more devulcanization experienced by this sample, caused by an increase of the ultrasonic amplitude and a decrease of the flow rate. For the same reason, the  $M_H$ ,  $t_{52}$  and  $t_{95}$  exhibited a similar trend as well. This behavior had previously been observed by Feng et al. [13]. The same trend can be also observed in the mechanical and rheological properties (Figure 7.4 and Figure 7.5), where the moduli showed lower values for samples devulcanized at a higher amplitudes.

The compound containing G-GTR showed a decrease in all curing parameters if compared to the one containing GTR (Figure 7.2). A decrease in  $M_H$  and  $M_L$  in presence of a GTR devulcanized by a biological treatment had already been observed in [14]. The torque decrease could be explained by a partial and superficial rupture of crosslink structure and by the formation of smaller chains on the surface acting as a plasticizer. Even the decrease in  $t_{52}$  and  $t_{95}$  had already been observed [15,16] and it might be attributed to the high surface reactivity of the biodesulfurized rubber.

After curing, the crosslink density of each vulcanized compound was determined and is shown in Figure 7.3.

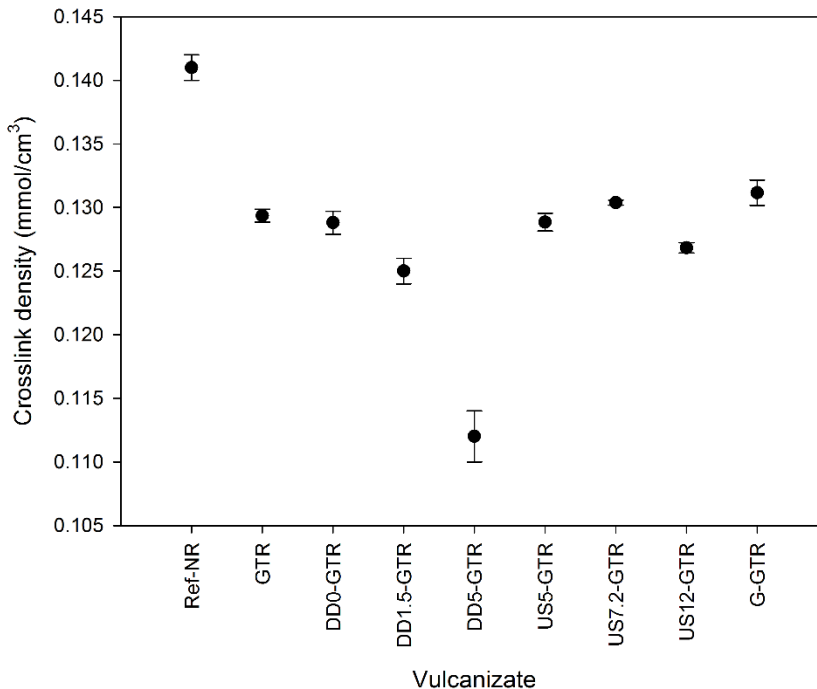


FIGURE 7.3: CROSSLINK DENSITY OF VULCANIZATES.

Ref-NR vulcanizate showed the highest crosslink density. Surprisingly, the incorporation of 10 phr of GTR caused a significant decrease of the crosslink density. An increase of devulcanizing agent from 0 wt% to 5 wt% led to a decrease of the crosslink density in vulcanized compounds containing DD-GTRs. The DD5-GTR vulcanizates showed the lowest crosslink density.

Among the US-GTRs vulcanizates, US12-GTR resulted the only sample showing a significant decrease in the crosslink density if compared to the GTR vulcanizate. This sample is the one that underwent a stronger devulcanization as can be observed in Table 7.6. The same trend for crosslink density of a revulcanized ultrasonically devulcanized GTR had been observed in [6,7].

The G-GTR vulcanizate was the only sample showing a crosslink density slightly higher when compared to the GTR vulcanizate. As previously observed in [8], the biological treatment is a selective and superficial process, therefore able to reduce the crosslink density only on the surface of GTR, keeping the bulk three-dimensional network.

### 7.2.2.2 MECHANICAL PROPERTIES OF VULCANIZED COMPOUNDS

The stress-strain curves of the different vulcanizates were analyzed and the moduli at 100 % and 300 % of elongation (M100 and M300), tensile strength (TS) and elongation at break (Eb) of each vulcanizate are shown in Figure 7.4. These mechanical properties displayed that all the vulcanizates containing GTR and X-GTRs exhibited worse properties than the Ref-NR, as already observed in Chapter 3 and in [9,17,18] especially considering the fact that each material was compounded at 10 phr.

The vulcanizates containing GTR treated in  $scCO_2$  with low amount of DD (DD0-GTR and DD1.5-GTR) showed similar mechanical properties compared to the vulcanizate containing GTR. However, these samples were treated keeping the temperature higher in order to reach the same degree of devulcanization obtained for the 5DD-GTR sample. In this case, the high temperature could generate a higher content of sol fraction with a lower molecular weight, leading to a slight decrease of moduli.

In Chapter 3, it had been demonstrated that unreacted DD can affect not only the curing properties, but also the mechanical properties of the vulcanizates containing such devulcanized GTR, in particular increasing the elongation at break and decreasing the modulus. The same behavior can be observed in the present chapter, where DD-GTRs vulcanizates experienced M100 decrease. On the other hand, Eb exhibited a slight increase by increasing the DD/rubber ratio from 0 wt%, to 1.5 wt% and to 5 wt%. In Figure 7.2 and Figure 7.3, it can be observed that even at concentrations of 1.5 wt% and 5 wt% of DD used during the devulcanization process was enough to interfere with the curing process and therefore with the crosslink density of vulcanizates, negatively affecting M100 and M300 and positively affecting Eb even when added at 10 phr (Figure 7.4). These results confirm that the supercritical fluid treatment might increase the compatibility of the GTR with the raw NR and the mechanical properties of vulcanizates. Therefore, the unreacted DD can lead to a deterioration of the mechanical properties, especially of M100 and M300.

The vulcanizate containing GTR treated at the highest ultrasonic amplitude, lowest flow rate and highest T (US12-GTR) showed higher TS and Eb if compared to the GTR vulcanizate. The Eb resulted even comparable with the one of the Ref-NR vulcanizate. On the other hand, this vulcanizate exhibited similar M100 to GTR vulcanizate, but slightly lower M300 (Figure 7.4). US5-GTR vulcanizate, containing GTR treated at the mildest conditions, behaved differently, showing



similar properties to the ones observed on the GTR vulcanizate. In this case, the treatment was insufficient to produce a strong devulcanization (Table 7.6), providing less compatibility with raw NR. Moreover, the TS and especially Eb did not show big differences with respect to the GTR composite since the degradation was kept low. The US7.2-GTR vulcanizate showed intermediate properties between the two previous conditions.

From these results, it can be observed that a strong ultrasonic treatment caused a breakage of sulfur crosslinks and rubber chain, generating sol fraction with a low molecular weight as reported on the same material in Chapter 6 and in [6]. This soluble polymeric fraction, along with the gel of lower crosslink density, provides enough active sites that can be re-cured, increasing the compatibility between various particles, resulting in better final properties. However, this low molecular weight sol fraction could be responsible for the decrease of M300 observed in vulcanizate containing US12-GTR.

The G-GTR vulcanizate, containing GTR treated by a biological process, showed high M100 and M300, better than the vulcanizate containing GTR and even comparable with the Ref-NR vulcanizate, but it exhibited similar final properties to the GTR vulcanizate, especially Eb. This behavior can be explained considering the fact that biological devulcanization is just superficial and cannot give a bulk treatment as shown in [8]. Moreover, since bacteria might remove sulfur from the GTR, the bulk particles crosslink network is maintained, resulting in a higher crosslink density of the vulcanizate (as shown in Figure 7.3). This behavior can be attributed to the gel content of the G-GTR, indeed the particles generate points for stress concentration and failure. Therefore, the final properties resulted close to the GTR vulcanizate ones.

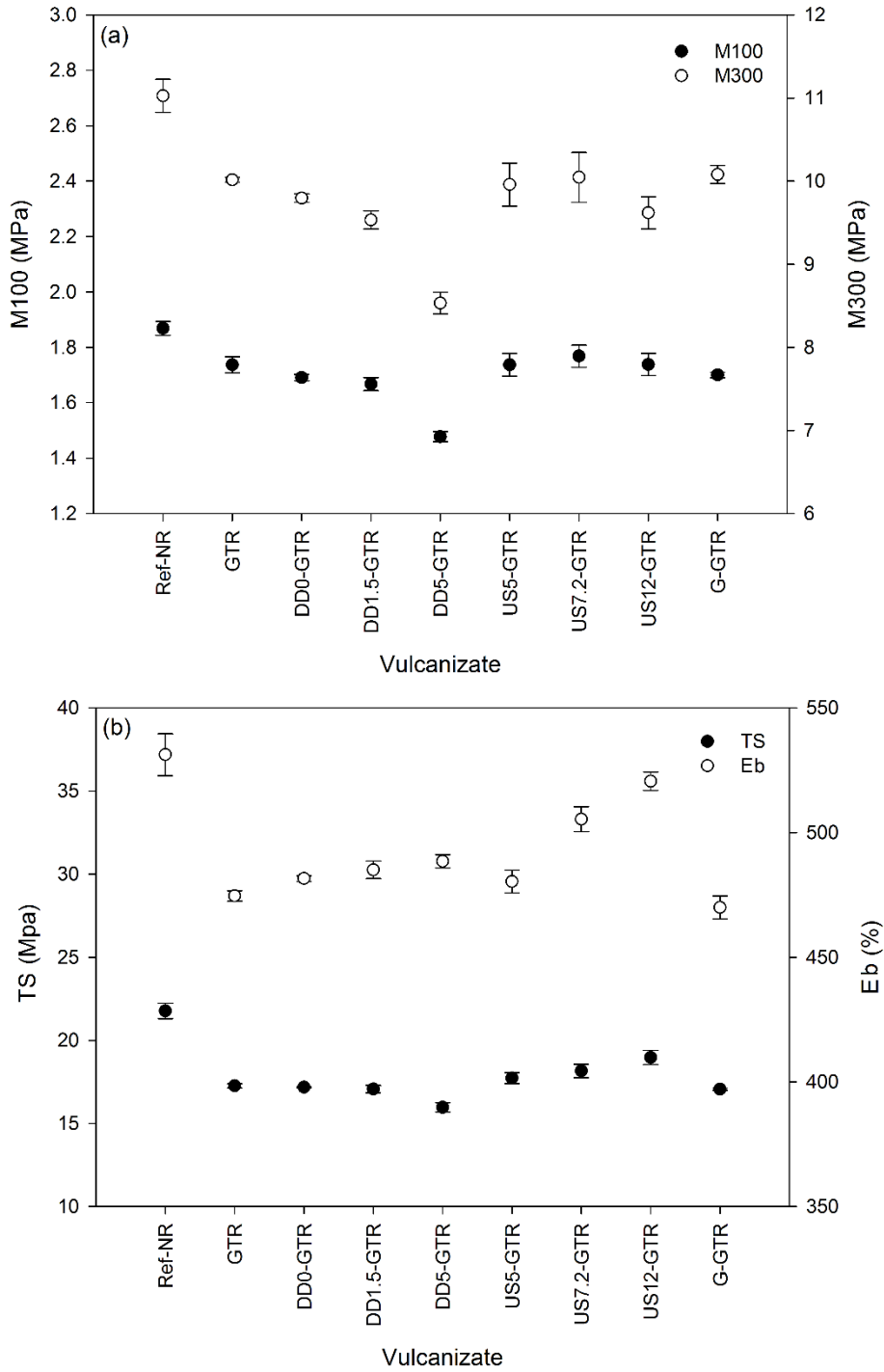


FIGURE 7.4: (a) MODULI AT 100% (M100) AND AT 300% (M300) OF ELONGATION, (b) TENSILE STRENGTH (TS) AND ELONGATION AT BREAK (Eb) FOR THE VULCANIZED COMPOUNDS.

## 7.2.2.3 DYNAMIC VISCOELASTIC PROPERTIES OF VULCANIZED COMPOUNDS

Figure 7.5 shows the frequency dependencies of the storage modulus,  $G'$  (a) and the loss tangent,  $\tan \delta$  (b) of various vulcanizates.

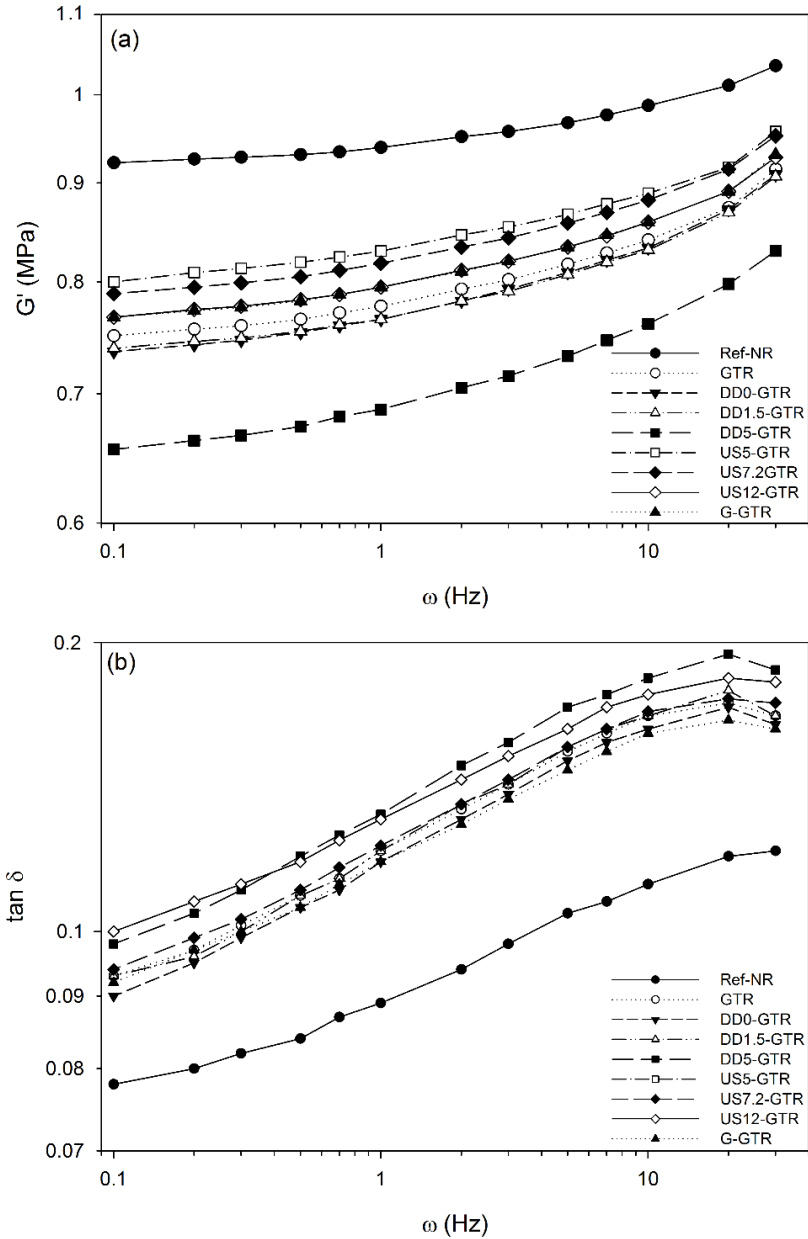


FIGURE 7.5: (a) STORAGE MODULUS ( $G'$ ) AND (b) LOSS TANGENT ( $\tan \delta$ ) OF VULCANIZED COMPOUNDS AS A FUNCTION OF FREQUENCY.

#### 7.2.2.3.1 STORAGE MODULUS

The reference vulcanizate (Ref-NR) showed the highest value of  $G'$ , confirming that the vulcanizate containing just NR had the highest elasticity compared to the other vulcanizates. The worsening of the storage modulus in GTR and X-GTRs vulcanizates is due to the presence of a certain amount of gel fraction. The gel fraction that can contribute to increase the storage modulus in the uncured compounds, at the same time leads to a decrease of  $G'$  after the vulcanization process. The latter is due to the fact that during the curing process the gel particles co-cure with the rubber matrix and their mobility and flexibility is lost providing the overall reduction in the elasticity.

The DD5-GTR vulcanizate showed the lowest  $G'$  and therefore the lowest elasticity. This behavior was caused by the unreacted DD that interfered with the revulcanization process leading to a worsening of properties. On the contrary, the DD0-GTR and DD1.5-GTR vulcanizates showed values of  $G'$  close to the GTR vulcanizate one, especially at high frequencies, confirming what already observed for the mechanical properties. When the content of DD was kept low, the properties of vulcanizates containing these material did not show the same worsening than the one experienced in presence of high amount of DD.

The G-GTR and US-GTRs vulcanizates, especially the US5-GTR and US7.2-GTR samples, containing GTR devulcanized at lower US amplitudes showed better elasticity if compared to the GTR vulcanizate. In this case, the degradation was lower, but the treatment was enough to reduce the crosslink density of the material. The US12-GTR vulcanizate showed lower  $G'$  compared to the other US-GTRs since the treatment can produce degradation with a sol fraction having lower molecular weight. The lower molecular weight of the sol part can lead to a decrease in the storage moduli.

The same behaviors can be observed by the Cole–Cole plot (Figure 7.6) where it is clear that different vulcanizates have different elasticity behavior, but lower than Ref-NR vulcanizate. At the same loss moduli, the Ref-NR vulcanizate showed the highest elasticity followed by US-GTRs and G-GTR having, nevertheless, higher elasticity compared to the GTR vulcanizate. Even in this case the DD5-GTR showed the lowest elasticity.

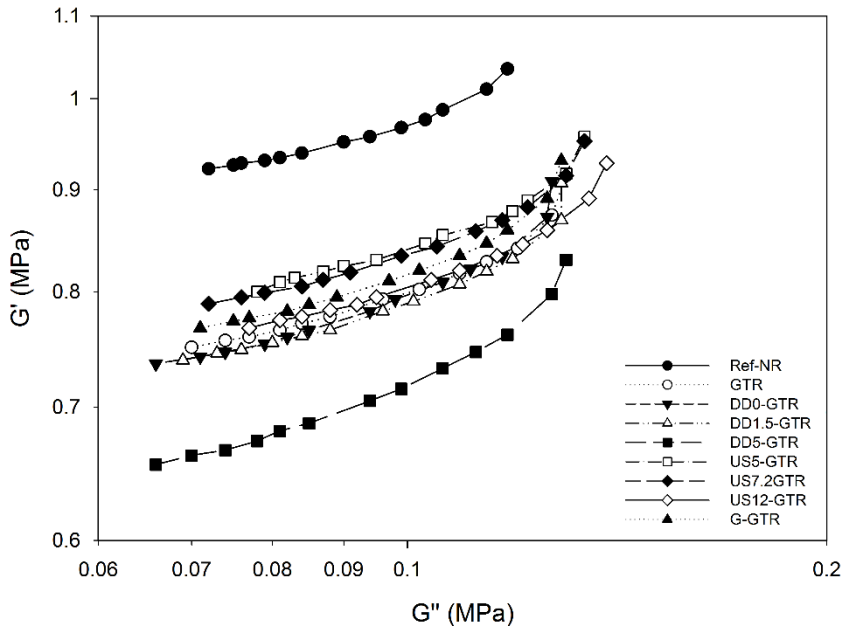


FIGURE 7.6: COLE-COLE PLOT FOR VULCANIZED COMPOUNDS.

#### 7.2.2.3.2 TANGENT DELTA

The  $\tan \delta$  of the vulcanizates is an important parameter since it is a measure of tire rolling resistance. The loss tangent is the ratio of the work converted into heat to the work recovered. In Figure 7.5, it can be observed that even in this case the Ref-NR vulcanizate showed the best properties. On the other hand, DD5-GTR vulcanizate exhibited the highest  $\tan \delta$ , especially at high frequencies. The US12-GTR vulcanizate showed higher values than other US-GTRs, since higher devulcanization temperature, ultrasonic amplitude and low flow rate led to worse  $\tan \delta$  properties due to the lower crosslink density and to the presence of higher sol fraction with low molecular weight. All the other samples showed an intermediate behavior close to the GTR vulcanizate, especially at low frequencies.

### 7.3 CONCLUSIONS

Several devulcanization processes at their optimal conditions were applied in this study for a devulcanization of a GTR. The devulcanized samples were analyzed and compounded in raw NR at 10 phr in order to have a direct comparison among these optimized techniques.

Each devulcanization process affected the structure of the GTR and therefore the properties of the compounds and vulcanizates containing the devulcanized materials.

The biological treatment resulted the mildest and most superficial devulcanization, with a small production of sol fraction. The mechanical and rheological properties of the vulcanizate containing this G-GTR were found to be better than the vulcanizate containing GTR, especially for moduli. Nevertheless, the final properties remained unchanged.

Samples from scCO<sub>2</sub> process led to differences in mechanical, rheological properties of the vulcanizates if compared to the ones with GTR, despite the fact that these materials did not show big differences in sol and gel fractions if compared to the GTR ones. When GTR was treated at the highest amount of devulcanizing agent, it showed the worst properties. The unreacted DD interferes with the curing process, worsening the mechanical and rheological properties being a limiting factor for the application of this technology.

The material from ultrasonic treatment showed the biggest differences in term of sol and gel fractions and in term of properties of vulcanized compounds. The moduli of vulcanizates containing these materials were similar to the one containing GTR, with a slight decrease for the sample treated at the highest ultrasonic amplitude. The final properties and storage modulus resulted the highest among the other devulcanization techniques. However, at the highest ultrasonic amplitude, the treatment produced a high amount of sol fraction that led to a reduction of moduli values and an increase of loss tangent value, despite the vulcanizate showed the best final properties.

Among the known devulcanization technologies, the ultrasonic method seems to be the most useful technique to control the investigated properties of the vulcanizates. Nevertheless, each of these studied technologies can be employed to enhance specific properties or extended to other properties not investigated in this thesis work.

Confidently, in future further novel and efficient *green* devulcanization technologies may be developed as well.

## REFERENCES

1. X. Zhang, C. Lu, M. Liang; Properties of natural rubber vulcanizates containing mechanochemically de-vulcanized ground tire rubber. *Journal of Polymer Research* 2009;16:411–419.

2. P.J. Flory, J.Jr. Rehner; Statistical mechanics of cross-linked polymer networks, I and II. *The Journal of Chemical Physics* 1943;11:512-520 and 521-526.
3. J.L. Valentín, J. Carretero-González, I. Mora-Barrantes, W. Chassé, K. Saalwächter; Uncertainties in the determination of crosslink density by equilibrium swelling experiments in Natural Rubber. *Macromolecules* 2008;41:4717-4729.
4. E. Bilgili, H. Arastoopour, B. Bernstein; Pulverization of rubber granulates using the solid state shear extrusion process Part II. Powder characterization. *Powder Technology* 2001;115:277–289.
5. G. Kraus; Swelling of filler-reinforced vulcanizates. *Journal of Applied Polymer Science* 1963;7:861-871.
6. A.I. Isayev, T. Liang, T.M. Lewis; Effect of particle size on ultrasonic devulcanization in twin-screw extruder. *Rubber Chemistry and Technology* 2014;87:86-102.
7. W. Feng, A.I. Isayev; Recycling of tire-curing bladder by ultrasonic devulcanization. *Polymer Engineering and Science* 2006;46:8-18.
8. C. Yao, S. Zhao, Y. Wang, B. Wang, M. Wei, M. Hu; Microbial desulfurization of waste latex rubber with *Alicyclobacillus* sp.. *Polymer Degradation and Stability* 2013;98:1724-1730.
9. V.V. Rajan, W.K. Dierkes, R. Joseph, J.W.M. Noordermeer; Recycling of NR based cured latex material reclaimed with 2,2'-dibenzamidodiphenyldisulphide in a truck tire tread compound. *Journal of Applied Polymer Science* 2006;102:4194-4206.
10. J. Shi, K. Jiang, D. Ren, H. Zou, Y. Wang, X. Lv, L. Zhang; Structure and performance of reclaimed rubber obtained by different methods. *Journal of Applied Polymer Science* 2013;129: 999-1007.
11. K. Jiang, J. Shi, Y. Ge, R. Zou, P. Yao, X. Li, L. Zhang; Complete devulcanization of sulfur-cured butyl rubber by using supercritical carbon dioxide. *Journal of Applied Polymer Science* 2013;127:2397–2406.
12. G.K. Jana, R.N. Mahaling, T. Rath, A. Kozolowska, M. Kozolowski, C.K. Das; Mechano-chemical recycling of sulfur cured natural rubber. *Polimery* 2007;52:131-136.
13. W. Feng, A.I. Isayev; Recycling of Tire-Curing Bladder by Ultrasonic Devulcanization. *Polymer Engineering and Science* 2006;46:8-18.

14. Y. Li, S. Zhao, Y. Wang; Improvement of the properties of natural rubber/ground tire rubber composites through biological desulfurization of GTR. *Journal of Polymer Research* 2012;19:9864-9871.
15. G. Jiang, S. Zhao, W. Li, J. Luo, Y. Wang, Q. Zhou, C. Zhang; Microbial desulfurization of SBR ground rubber by *Sphingomonas* sp. and its utilization as filler in NR compounds. *Polymer for Advanced Technologies* 2010;22:2344-2351.
16. G. Jiang, S. Zhao, J. Luo, Y. Wang, W. Yu, C. Zhang; Microbial Desulfurization for NR Ground Rubber by *Thiobacillus ferrooxidans*. *Journal of Applied Polymer Science* 2010;116:2768–2774.
17. S. Li, J. Lamminmäki, K. Hanhi; Effect of ground rubber powder on properties of natural rubber. *Macromolecular Symposia* 2004;216:209-216.
18. A.K. Naskar, S.K. De, A.K. Bhowmick, P.K. Pramanik, R. Mukhopadhyay; Characterization of ground rubber tire and its effect on natural rubber compound. *Rubber Chemistry and Technology* 2000;73:902-911.



## SCIENTIFIC CONTRIBUTIONS

### RESEARCH PAPERS

- I. Mangili, E. Collina, M. Anzano, D. Pitea, M. Lasagni; Characterization and supercritical CO<sub>2</sub> devulcanization of cryo-ground tire rubber: Influence of devulcanization process on reclaimed material. *Polymer Degradation and Stability* 2014;102:15-24.
- I. Mangili, M. Oliveri, M. Anzano, E. Collina, D. Pitea, M. Lasagni; Full factorial experimental design to study the devulcanization of ground tire rubber in supercritical carbon dioxide. *The Journal of Supercritical Fluids* 2014;92:249-256.
- I. Mangili, M. Lasagni, K. Huang, A.I. Isayev; Modeling and optimization of ultrasonic devulcanization using the response surface methodology based on central composite face-centered design. Submitted 2015.
- V. Tatangelo, I. Mangili, P. Caracino, G. Bestetti, E. Collina, M. Lasagni, A. Franzetti; Experimental design approach to study biological devulcanization of ground rubber by *Gordonia desulfuricans* 213E strain. Submitted 2015.
- I. Mangili, V. Tatangelo, P. Caracino, M. Anzano, E. Collina, M. Lasagni, A. Franzetti, A.I. Isayev; Properties of Natural Rubber Compounds Containing Devulcanized Ground Tire Rubber from Several Methods, *in preparation*.

### CONFERENCE CONTRIBUTIONS

- D. Pitea, C. Acaia, E. Collina, M. Lasagni, I. Mangili, G. Gerosa et al.; Sewage sludge characterization for the assessment of an integrated drying and combustion system for sludge disposal. *Industrial economy: I principi, le applicazioni a supporto della green economy*. Maggioli, Atti dei Seminari Ecomondo, 2011.
- I. Mangili, M. Lasagni, E. Collina, M. Anzano, D. Pitea; Characterization and supercritical CO<sub>2</sub> devulcanization of commercial cryo-ground and carbon black filled tires. XIV Congresso Nazionale di Chimica dell'Ambiente e dei beni culturali. "La chimica nella società sostenibile", 2013.
- I. Mangili; Sewage Sludge from Urban Wastewater Treatment Plant: Energy Recovery and Environmental Assessment. XIII Congresso Nazionale di Chimica dell'Ambiente e dei Beni Culturali, 2012.
- I. Mangili, M. Lasagni, K. Huang, A.I. Isayev; Optimization of ultrasonic devulcanization of cryo-ground tire rubber. International Rubber Expo, 186th Technical Meeting & Educational Symposium, 2014.



## ACKNOWLEDGMENTS

I would like to express my sincere gratitude to many people without whom this work could have never been accomplished.

First of all, Prof. Marina Lasagni for being my guide during these three years. Thanks for supporting me and for excellent guidelines on research.

I would also like to thank Distinguished Prof. Avram I. Isayev for accepting me as a visiting researcher in his laboratories, making me a part of his research group and giving me the opportunity to meet some really smart and friendly colleagues.

My sincere appreciation extends to Pirelli Labs SpA, in particular to Dr. Paola Caracino for being my external tutor, supporting my research with punctual and precise data, thoughtful advice and suggestions; I do apologize for hundreds of e-mails and calls.

I would also like to thank Prof. Demetrio Pitea, Dr. Elena Collina, Dr. Elsa Piccinelli and Dr. Manuela Anzano for their support and patient help and Cesare Mannino and Matteo Oliveri for carrying out part of my project while I was in the States.

Special thanks go to Valeria and Federica who shared with me the research project but especially the Ph.D. experience.

My sincere gratitude goes to my parents for giving me the devotion for work. Thanks go to all my friends and especially to Simone for precious revisions of published papers and for keeping me motivated.

Last but not the least, thanks go to Fondazione Tronchetti Provera for sponsoring my Ph.D. program, to Akrochem Corporation for providing some materials used during research activities and to the Rubber Division of the American Chemical Society for the award at the 2014 International Elastomer Conference.